1967

Stresses in a thick spherical shell

David Wayne Moore

Department:

STRESSES IN A THICK SPHERICAL SHELL

BY

DAVID W. MOORE - 1938 -

A

THESIS

submitted to the faculty of

THE UNIVERSITY OF MISSOURI AT ROLLA

in partial fulfillment of the requirements for the

Degree of

MASTER OF SCIENCE IN ENGINEERING MECHANICS

Rolla, Missouri

1967

Approved by

Peter G Hanson (advisor)

Fred F. Rasche

Larry E Farmer

D W Moore

ABSTRACT

This thesis reports a method to evaluate the stresses in a segment of a thick spherical shell. In the numerical examples loads due to thermal expansion as the shell is constrained at the free edge and a dead load acting vertically downward were considered for a shell assumed pinned but free to rotate and for a shell assumed completely fixed at the edge. A concrete shell was specifically studied but the method would also apply to a shell of any homogeneous, isotropic material.

PREFACE

The author wishes to thank Dr. Peter G. Hansen for the suggestion of this topic and for his guidance and advice relating to this thesis.

TABLE OF CONTENTS

LIST OF FIGURES

FIGURE PAGE

FIGURE PAGE

LIST OF SYMBOLS

D - Measure of axial stiffness.

ds_c - Width of small element at centroidal surface.

E - Modulus of elasticity.

H - Horizontal circumferential load at supported edge of shell.

I - Moment of inertia.

K - Measure of bending stiffness.

M_ϕ - Meridional moment.

M_θ - Circumferential moment.

N_ϕ - Axial load in meridional direction.

N_θ - Axial load in circumferential direction.

$\underline{P}$ - Total vertical load in pounds.

p - Vertical applied load in psi. of projected area.

p_w - Shell weight per unit area of middle surface.

Q_ϕ - Transverse shear load.

R_c - Radius of centroid surface.

R_i - Radius of inner surface.

R_o - Radius of outer surface.

R_s - Radius of middle surface.

r - Radius of any surface.

T - Temperature increase.

t - Thickness of shell.

u - Radial expansion.

V - Vertical circumferential load at supported edge of shell.

X - Rotation of element of shell.

Z - Area factor due to curvature.

z' - Solution to hypergeometric differential equation.

z - Coordinate along thickness of shell.

α - Coefficient of thermal expansion.

δ - Horizontal deflection.

ε - Axial strain.

ϕ - Meridional angle.

ν - Poisson's ratio.

σ_θ - Stress in circumferential direction.

σ_ϕ - Stress in meridional direction.

I. INTRODUCTION

Many companies in the United States design and build chemical furnaces. In the past these furnaces have been approximately eight feet in diameter. A drawing of a furnace, sufficient in detail for our discussion, is shown in Figure 1. In recent times the trend in industry has been to achieve maximum production and efficiency with a minimum outlay of capital and equipment. With respect to the chemical application under consideration, this has been partially achieved by designing furnaces up to 24 feet in diameter, whereby the complexities in design have been increased. In particular, additional factors must be considered for proper design of the spherical dome separating the solid charge from the flame.

A method for determining the stresses in a thick spherical dome and hence a basis for making an engineering decision provides the subject for this thesis. Figure 2 shows the assumed loading of the dome. The following cases are studied in the investigation:

(A) $\underline{P} = 0$, $M_\phi = 0$ (Pinned but free to rotate at edge).

(B) $\underline{P} = 0$, Rotation = 0 (Fixed at edge).

(C) $\underline{P}$ = Value of charge "dead load", $M_\phi = 0$.

(D) $\underline{P}$ = Value of charge "dead load", Rotation = 0.

It should be noted that temperature effects were included in all of the above cases. For cases (C) and (D) involving the vertical load a value of p = 25,000 lbs./ft^2.

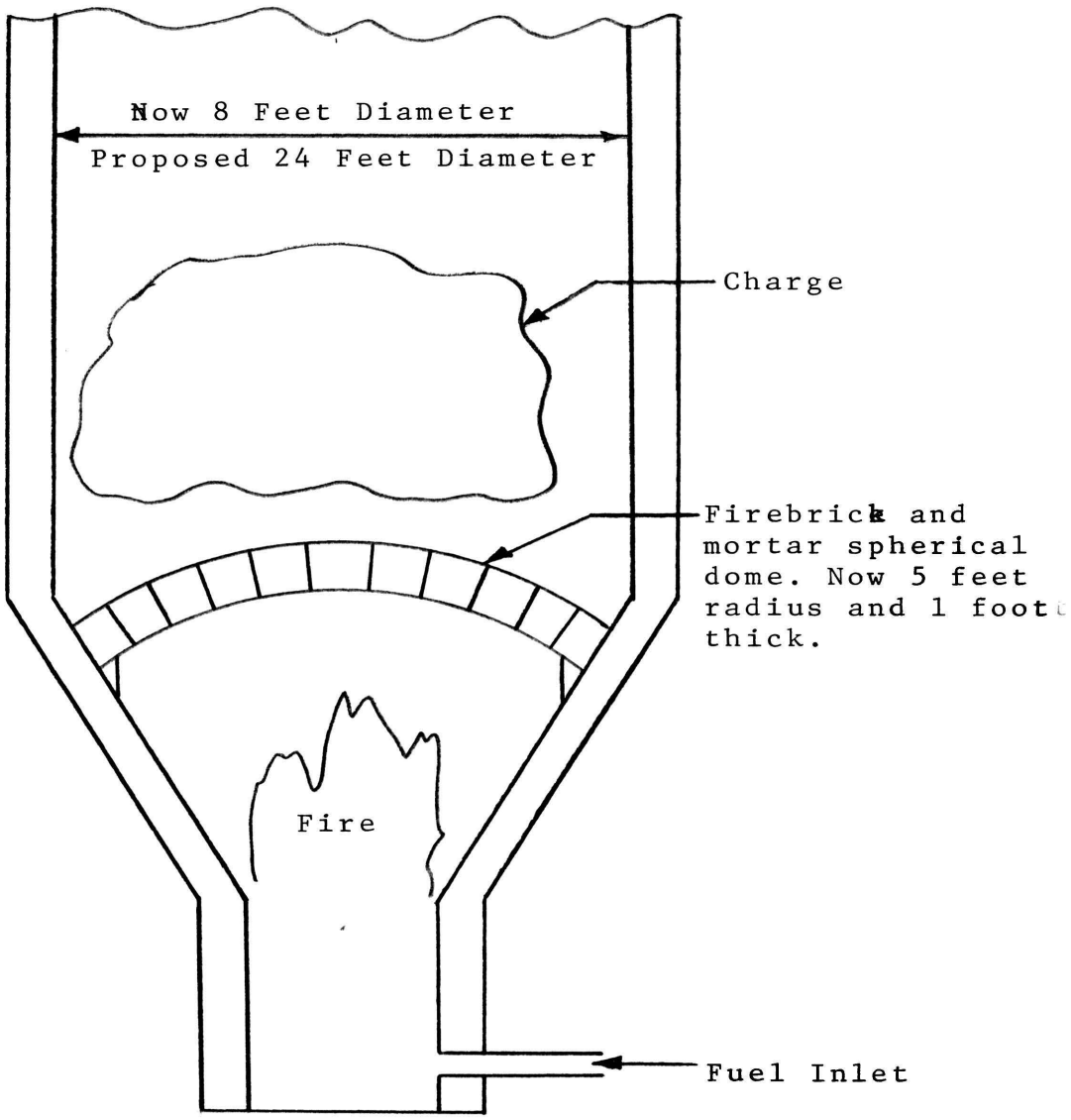

Figure 11. Details of Chemical Furnace

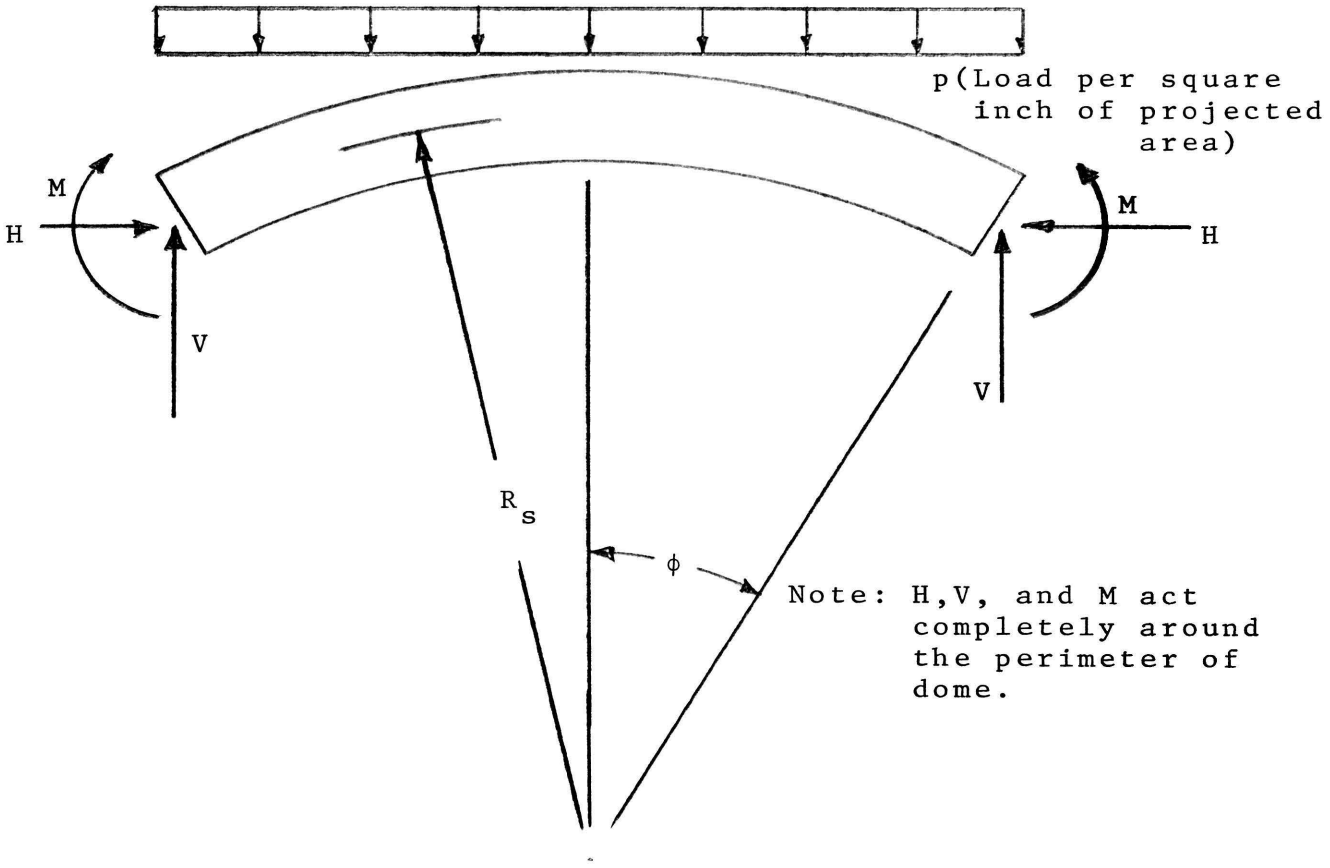

Figure 2. Loading of Dome

(173.6 psi.) was used which is the present design value of the eight foot diameter furnace. As will be shown later this value of vertical load only made a very small change from cases (A) and (B).

Cases (A) and (B) do not specifically apply to the furnace problem under consideration but the usefulness of the solution to these cases could be of value in other situations. It should also be stated that only the pinned ($M_\phi = 0$) and fixed (rotation = 0) edge conditions have been studied whereas the actual construction will fall somewhere between these two cases. This should provide limiting

values for the loads and stresses. With this knowledge an estimate of the actual stresses could be made assuming some percentage of fixity.

II. REVIEW OF LITERATURE

Many books and technical publications have been written concerning shells, considering various loadings and configurations of such, examining various methods for exact and approximate solutions, and studying some physically realistic cases as well as some theoretically intriguing situations. Generally the literature very thoroughly covers the field of thin shells with only a brief discussion concerning thick shells.

Several books on shells were reviewed and a rather comprehensive bibliography on shells was also compiled. The part appropriate for thick shells is rather small.

Fluegge[1] spends by far the majority of his book in the consideration of thin shells but he does make a brief statement concerning thick shells. His statement is:

> "If the shell thickness is not very small compared with the radii of curvature, it may be worthwhile to take the trapezoidal shape of the cross-section into account; but then one should also make use of the basic ideas of bars of great curvature and consider the corresponding non-linearity in the stress distribution".

This suggestion was used as will be explained later.

III. DISCUSSION

A brief outline of the complete method will be presented before all of the details are explained.

Part A. The thermal expansion of the spherical shell due to a temperature increase is determined. In cases (A) and (B) (Page 1), when the vertical load is zero, the restraint of the thermal expansion is what causes the loads (H only). If a horizontal load could be developed by some other means the discussion for cases (A) and (B) (Page 1) would still be appropriate.

Part B. An element of the shell with all the internal forces acting on it was taken. By writing the equations of equilibrium, load-displacement relationships, and solving the resulting hypergeometric differential equation it is possible to obtain the expressions for the loads at any cross-section of the shell. The solution is in the form of a hypergeometric series.

Up to this point everything is equally applicable to thick and thin shells. The next step for thin shells would be relatively easy. For thick shells the problem becomes rather complicated.

Part C. An expression giving the stress distribution across the thickness of the shell is found. This expression is obtained by considering the loads that act on the faces of an element and the change in shape of the element due to these loads. It will be shown that the stress expressions

developed in Part C are also quite appropriate for thin shells as well as correct for thick shells.

It should be stated that at all times the attempt was made to keep the resulting method as general as possible while realizing that it is already limited to a spherical shell of constant thickness loaded by an axially symmetric load.

A. Thermal Expansion

Completing the derivation of Timoshenko[2] it is possible to obtain an expression for the radial expansion of a hollow spherical shell due to a temperature increase which is

$$u = \left[\frac{3\,\alpha R_o}{R_o^3 - R_i^3}\right] \int_{R_i}^{R_o} T(r)\, r^2\, dr \qquad (1)$$

where

u = radial expansion.

α = coefficient of thermal expansion.

R_o = outer radius.

R_i = inner radius.

$T(r)$ = temperature as a function of the radius.

r = radius to any point of shell.

The temperature across the thickness of the shell will be constant after the furnace has operated for some period of time. For $T(r) = T$ = constant temperature then

$$u_{r=R_o} = \alpha R_o T \,. \qquad (2)$$

Thus the expression for the radial expansion due to a temperature increase, constant across the thickness, is rather simple.

In cases (A) and (B) (Page 1), for a shell restrained from expanding, a horizontal load H (See Figure 2.) is found that causes a deflection equal and opposite to the horizontal component of the thermal expansion. In cases (C) and (D) it is a combination of the thermal expansion and the outward deflection due to the vertical load p that the horizontal load H must overcome. And finally in cases (B) and (D), at the fixed edge, a moment M will cause the rotation to be zero.

Timoshenko[3] determines, based on the equilibrium equations, stress-strain relationships, and the strain-displacement relationships, an expression for the deflection of a spherical shell due to a horizontal load H (See Figure 2.). This equation is

$$\delta = \frac{R_s \sin\phi}{E\ t} (N_\theta - \nu N_\phi) \qquad (3)$$

where

δ = Horizontal deflection at angle ϕ.

R_s = Radius to middle surface.

ϕ = coordinate angle of spherical shell.

E = Modulus of elasticity of shell material.

t = Thickness of shell.

ν = Poisson's ratio.

N_θ = Axial load in θ (circumferential) direction.

N_ϕ = Axial load in ϕ (meridional) direction.

Equation (3) is applicable to the loading situation of all four cases considered (A), (B), (C) and (D). The expressions for N_θ and N_ϕ derived later will differ between the first two and the latter. The differences take into account the vertical load in cases (C) and (D).

In a problem involving both a temperature increase and other loads the usual stress-strain relationships must be modified to account for the strain in an element due to the temperature increase. (See Boresi[4].) However when the temperature is constant throughout the body, the modification required for the thermal strain drops out and the standard stress-strain relations are valid. That is why it is correct to use equation (3) even though it was derived without being based on any temperature considerations.

Equation (2) forms one boundary condition for the overall problem. When the horizontal component of the radial expansion is found it can be substituted into equation (3), providing a relationship between N_θ and N_ϕ at the free edge of the shell. If a gap is provided for a part of the thermal expansion then the "opposite" deflection of the restraining load will be reduced accordingly. The loads vary linearly with the thermal expansion, hence if a gap is provided for one-half of the thermal expansion the loads are only reduced by fifty percent and are not completely relieved.

B. Variation of Loads

Consider an element of a shell as shown in Figure 3.

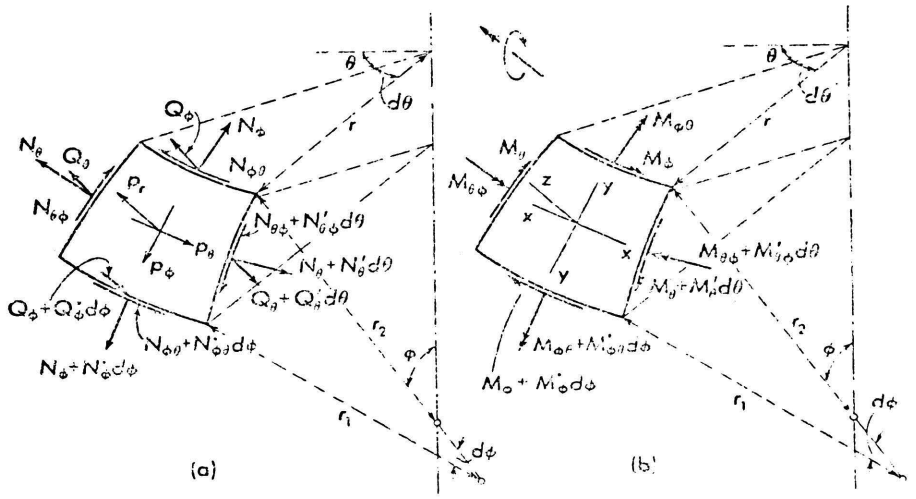

From Fluegge[1] $( )^{\cdot} = \frac{d( )}{d\theta}$ $( )' = \frac{d( )}{d\phi}$

Figure 3. Loads on Element of Shell of Any Shape

For a spherical shell with an axially symmetric load there will not be any variation of load with respect to θ; $N_{\theta\phi}$, $N_{\phi\theta}$, $M_{\theta\phi}$, $M_{\phi\theta}$, Q_{θ}, and p_{θ} will all be zero; the radius of curvature will be R_s, and $r = R_s \sin\phi$. It was found in a separate study (See Appendix 1.) that the stresses caused by the weight of the shell were very small compared to the stresses caused by the other loads. Therefore the body forces p_{ϕ} and p_r will also be dropped. This is true because of the sizes of shells that were considered.

For shells appreciably larger the shells own weight would have to be considered.

Following the derivation of Fluegge[1] (pages 312-324) the equations of equilibrium and the load-displacement relationships lead to the following differential equation

$$\frac{d^2Q_\phi}{d\phi^2} + \frac{dQ_\phi}{d\phi}\cot\phi - Q_\phi \cot^2\phi + 2im^2Q_\phi = 0 \qquad (4)$$

where $i = \sqrt{-1}$

$$m^4 = 3(1-\nu^2)\frac{R_s^2}{t^2} - \frac{\nu^2}{4} \qquad (5)$$

Equation (4) is a second-order differential equation with variable coefficients. Introducing the new variables

$$x = \sin^2\phi \qquad (6)$$

and

$$Q_\phi = z' \sin\phi \qquad (7)$$

transforms equation (4) into

$$\frac{d^2z'}{dx^2} + \frac{4-5x}{2x(1-x)}\frac{dz'}{dx} - \frac{1-2im^2}{4x(1-x)}z' = 0 \qquad (8)$$

This is a hypergeometric differential equation (See reference (5) or any differential equations textbook.) which in its general form is

$$\frac{d^2z'}{dx^2} + \frac{\gamma-(1+\alpha+\beta)x}{x(1-x)}\frac{dz'}{dx} - \frac{\alpha\beta}{x(1-x)}z' = 0 \qquad (9)$$

The solution to equation (9) is the following

$$z'_a = 1 + \frac{\alpha\beta}{1!\gamma}x + \frac{\alpha(\alpha+1)\beta(\beta+1)}{2!\gamma(\gamma+1)}x^2 + \frac{\alpha(\alpha+1)(\alpha+2)\beta(\beta+1)(\beta+2)}{3!\gamma(\gamma+1)(\gamma+2)}x^3 + \ldots \qquad (10)$$

From equations (8) and (9) it is possible to show that

$$\alpha = \frac{1}{4}\left(3 - \sqrt{5 + 8im^2}\right) \tag{11}$$

$$\beta = \frac{1}{4}\left(3 + \sqrt{5 + 8im^2}\right) \tag{12}$$

$$\gamma = 2 \tag{13}$$

Substituting equations (11), (12) and (13) into equation (10) gives

$$z'_a = 1 + \frac{(1 - 2im^2)}{1!(4)(2)} x + \frac{(1 - 2im^2)(11 - 2im^2)}{2!\ (4)\ (4)\ (2)\ (3)} x^2 + \frac{(1 - 2im^2)(11 - 2im^2)(29 - 2im^2)}{3!\ (4)(4)(4)(2)(3)(4)} x^3 + \ldots \tag{14}$$

Equation (14) has a limitation that $|x| < 1.0$. Remembering that $x = \sin^2\phi$ this means we are restricted to ϕ angles less than ninety degrees. For shells having a ϕ angle greater than ninety degrees it is necessary to consider the shell in two parts and use both the solution shown by Fluegge[1] and the solution developed here. Using both solutions, which are applicable for different regions of the shell, it would be possible to determine the loads in a shell for ϕ greater than ninety degrees.

In equation (14) a fraction is multiplied on the nth term to form the (n + 1) term. The first part of the additional term of the numerator increases in the following manner: 1, 11, 29, 55, 89, . . ., each number increases by the difference between the preceding two numbers plus eight. The general expression for the denominator is $4^n\ n!(n + 1)!$.

The real and imaginary parts of equation (14) also form linear independent solutions to the differential

equation (equation 8). These two solutions can be obtained in the following manner:

Let $\bar{z}'_a$ = conjugate complex of z'_a (equation (13))

$$z'_1 = \frac{1}{2}\left(z'_a + \bar{z}'_a\right) \tag{15}$$

$$z'_2 = \frac{i}{2}\left(z'_a - \bar{z}'_a\right) \tag{16}$$

Then the solution of equation (4) becomes

$$Q\phi = z'_{total} \sin\phi = \left(C_1 z'_1 + C_2 z'_2\right) \sin\phi \tag{17}$$

where C_1 and C_2 are constants to be determined from the boundary conditions. Carrying out the steps suggested by equations (15) and (16) gives

$$z'_1 = 1 + \frac{1}{4\ 1!2!}\sin^2\phi + \frac{(11 - 4m^4)}{4^2\ 2!\ 3!}\sin^4\phi + \frac{(319 - 164m^4)}{4^3\ 3!\ 4!}$$

$$\sin^6\phi + \frac{(17545 - 10456m^4 + 16m^8)}{4^4\ 4!\ 5!}\sin^8\phi + \ldots \tag{18}$$

and

$$z'_2 = \frac{2m^2}{4\ 1!2!}\sin^2\phi + \frac{24m^2}{4^2\ 2!\ 3!}\sin^4\phi + \frac{(718m^2 - 8m^6)}{4^3\ 3!\ 4!}\sin^6\phi +$$

$$\frac{(40228m^2 - 768m^6)}{4^4\ 4!\ 5!}\sin^8\phi + \ldots \tag{19}$$

From Fluegge in reference 1

$$N_\phi = -Q_\phi \cot\phi - \frac{\underline{P}}{2\pi R_s \sin^2\phi} \tag{20}$$

$$N_\theta = -\frac{dQ_\phi}{d\phi} + \frac{\underline{P}}{2\pi R_s \sin^2\phi} \tag{21}$$

$$M_{\phi} = \frac{K}{R_s}\left[\frac{dX}{d\phi} + \nu X \cot\phi\right] \tag{22}$$

$$M_{\theta} = \frac{K}{R_s}\left[X \cot\phi + \nu\frac{dX}{d\phi}\right] \tag{23}$$

where

$\underline{P}$ = total vertical load at any angle ϕ

$$K = \frac{Et^3}{12(1 - \nu^2)} \tag{24}$$

$$X = \frac{(2m^2 z'_2 - \nu z'_1)C_1 - (2m^2 z'_1 + \nu z'_2)C_2 \quad \sin\phi}{D(1 - \nu^2)} \tag{25}$$

$$D = \frac{Et}{1 - \nu^2} \tag{26}$$

All loads are in appropriate units per unit width.

The last part of equations (20) and (21), which only appears in these equations when there is a vertical load, are written in terms of the total vertical load $\underline{P}$. In terms of the load per square inch (p = 173.6 psi.) $\underline{P} = \pi(R_s \sin\phi)^2 p$. At any value of ϕ the $\sin^2\phi$ terms cancel out and the last part of the equations become constant values modifying the axial loads N_{ϕ} and N_{θ}.

Hence, once the series z'_1 and z'_2 are obtained it is possible to calculate all the loads (Q_{ϕ}, N_{ϕ}, N_{θ}, M_{ϕ} and M_{θ}) in terms of the constants C_1 and C_2. A computer program (See Appendix 2.) was written to perform the necessary calculations. The series were calculated until the difference between succeeding terms was 0.00001. Then the boundary conditions are considered and the constants C_1 and C_2 are

evaluated. Using the deflection boundary condition previously discussed and the load boundary conditions at the free edge of the shell, shown in Figure 4, it is possible to obtain C_1, C_2 and H. V can be determined, when applicable, by summing forces in the vertical direction. After the constants are evaluated it is possible to obtain the loads acting on any cross-section of the shell.

C. Stress Distribution

Knowing the loads at a cross-section from part B, the problem now is to find how the stresses are distributed across the thickness.

A derivation similar to that used on an element of a curved beam is followed except that on a shell element it is necessary to consider loads and stresses in two directions along with the curvature in two directions. The derivation assumes that

(1) Small deflections exist,

(2) Plane sections remain plane,

(3) Displacement of the neutral surface is zero,

(4) Elastic limit not exceeded.

The procedure followed is

(1) Apply a moment to an element,

(2) Obtain an expression for the strain as the element deforms by considering the curvature and the change in shape,

(3) Use Hooke's Law to determine the stress-strain relationships,

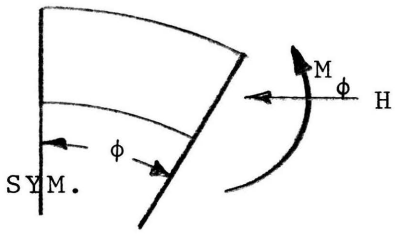

a) Case (A)

Zero Vertical Load
Boundary Conditions,

$$\left.\begin{array}{l} \text{At } \phi=\phi_o \quad M_\phi = 0 \\ \text{At } \phi=\phi_o \quad Q_\phi = H\sin\phi \end{array}\right\} \quad (27)$$

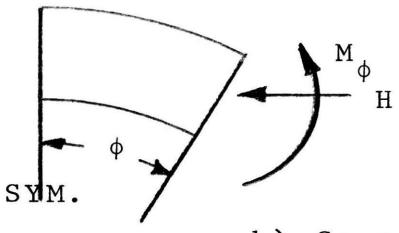

b) Case (B)

Zero Vertical Load
Boundary Conditions,

$$\left.\begin{array}{l} \text{At } \phi=\phi_o \quad \text{Rotation} = 0 \\ \text{At } \phi=\phi_o \quad Q_\phi = H\sin\phi \end{array}\right\} \quad (28)$$

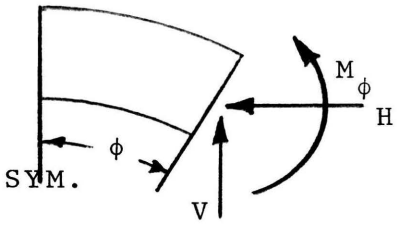

c) Case (C)

173.6 psi. Vertical Load
Boundary Conditions,

$$\left.\begin{array}{l} \text{At } \phi=\phi_o \quad M_\phi = 0 \\ \text{At } \phi=\phi_o \quad Q_\phi = H\sin\phi - V\cos\phi \end{array}\right\} \quad (29)$$

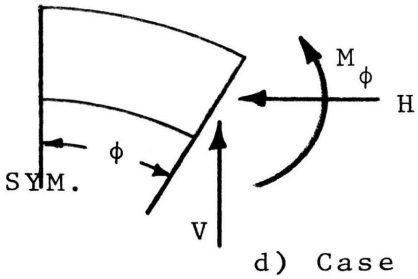

d) Case (D)

173.6 psi. Vertical Load
Boundary Conditions,

$$\left.\begin{array}{l} \text{At } \phi=\phi_o \quad \text{Rotation} = 0 \\ \text{At } \phi=\phi_o \quad Q_\phi = H\sin\phi - V\cos\phi \end{array}\right\} \quad (30)$$

Figure 4. Load Conditions and Boundary Conditions

and (4) Use equations of equilibrium relating stresses on a cross-section to the load on the cross-section.

Figure 5 shows an element and the change in shape caused by the applied moment.

From the stresses acting on face CDGH of Figure 5c the following can be obtained

$$\int_{area} \sigma \, dA = 0 \tag{31}$$

$$M = \int_{area} \sigma z \, dA \tag{32}$$

A load (moment) is only shown on one face but there is also a moment acting on the face perpendicular to CDGH. Hence we have a biaxial stress state. Remembering Fluegge's statement copied earlier (See page 5), the following considers the change in shape of the element due to the load. Because of the spherical shape of the element it is possible that the neutral surface, the centroidal surface and the middle surface will all be different. We have assumed that plane sections remain plane after loading so that the deformations will be proportional to the distance from the neutral surface. Strains will not be proportional because of the different original length of each fiber.

From Figure 5

ε_c = strain in centroid element

$$\varepsilon_c = \frac{KK'}{LK} \tag{33}$$

$$KK' = \varepsilon_c LK = \varepsilon_c R_c d\theta \tag{34}$$

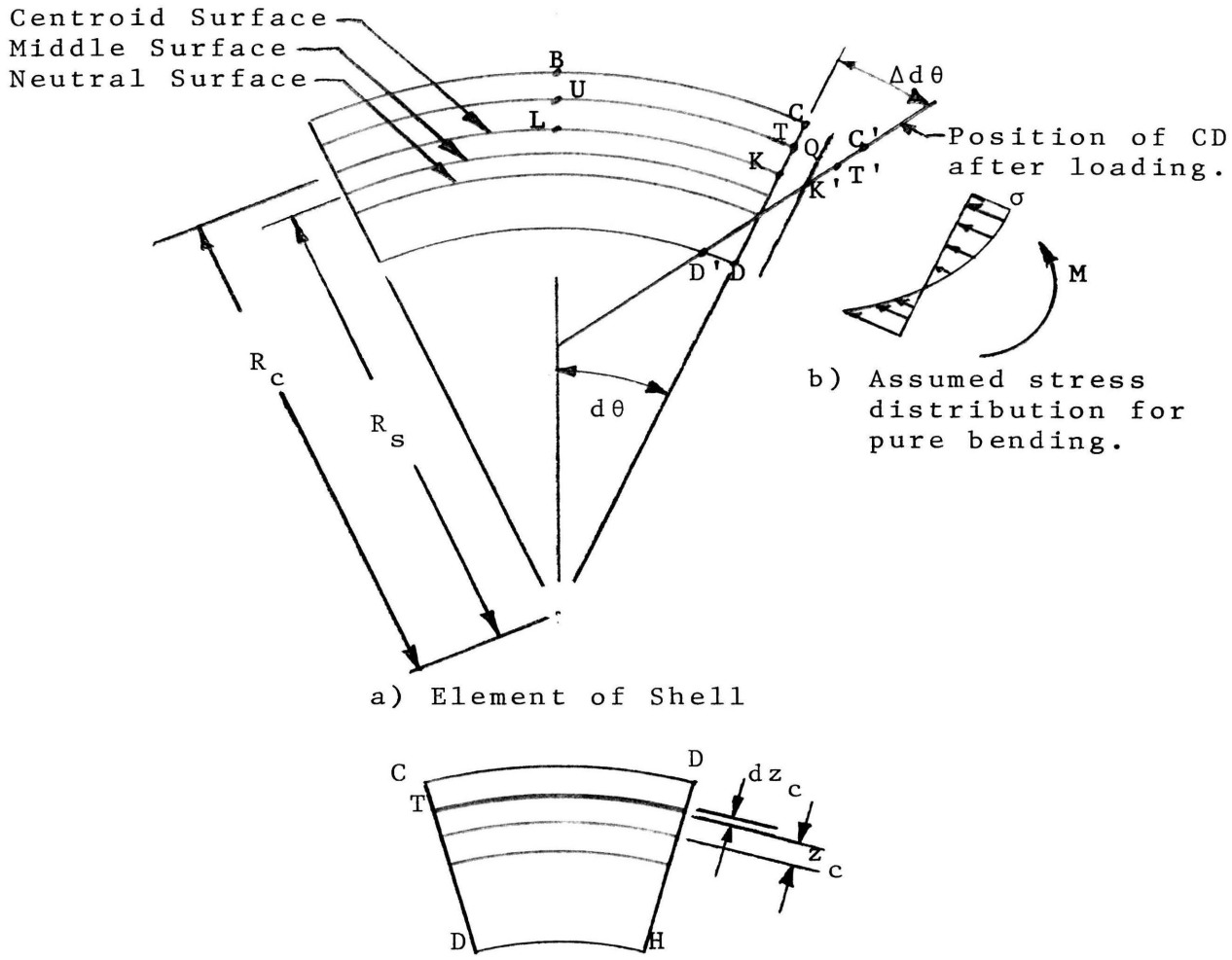

Figure 5. Change in Shape of Element Due to Bending Moment

At some distance z from the centroid surface

$$\varepsilon(z) = \frac{TT'}{UT} = \frac{TQ+QT'}{UT} = \frac{KK'+QT'}{UT} \tag{35}$$

$$QT' = z\Delta d\theta \tag{36}$$

$$UT = (R_c+z)\,d\theta \tag{37}$$

$$\varepsilon(z) = \frac{\varepsilon_c R_c\, d\theta + z\Delta d\theta}{(R_c+z)\,d\theta} = \frac{\varepsilon_c R_c + z\frac{\Delta d\theta}{d\theta}}{R_c+z} \tag{38}$$

Let $\omega = \frac{\Delta d\theta}{d\theta}$ and simplify

$$\varepsilon(z) = \varepsilon_c + \frac{z(\omega-\varepsilon_c)}{R_c+z} \tag{39}$$

Equation (39) is due to the moment on one face of the element. Considering the moment on both faces gives

$$\varepsilon(z)_\theta = \varepsilon_{c_\theta} + \frac{z(\omega-\varepsilon_c)_\theta}{R_c+z} \tag{40}$$

$$\varepsilon(z)_\phi = \varepsilon_{c_\phi} + \frac{z(\omega-\varepsilon_c)_\phi}{R_c+z} \tag{41}$$

Relating stress and strain in a biaxial stress state gives

$$\sigma_\theta = \frac{E}{1-\nu^2}\left\{\varepsilon_{c_\theta} + \frac{z(\omega-\varepsilon_c)_\theta}{R_c+z} + \nu\left[\varepsilon_{c_\phi} + \frac{z(\omega-\varepsilon_c)_\phi}{R_c+z}\right]\right\} \tag{42}$$

$$\sigma_\phi = \frac{E}{1-\nu^2}\left\{\varepsilon_{c_\phi} + \frac{z(\omega-\varepsilon_c)_\phi}{R_c+z} + \nu\left[\varepsilon_{c_\theta} + \frac{z(\omega-\varepsilon_c)\theta}{R_c+z}\right]\right\} \tag{43}$$

Substituting equations (42) and (43) into equations (31) and (32) gives the following

$$\int_{\text{Area}} \frac{E}{1-\nu^2}\left\{\varepsilon_{c_\theta} + \frac{z(\omega-\varepsilon_c)_\theta}{R_c+z} + \nu\left[\varepsilon_{c_\phi} + \frac{z(\omega-\varepsilon_c)_\phi}{R_c+z}\right]\right\} dA = 0 \tag{44}$$

$$M_\theta = \int_{\text{Area}} \frac{E}{1-\nu^2}\left\{\varepsilon_{c_\theta} + \frac{z(\omega-\varepsilon_c)_\theta}{R_c+z} + \nu\left[\varepsilon_{c_\phi} + \frac{z(\omega-\varepsilon_c)_\phi}{R_c+z}\right]\right\} z\,dA \tag{45}$$

and

$$\int_{\text{Area}} \frac{E}{1-\nu^2}\left\{\varepsilon_{c_\phi} + \frac{z(\omega-\varepsilon_c)_\phi}{R_c+z} + \nu\left[\varepsilon_{c_\theta} + \frac{z(\omega-\varepsilon_c)_\theta}{R_c+z}\right]\right\} dA = 0 \tag{46}$$

$$M_\phi = \int_{\text{Area}} \frac{E}{1-\nu^2}\left\{\varepsilon_{c_\phi} + \frac{z(\omega-\varepsilon_c)_\phi}{R_c+z} + \nu\left[\varepsilon_{c_\theta} + \frac{z(\omega-\varepsilon_c)_\theta}{R_c+z}\right]\right\} z\,dA \tag{47}$$

The above four equations ((44) through (47)) can be solved for ε_{c_ϕ}, ε_{c_θ}, $(\omega-\varepsilon_c)_\phi$ and $(\omega-\varepsilon_c)_\theta$. These are then substituted back in to equations (42) and (43) which upon

simplifying yield

$$\sigma_\theta(z) = - \frac{M_\theta[(R_c + z)Z + z]}{(R_c + z)\, Z\, R_c\, t} \tag{48}$$

and

$$\sigma_\phi(z) = - \frac{M_\phi[(R_c + z)\, Z + z]}{(R_c + z)\, Z\, R_c\, t} \tag{49}$$

where

M_ϕ and M_θ = Moment in in.-lbs./unit width.

Z = Area factor due to curvature.

$$Z = - \frac{1}{A} \int_{\text{area}} \frac{z_c}{R_c + z_c}\, dA \ .$$

$$Z = \frac{t^2}{12\, R_s^2} \text{ for element of spherical shell}$$

(See Appendix 3.).

R_s = Radius to middle surface.

z_c = Distance measured outward from centroidal surface.

In equations (48) and (49), due to our sign convention, a positive moment at a positive distance z gives a compression stress, so the minus signs are added to correspond to the usual sign convention on stresses.

Rewriting equations (48) and (49) using the expressions in Appendix 3 for R_c and Z gives

$$\sigma_\theta(z) = - M_\theta \frac{12\, R_s}{t^3} \left[\frac{12\, R_s^2 t^2 + t^4 + (12\, R_s t^2 + 144\, R_s^3)z}{144 R_s^4 + 24 R_s^2 t^2 + t^4 + (12 R_s t^2 + 144 R_s^3)z} \right] \tag{50}$$

$$\sigma_{\phi}(z) = - M_{\phi} \frac{12R_s}{t^3}\left[\frac{12R_s^2t^2 + t^4 + (12R_st^2 + 144R_s^3)z}{144R_s^4 + 24R_s^2t^2 + t^4 + (12R_st^2 + 144R_s^3)z}\right] \tag{51}$$

An interesting point is to find the location of the neutral surface for pure bending. Taking the numerator of equation (50) or (51) and setting it equal to zero gives

$$z = - \frac{t^2}{12R_s} \tag{52}$$

It was found in Appendix 3 that this is the distance between the centroid and middle surfaces. So the neutral surface coincides with the middle surface for pure bending.

The maximum stress on the cross-section for pure bending will occur at the inner radius. With an accompanying axial load the maximum stress will occur at the inner or outer radius depending on the directions of the moment and axial load. Using the fact that

$$z_{outer} = \frac{t}{2} - \frac{t^2}{12R_s} \tag{53}$$

$$z_{inner} = - \left(\frac{t}{2} + \frac{t^2}{12R_s}\right) \tag{54}$$

and substituting these equations in equations (50) and (51) yields

$$\sigma_{\theta}(z_{outer}) = - M_{\theta} \frac{12R_s}{R_ot^2}\left[\frac{R_ot - 6R_s^2 - R_st}{12R_s^2 + t^2}\right] \tag{55}$$

$$\sigma_\theta(z_{inner}) = - M_\theta \frac{12R_S}{R_i t^2} \left[\frac{R_i t - 6R_s^2 - R_s t}{12R_s^2 + t^2} \right] \qquad (56)$$

A corresponding pair of equations will occur for $\sigma_\phi(z_{outer})$ and $\sigma_\phi(z_{inner})$ with M_ϕ substituted for M_θ.

A check on the entire process is to see what happens to equations (50) and (51) as R_s approaches infinity. When this is done

$$\sigma_\theta(z) = - M_\theta \frac{12}{t^3} z \quad . \qquad (57)$$

For a beam of unit width

$$I = \frac{t^3}{12}$$

so equation (57) simplifies to

$$\sigma_\theta(z) = - \frac{M_\theta z}{I} \qquad (58)$$

which is the expected answer for a beam with an infinite radius of curvature, i.e., a straight beam.

Equations (50), (51), (55) and (56) give the stresses when an element is loaded only in bending. A rather standard assumption to make concerning the axial load is to consider the axial stress uniform over the cross-section. Fluegge[1] does this for thin shells and Seely and Smith[6] do it for curved beams. Hence

$$\sigma_\theta = \frac{N_\theta}{t} \qquad (59)$$

and

$$\sigma_\phi = \frac{N_\phi}{t} \qquad (60)$$

where

N_θ = Circumferential axial load in pounds/unit width.

N_ϕ = Meridional axial load in pounds/unit width.

Therefore combining the stress equations for axial load and moment in the θ and ϕ directions will give the total normal stress at any z distance from the centroid surface for a given axial load and moment.

IV. RESULTS

A very brief review is perhaps in order. Remember that the original problem was to obtain the stress distribution in a thick spherical shell, where the shell specifically under consideration was a dome in a chemical furnace. Usually these domes are made of mortar and firebrick. So while trying to obtain the stress distribution for any thick shell it was also a goal to obtain the geometrical dimensions for the dome in the furnace such that tension stresses would not occur. Significant tension stresses could cause cracks to occur which would seriously limit the ability of the shell to carry any transverse shear. However, it is felt that the shell would probably not collapse even though some tension stresses did occur.

The computer program, shown in Appendix 2, evaluates the required equations of section III of this thesis.

From the practical design standpoint there is a limit to the height of the dome section. It is required that the dome be kept reasonably shallow for the best operating characteristics of the furnace. This helps out the desired goal of no significant tension stresses, because as the height is decreased the bending due to the applied loads will also decrease.

Hence with the cylindrical diameter of the furnace given (See Figure 1.) and for various heights of the dome it is possible to obtain the corresponding spherical radius.

For various spherical radii and thicknesses the stress distributions across the cross-section were found.

Shown in Figures 6 through 14 are the stress distributions across the thickness for a bending moment of 10,000 in.-lbs. It should be noted that some of the figures are for the same R_s/t ratio and the stress distribution is different. Referring back to equation (50), multiply and divide by $1/t^4$ which gives

$$\sigma_\theta(z) = - M_\theta \frac{12}{t^2}\left(\frac{R_s}{t}\right)\left\{\frac{12\left(\frac{R_s}{t}\right)^2 + 1 + \left[\frac{12}{t}\left(\frac{R_s}{t}\right) + \frac{144}{t}\left(\frac{R_s}{t}\right)^3\right]z}{\left(\frac{R_s}{t}\right)^4 + 24\left(\frac{R_s}{t}\right)^2 + 1 + \left[\frac{12}{t}\left(\frac{R_s}{t}\right) + \frac{144}{t}\left(\frac{R_s}{t}\right)^3\right]z}\right\} \quad (61)$$

The same procedure could be applied to equation (51) and $\sigma_\phi(z)$ would be obtained. It can be seen in equation (61) that all terms contain R_s/t or t. Hence $\sigma(z)$ is a function of t and R_s/t, so even with the same R_s/t ratio the stress distribution will be different. Also in Figures 6 through 14 the stress distribution assuming Mc/I (straight beam theory) for a section of unit width is shown.

For other values of (R_s/t) the stress distribution isn't shown. However, Figure 15 shows the maximum error that occurs using the conventional $\frac{Mc}{I}$ in a thick shell rather than the stress equations developed in this thesis. It was found that the error in using $\frac{Mc}{I}$ was dependent on the R_s/t ratio and only slightly affected by the thickness. Comparing equations (58) and (61) and realizing that I/z is a function of t^2, similar to the first constant in

equation (61), it can be seen that in calculating the error the first t^2 terms would cancel. In the last part of equation (61) there are some 1/t terms in the numerator and the denominator. They only cause a very small change in $\sigma(z)$ for any given R_s/t value. Hence it was felt that once the error was determined it wasn't necessary to show the complete bending stress distribution for any other cases. Usually we are interested in the maximum stress, which occurs at the inside radius for bending of a spherical shell, rather than a smaller value at some interior point.

Now after a rather thorough discussion of the stresses due to bending the next step is to calculate the loads and stresses that exist for an actual loading condition.

Shells investigated included those with a rise of 2.0, 3.0, 4.0, 5.0 and 10.0 feet and a R_s/t ratio of 2.5, 5.0, 10.0 and 20.0. In each case the computer program shown in Appendix 2 was used to calculate the loads N_ϕ, N_θ, Q_ϕ, M_ϕ and M_θ at two degree intervals from the free edge to top ($\phi = 0$). Then the stresses σ_θ and σ_ϕ were calculated at the inner and outer radii at each cross-section where the loads were calculated. The program also will determine the stress-distribution across the thickness due to a bending moment of 10,000 in.-lbs.

Figures 16 through 47 present the results of the study for a rise of 3.0', for each of the loading conditions and for each of the R_s/t ratios. The figures should be considered in pairs, the first presents the

loads vs. ϕ and the second presents the stresses vs. ϕ. Figures 16 through 23 are for Case A (page 1), the next eight figures for Case B, Figures 32 through 39 for Case C, and the last eight figures for Case D.

The figures show that for a given loading condition and method of support the loads (N_θ, N_ϕ, M_θ and M_ϕ) get smaller as the shell gets thinner (R_s/t increases). This is an expected result. The thicker the shell the greater the horizontal load H to overcome the thermal expansion. Also as the loads decrease the accompanying figures of stress vs. ϕ show that the magnitude of the maximum stresses decreases even though the shell is becoming thinner.

When the edge of the shell is fixed rather than just simply supported the maximum value of the loads (N_θ, N_ϕ, M_θ and M_ϕ) increase in magnitude for the same vertical load (p) and R_s/t ratio. In the fixed cases the maximum loads (N_θ, N_ϕ, M_θ and M_ϕ) occur at the edge while in the simply supported case the maximum moment (M_θ and M_ϕ) is at the top $\phi = 0$. Generally the fixed edge reduced the maximum value of the tension stresses, it reduced the area of shell in tension, and it reduced the amount of the shell thickness in tension at any value of ϕ. An exception to this is in the immediate area of the fixed edge where the tension bending stress due to M_ϕ always overcomes the compression stress due to $N\phi$.

The last comparison is made between the cases when the vertical load is zero and when it has a value. The

vertical load of 173.6 lb./in.^{2} has only a very slight effect (less than five per cent) on the values of the loads and stresses. It does increase the maximum value of the loads (N_θ, N_ϕ, M_θ and M_ϕ) and stresses, which is the expected change for an added load of this type, but not significantly. The vertical load slightly increased the magnitude of the compression stresses and slightly decreased the tension stresses.

Figures 16 through 47 show the data only for a rise of 3.0 feet. The loads and stresses were also obtained for rises of 2.0, 4.0, 5.0 and 10.0 feet. It doesn't appear to be of any value to show these results as the same statements made on the last few pages also apply to these other cases. The reason that a rise of three feet was chosen is that it had the lowest tension stresses of all the values of rise considered.

One special item should be mentioned concerning the values of the loads as ϕ approaches zero. Working with equations (17), (20) and (21) it turns out that for $\underline{P}$ equal zero (no vertical load) as ϕ approaches zero N_ϕ equals N_θ. When there is a vertical load on the shell N_ϕ doesn't become equal to N_θ as ϕ approaches zero. Re-writing equations (20) and (21) in a slightly different form

$$N_\phi = - (C_1 z'_1 + C_2 z'_2) \cos\phi - \frac{p R_s}{2} \qquad (20a)$$

$$N_\theta = - (C_1 z'_1 + C_2 z'_2) \cos\phi - (C_1 \frac{dz'_1}{d\phi} + C_2 \frac{dz'_2}{d\phi}) \sin\phi + \frac{p R_s}{2} \qquad (20b)$$

Equations (20a) and (20b), as ϕ approaches zero, will differ by the sign on the last term. This will be observed by looking at the appropriate figures.

V. CONCLUSIONS

This thesis has developed a method to determine the stresses in a thick spherical shell due to bending and due to a combination of bending and axial load. The method is based on the analogy of a curved beam and considers that in a shell stresses act in two directions. The method, which is based on a constant temperature across the thickness, must be regarded as an approximation to a more exact solution because of the curved beam analogy that was used.

It was found as shown in Figure 15 that for thin shells the elementary beam formula $\left(\frac{Mc}{I}\right)$ is a good approximation but it does give some error. At R_s/t equal to twenty the error is three per cent. As the shell becomes thicker (R_s/t decreasing) the error increases.

For the load conditions and boundary conditions considered a shell completely free of tension wasn't found. In comparing Figures 33 and 41 it is felt that if partial fixity were considered this configuration would be free of tension.

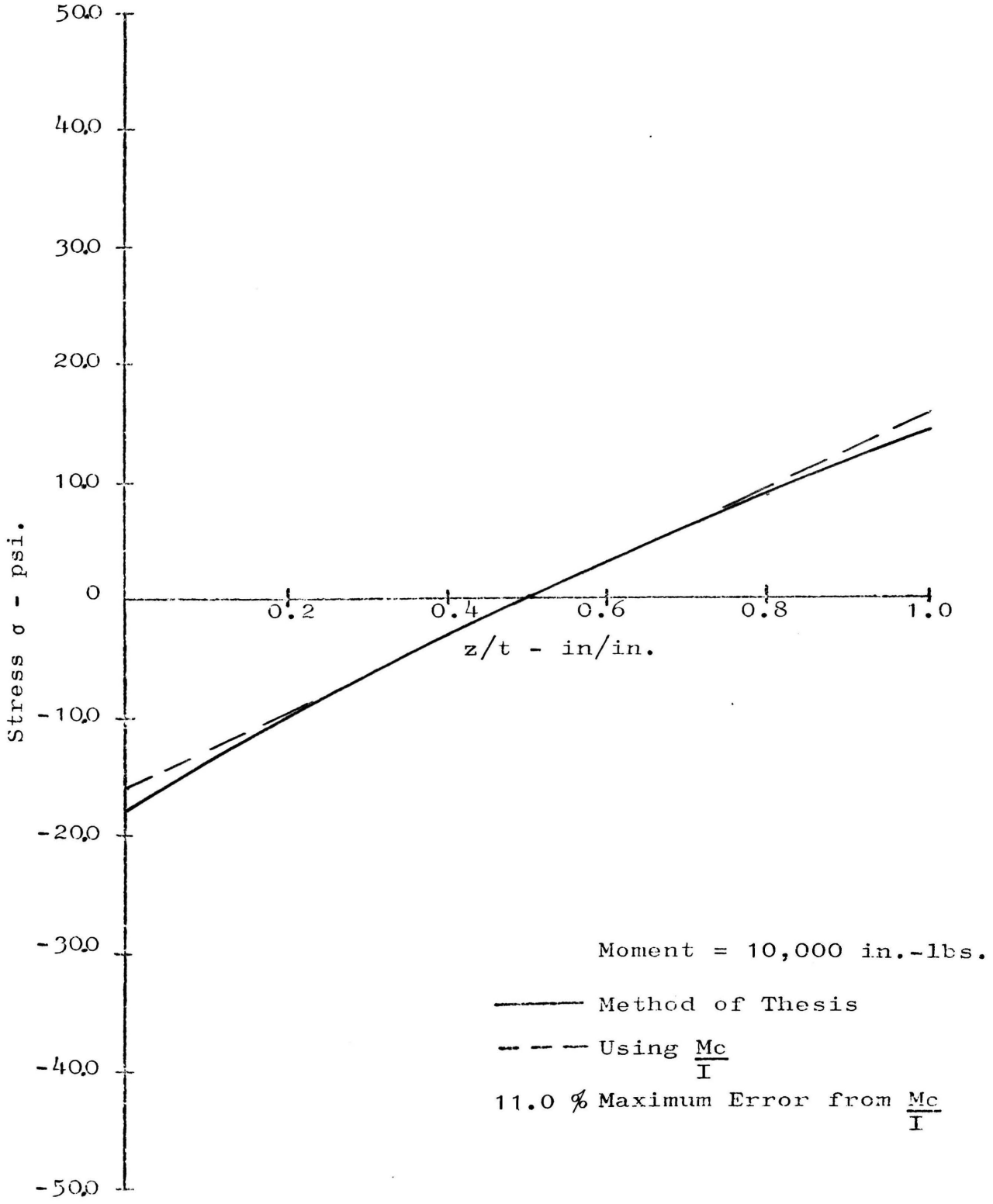

Figure 6. Stress vs. Thickness, Rise = 3.0 ft., R_s/t = 5.0 , Thickness = 61.2 in.

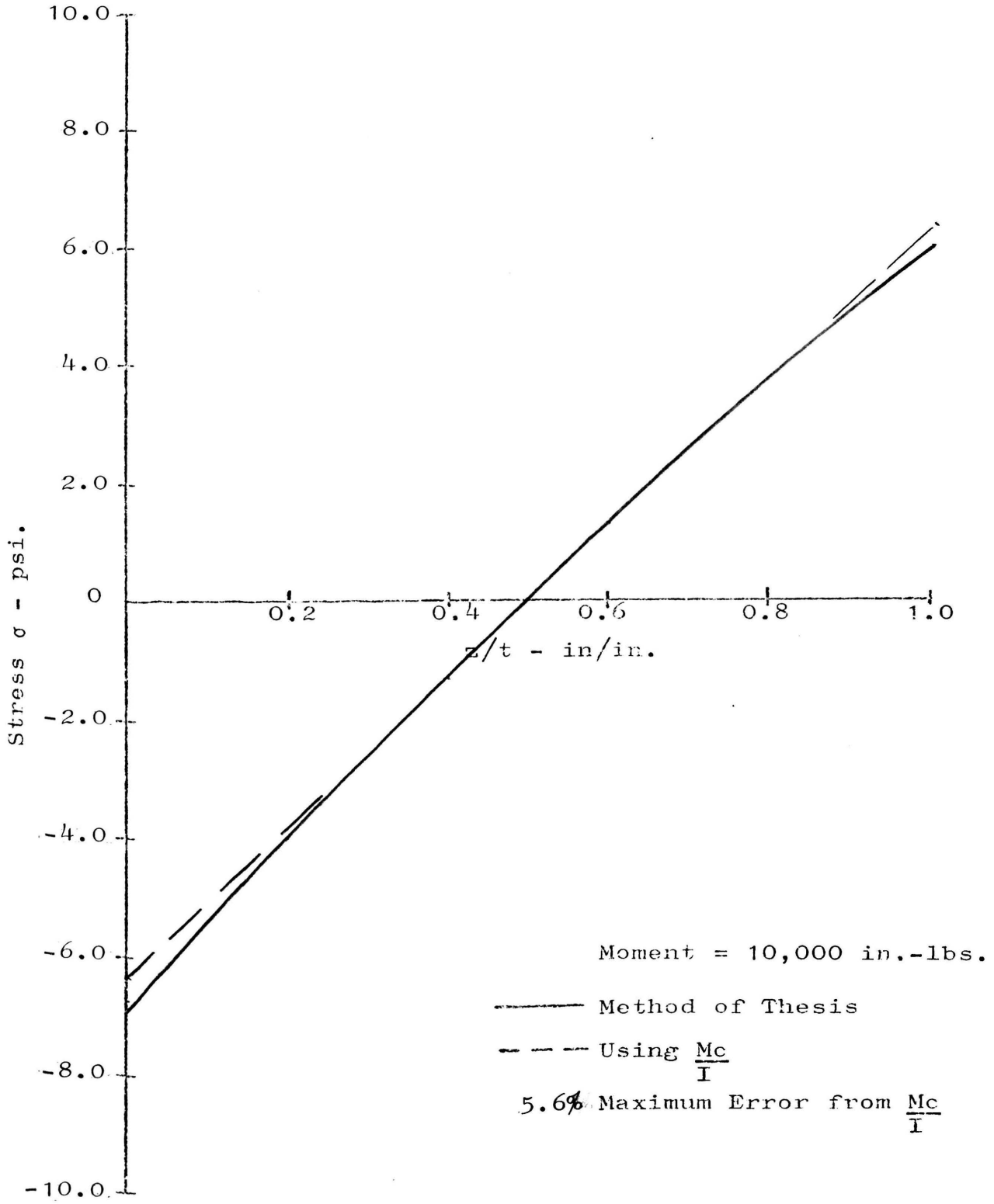

Figure 7. Stress vs. Thickness, Rise = 3.0 ft., R_s/t = 10.0, Thickness = 30.6 in.

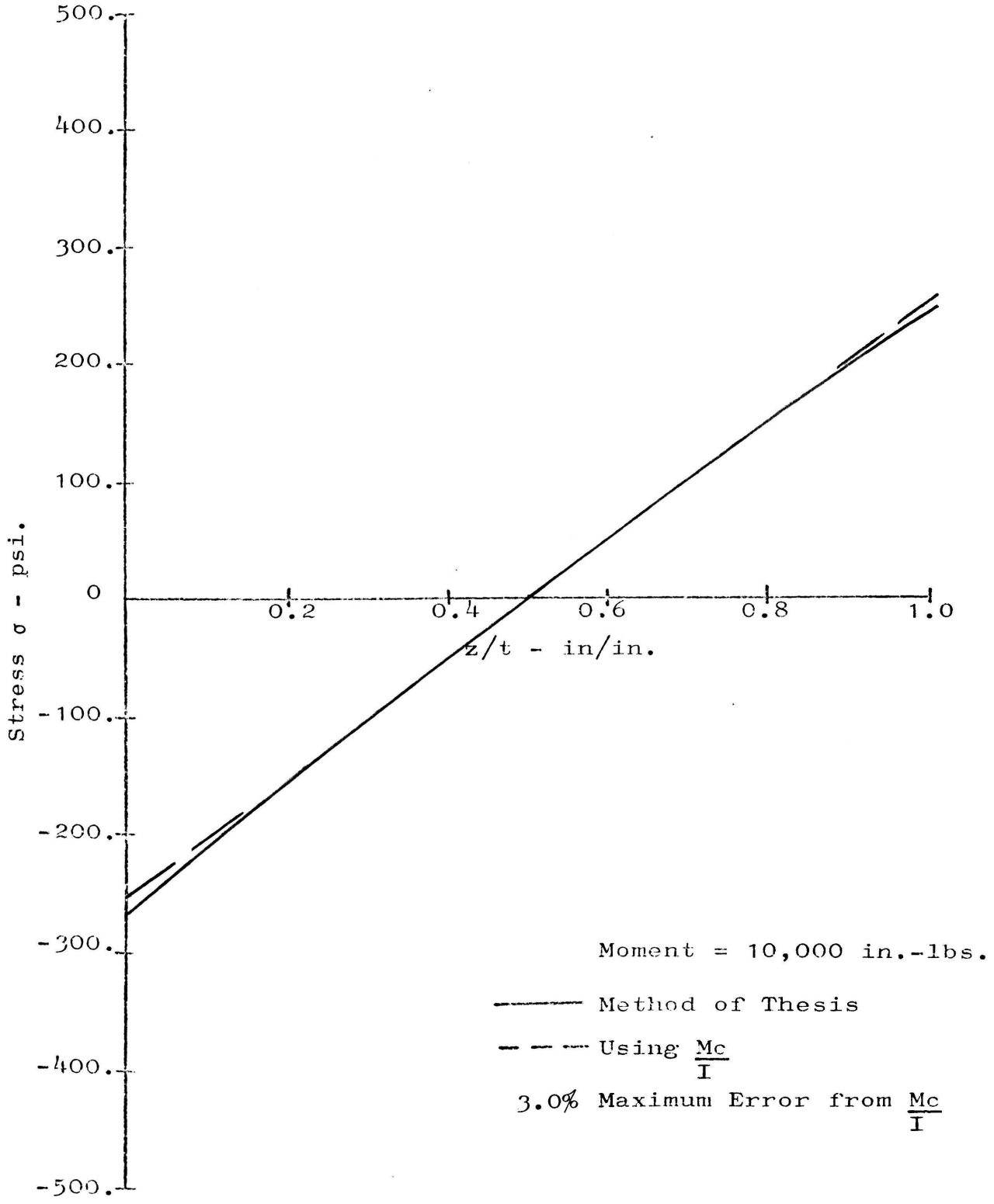

Figure 8. Stress vs. Thickness, Rise = 3.0 ft., R_s/t = 20.0, Thickness = 15.3 in.

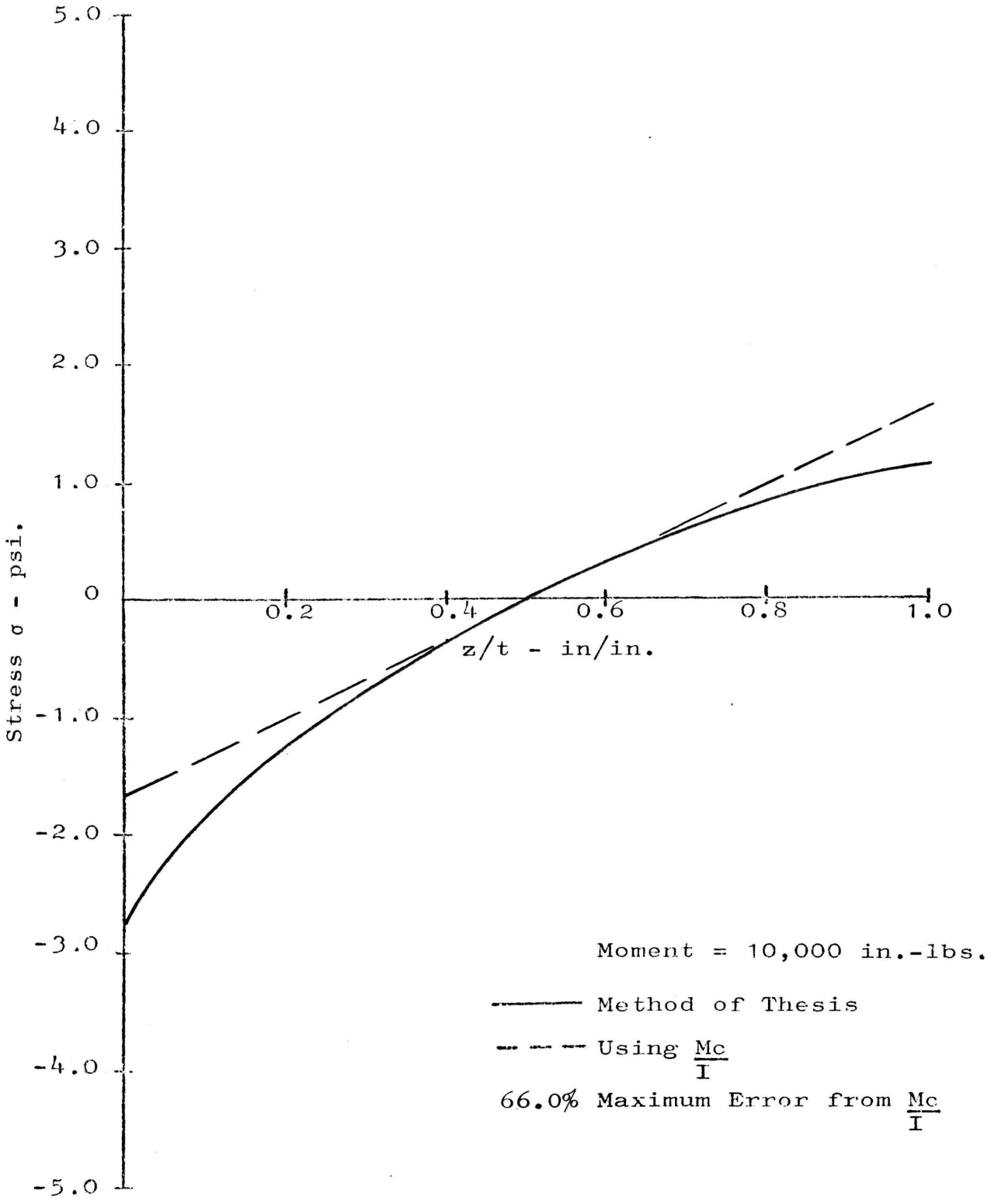

Figure 9. Stress vs. Thickness, Rise = 4.0 ft., R_s/t = 1.25, Thickness = 192.0 in.

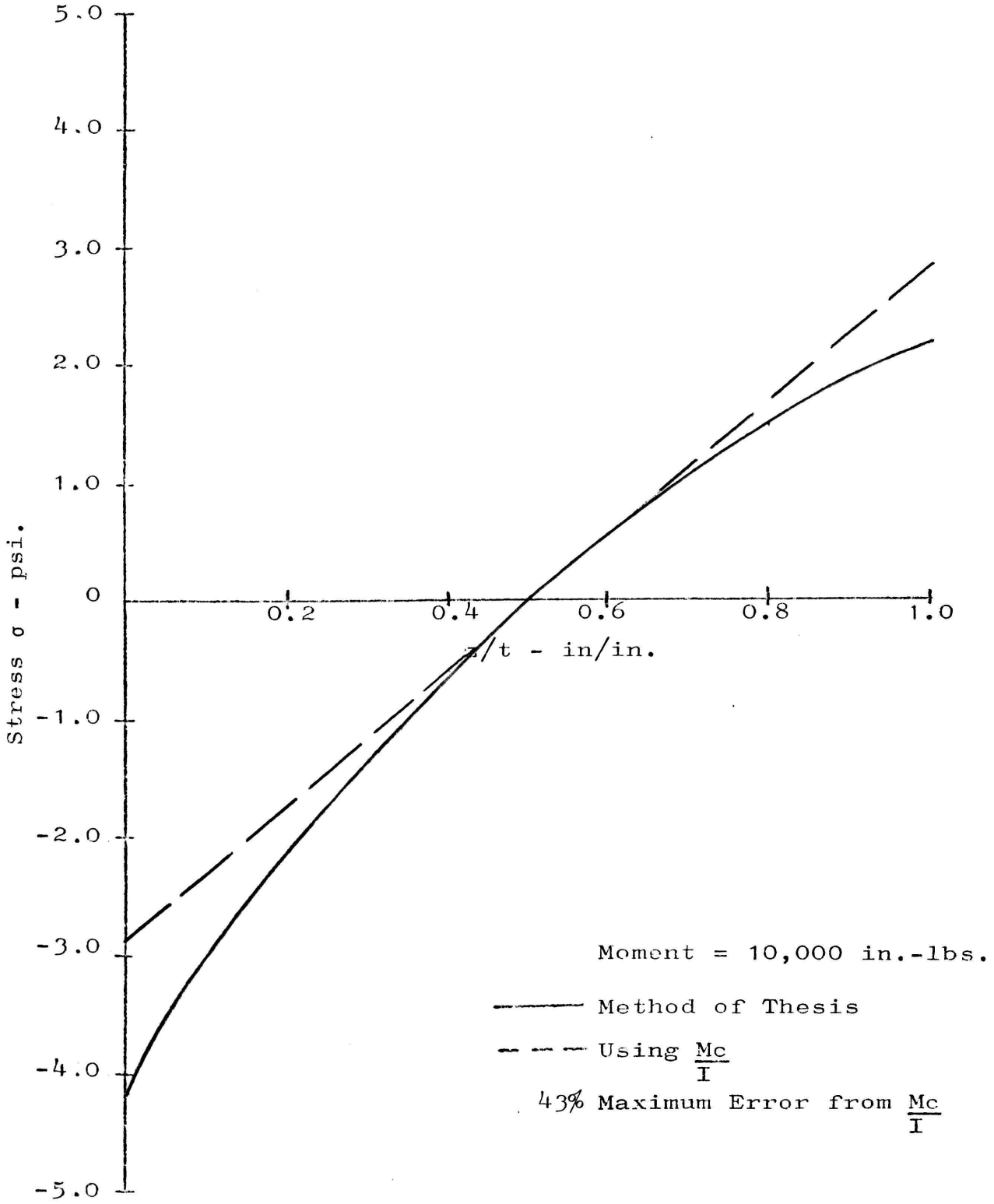

Figure 10. Stress vs. Thickness, Rise = 4.0 ft., R_s/t = 1.67, Thickness = 144.0 in.

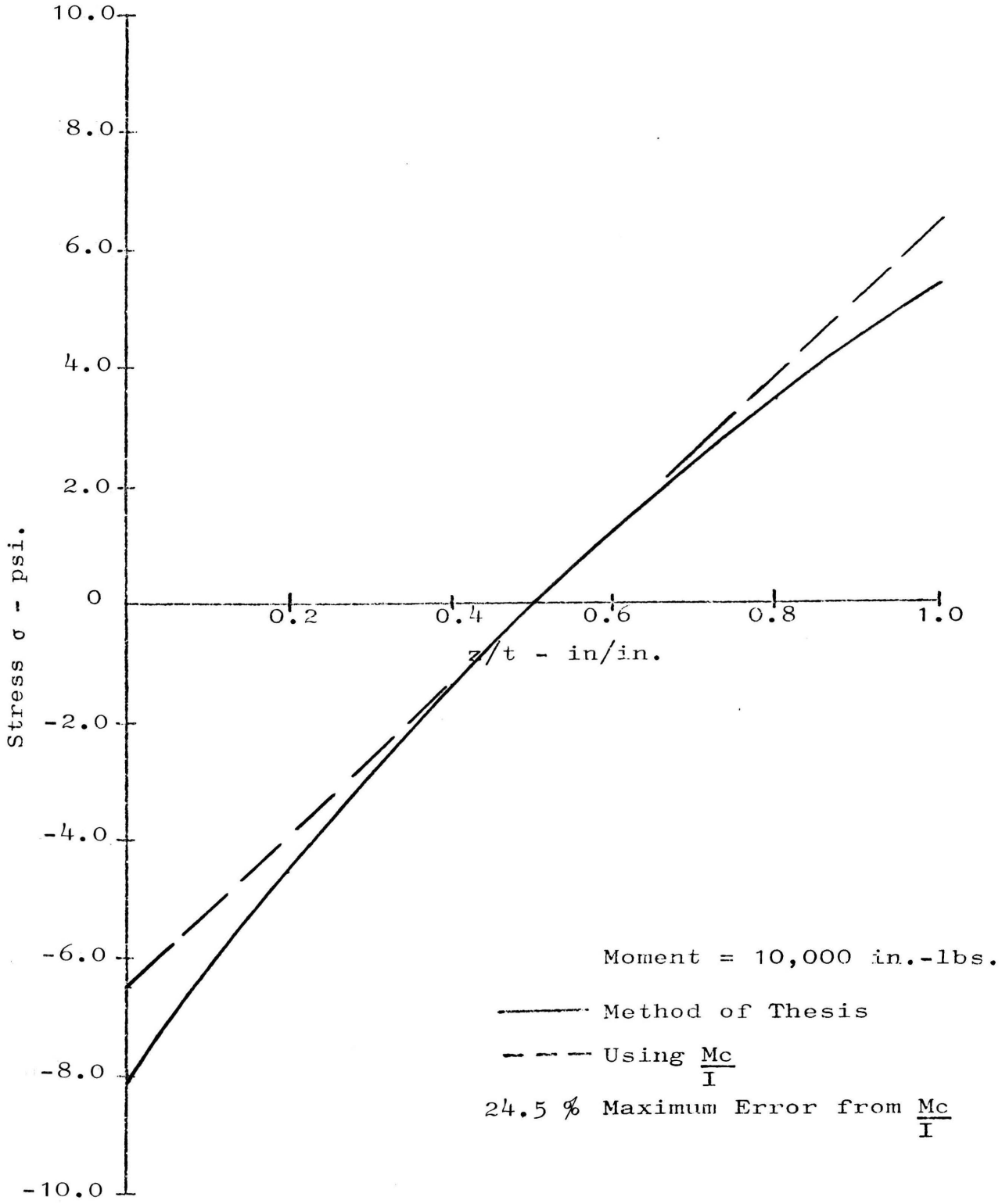

Figure 11. Stress vs. Thickness, Rise = 4.0 ft., R_s/t = 2.5 , Thickness = 96.0 in.

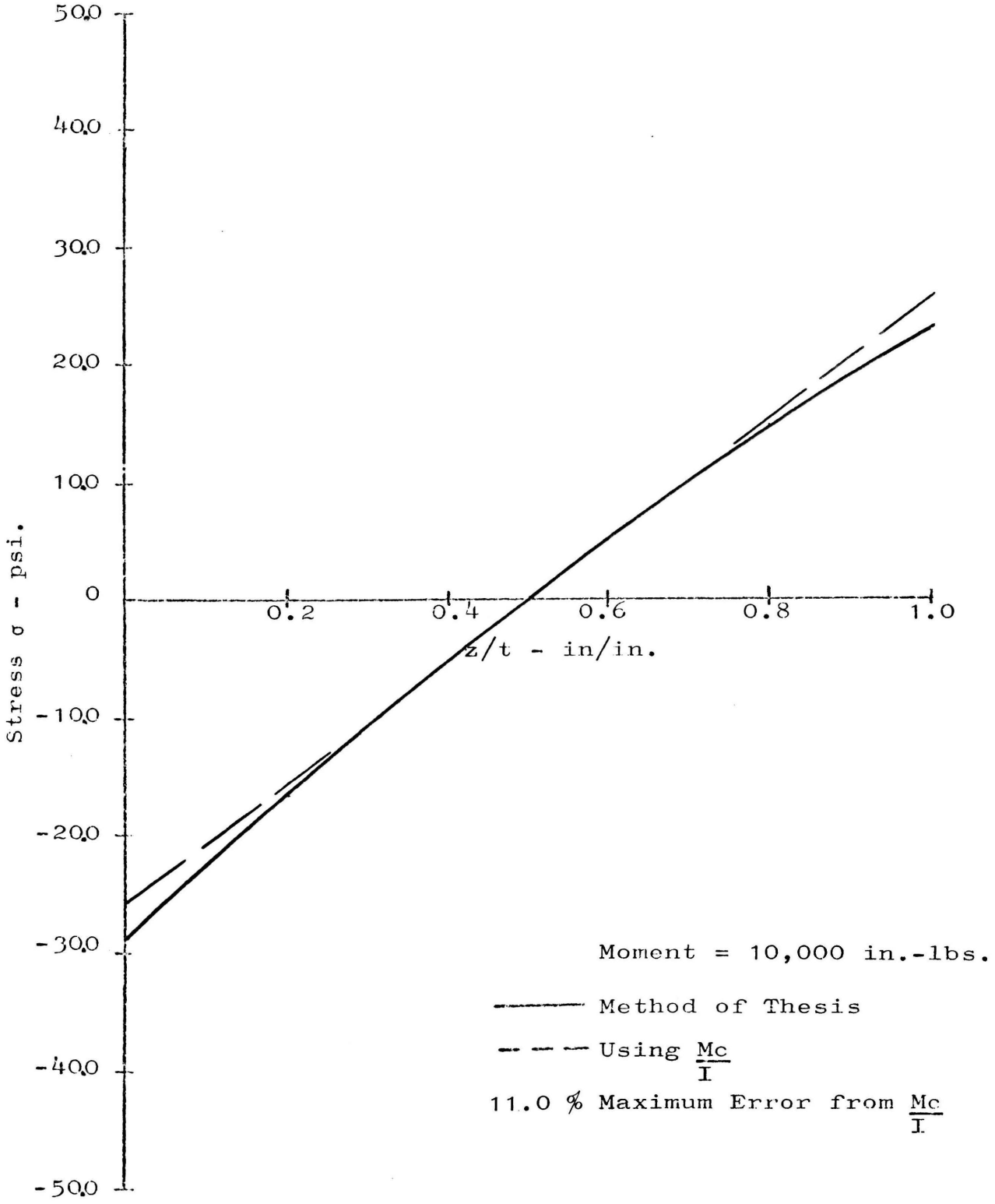

Figure 12. Stress vs. Thickness, Rise = 4.0 ft., R_s/t = 5.0 , Thickness = 48.0 in.

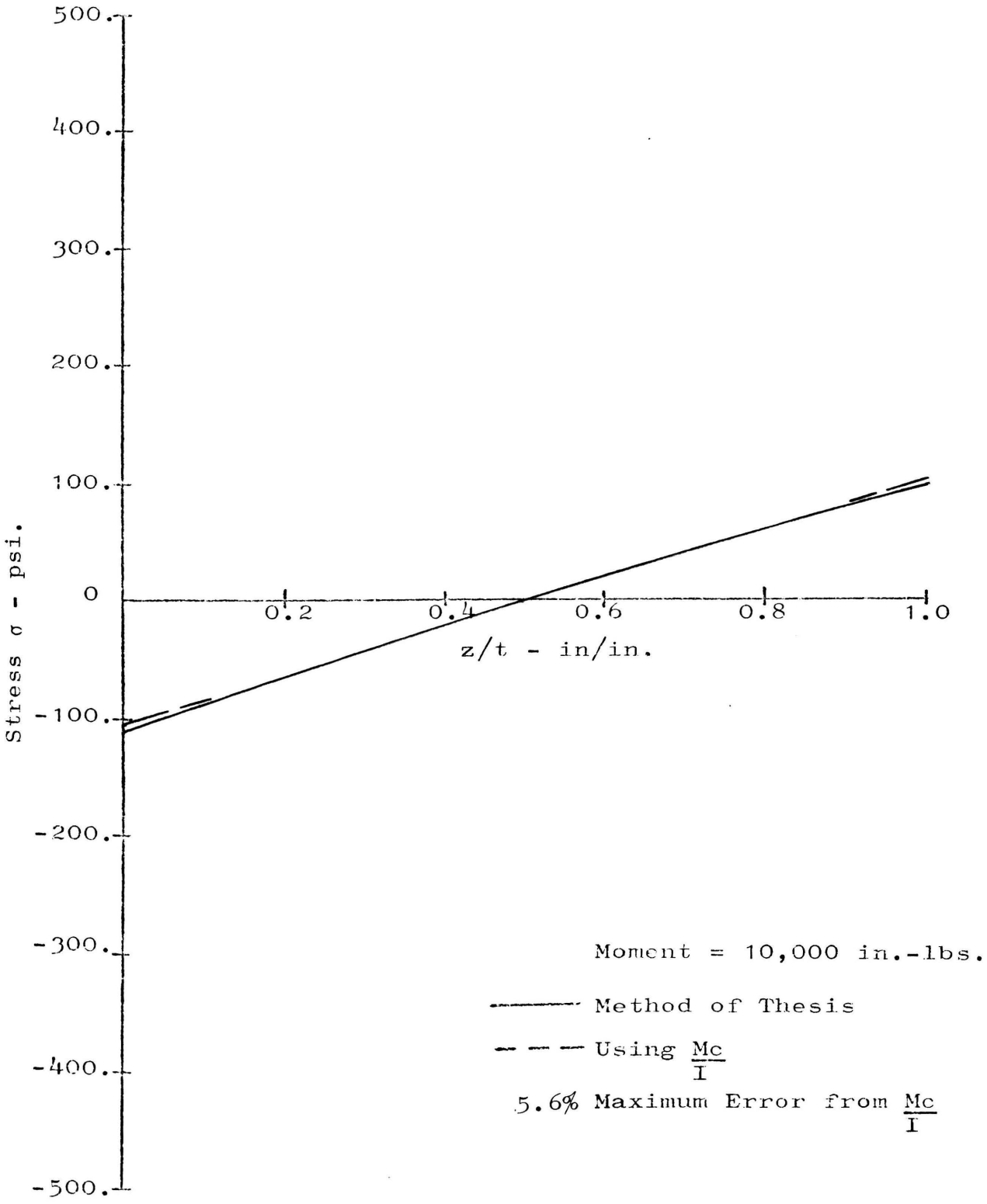

Figure 13. Stress vs. Thickness, Rise = 4.0 ft., R_s/t = 10.0 , Thickness = 24.0 in.

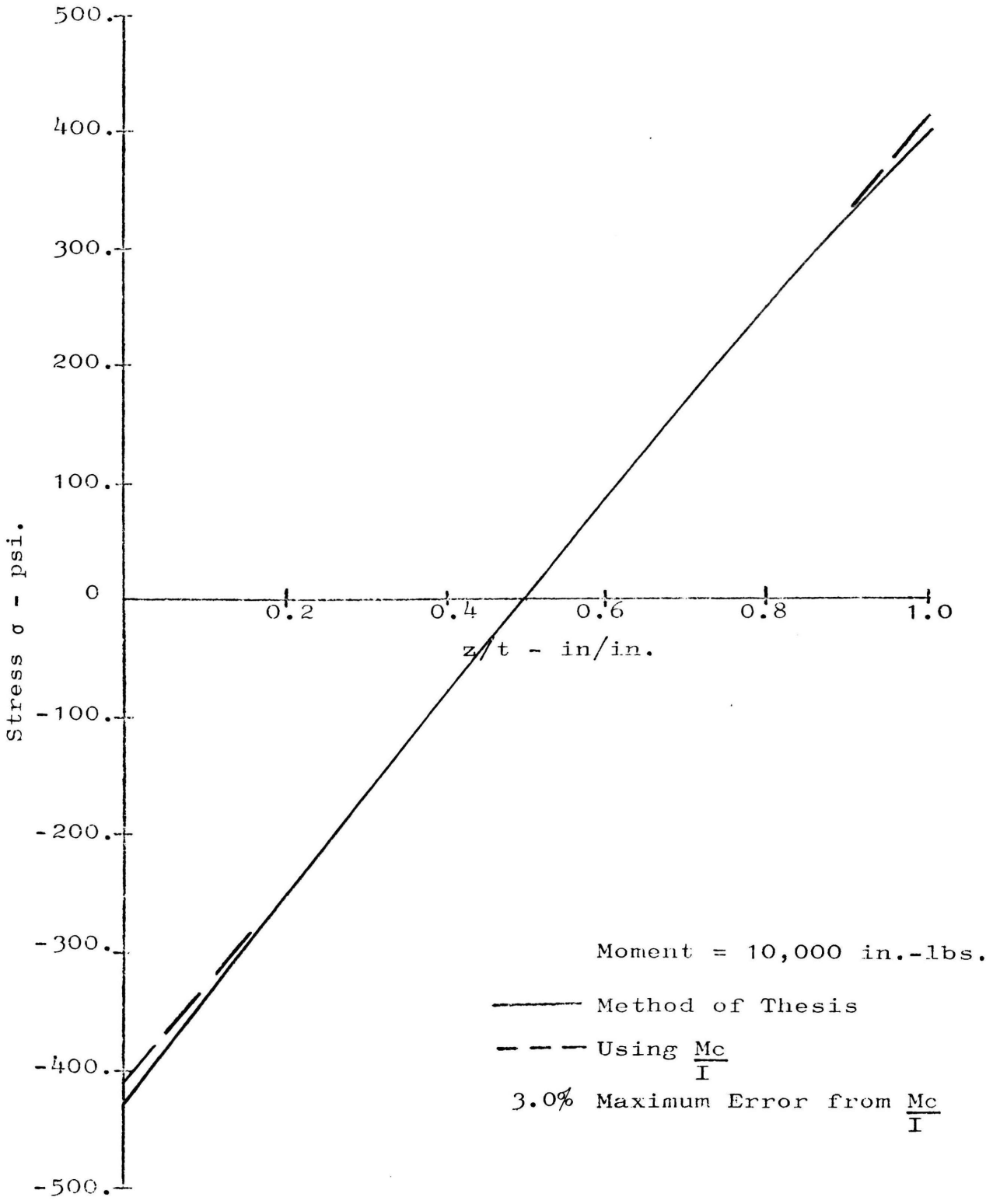

Figure 14. Stress vs. Thickness, Rise = 4.0 ft., R_s/t = 20.0, Thickness = 12.0 in.

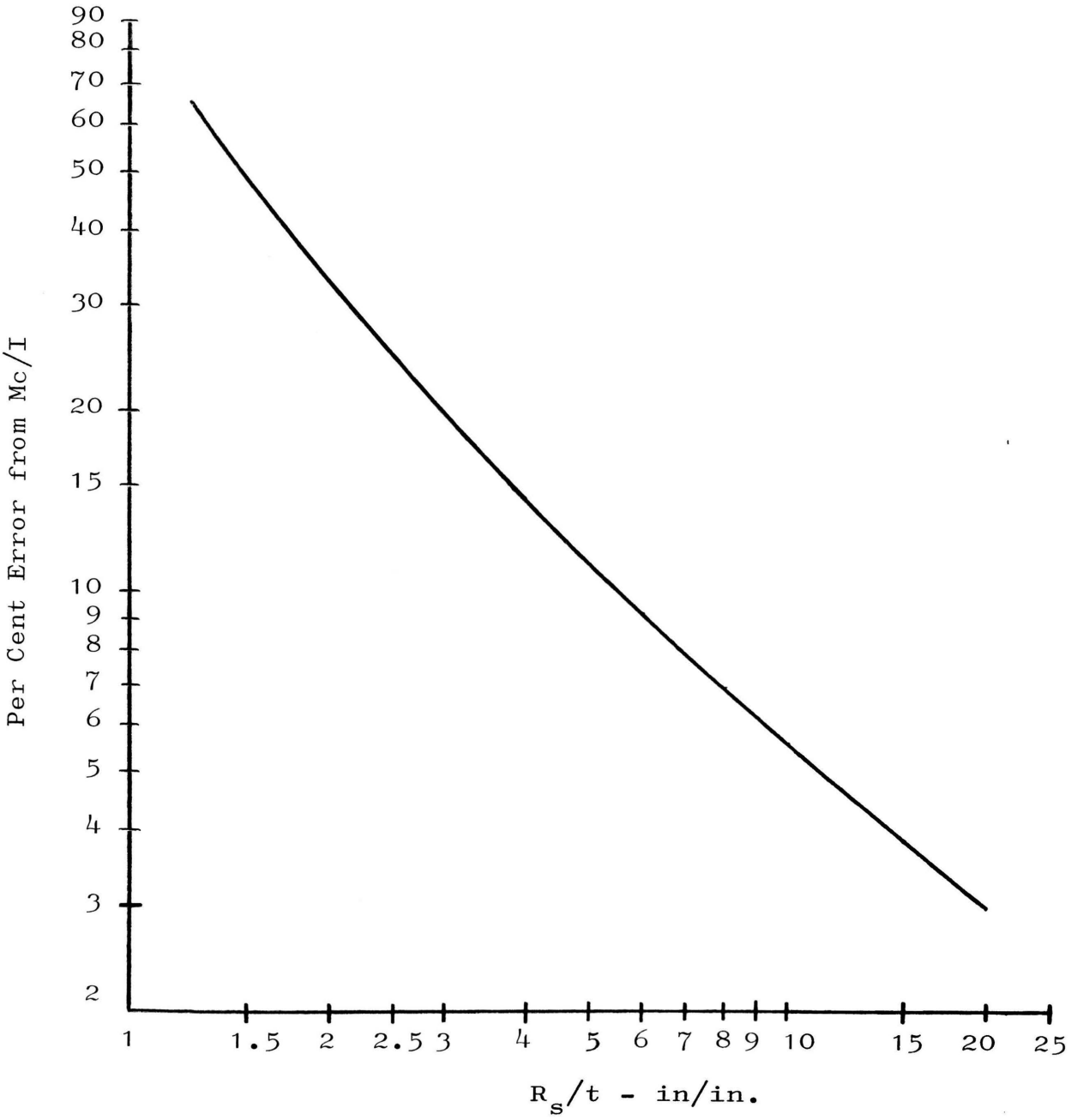

Figure 15. Error Using Elementary Bending Formula $\left(\frac{Mc}{I}\right)$

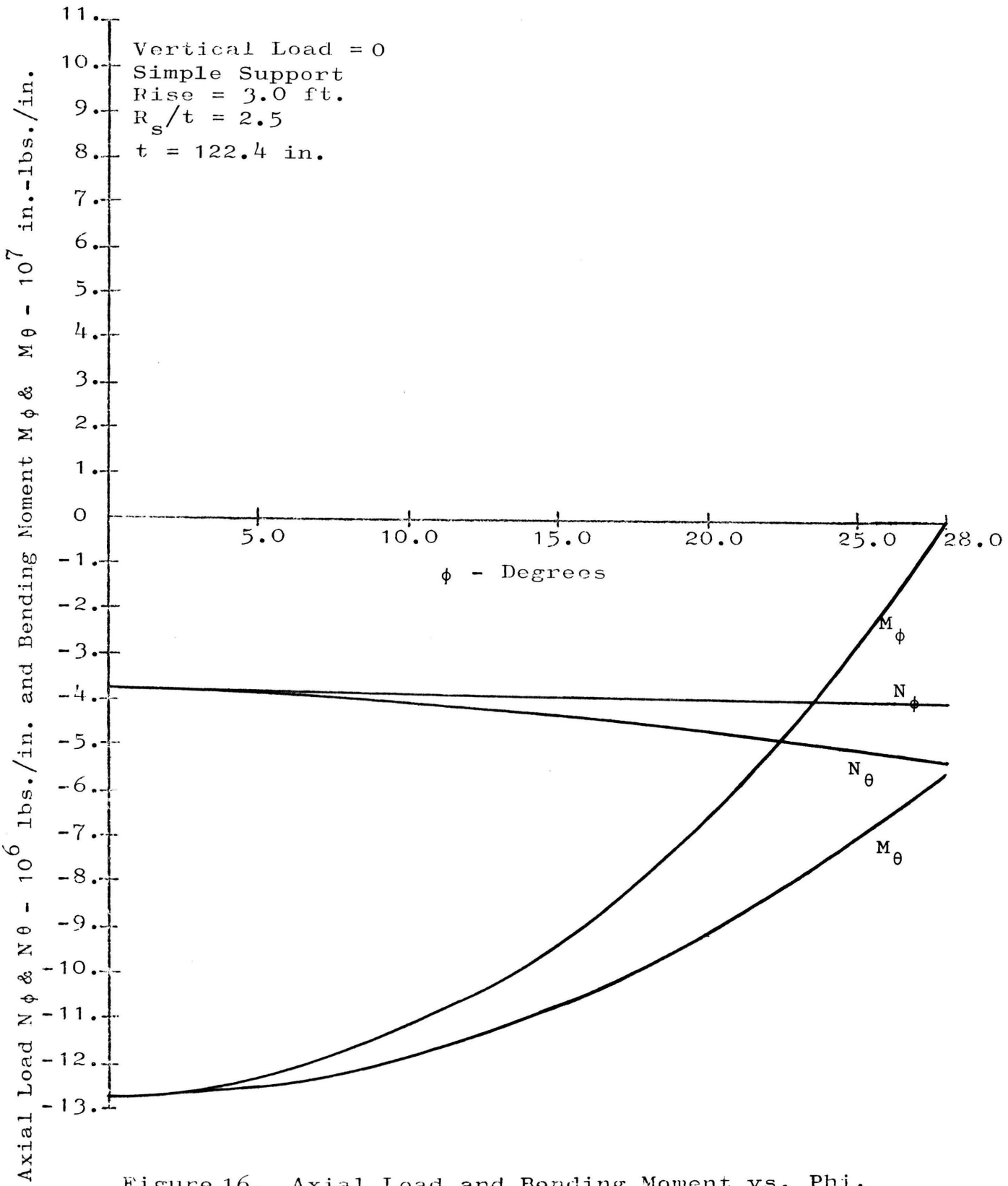

Figure 16. Axial Load and Bending Moment vs. Phi, Case A, R_s/t = 2.5

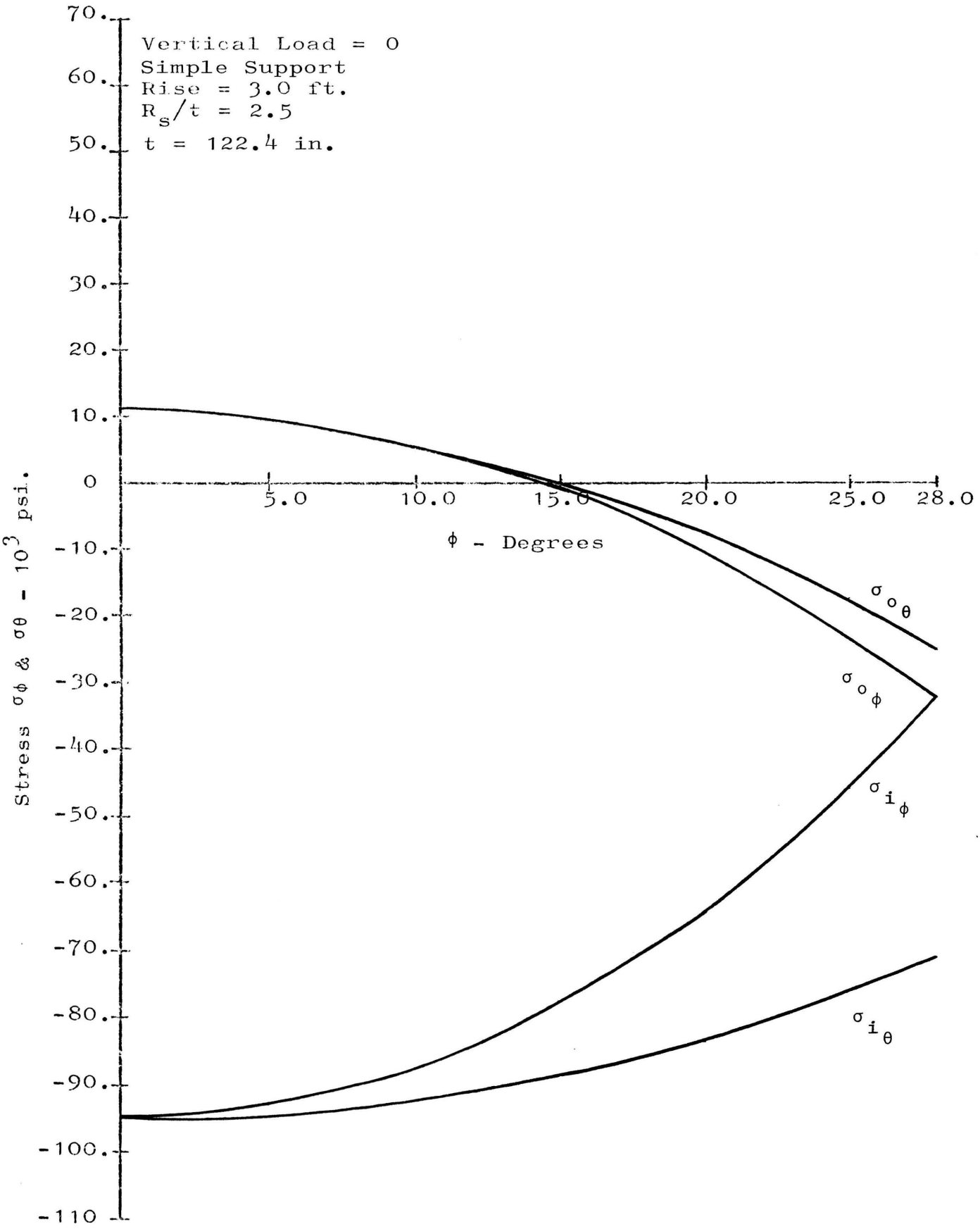

Figure 17. Stress vs. Phi, Case A, R_s/t = 2.5

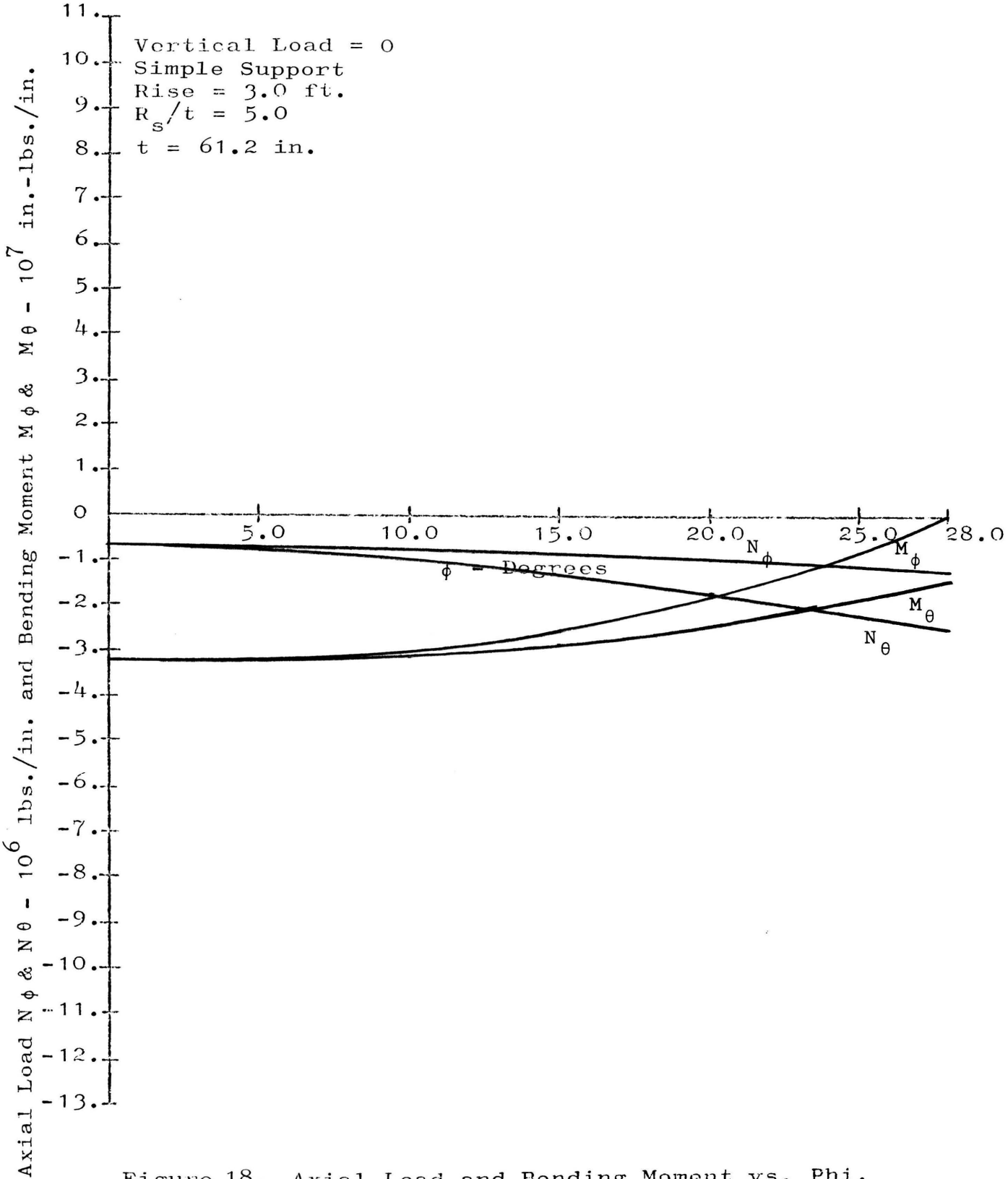

Figure 18. Axial Load and Bending Moment vs. Phi, Case A, R_s/t = 5.0

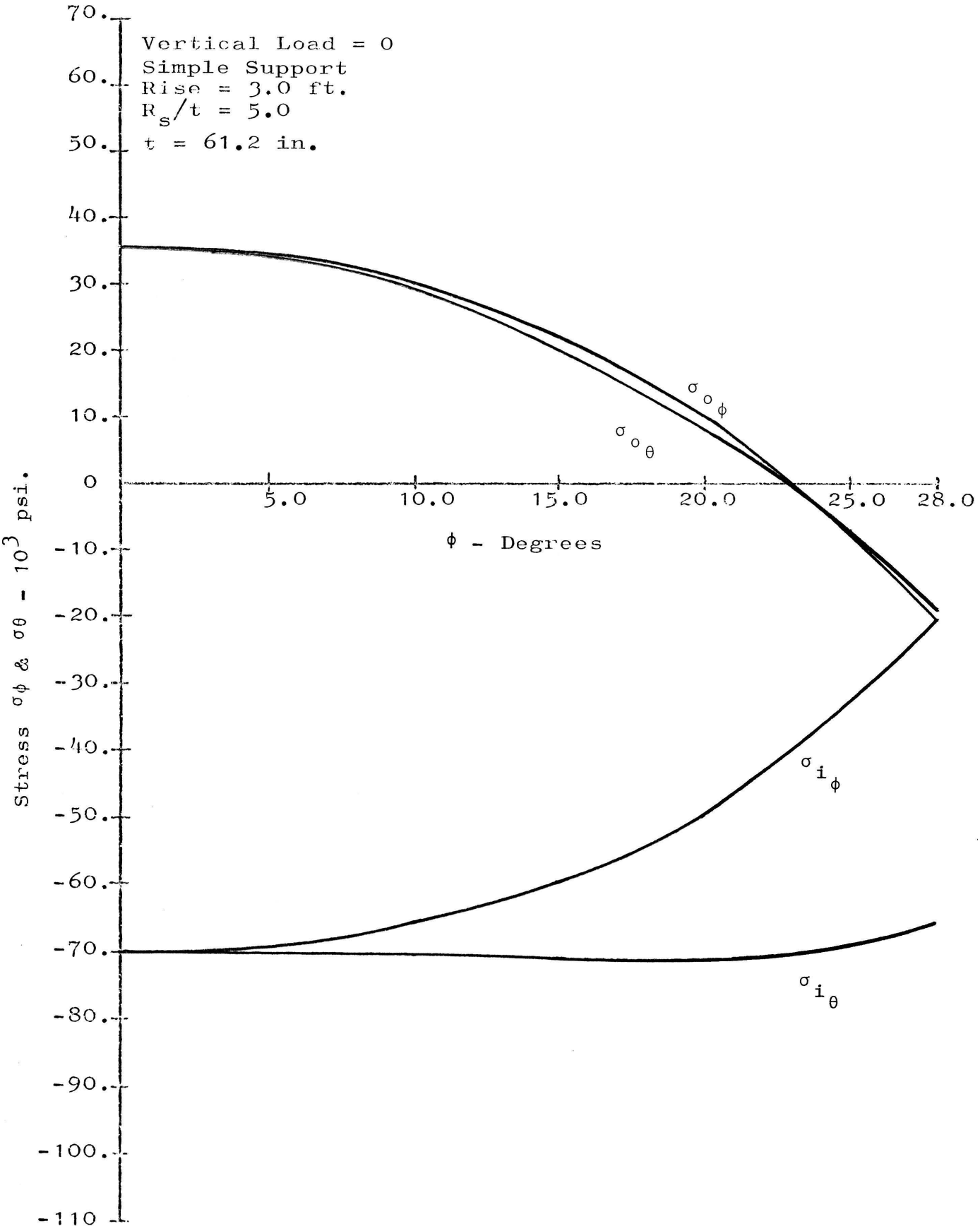

Figure 19. Stress vs. Phi, Case A, R_s/t = 5.0

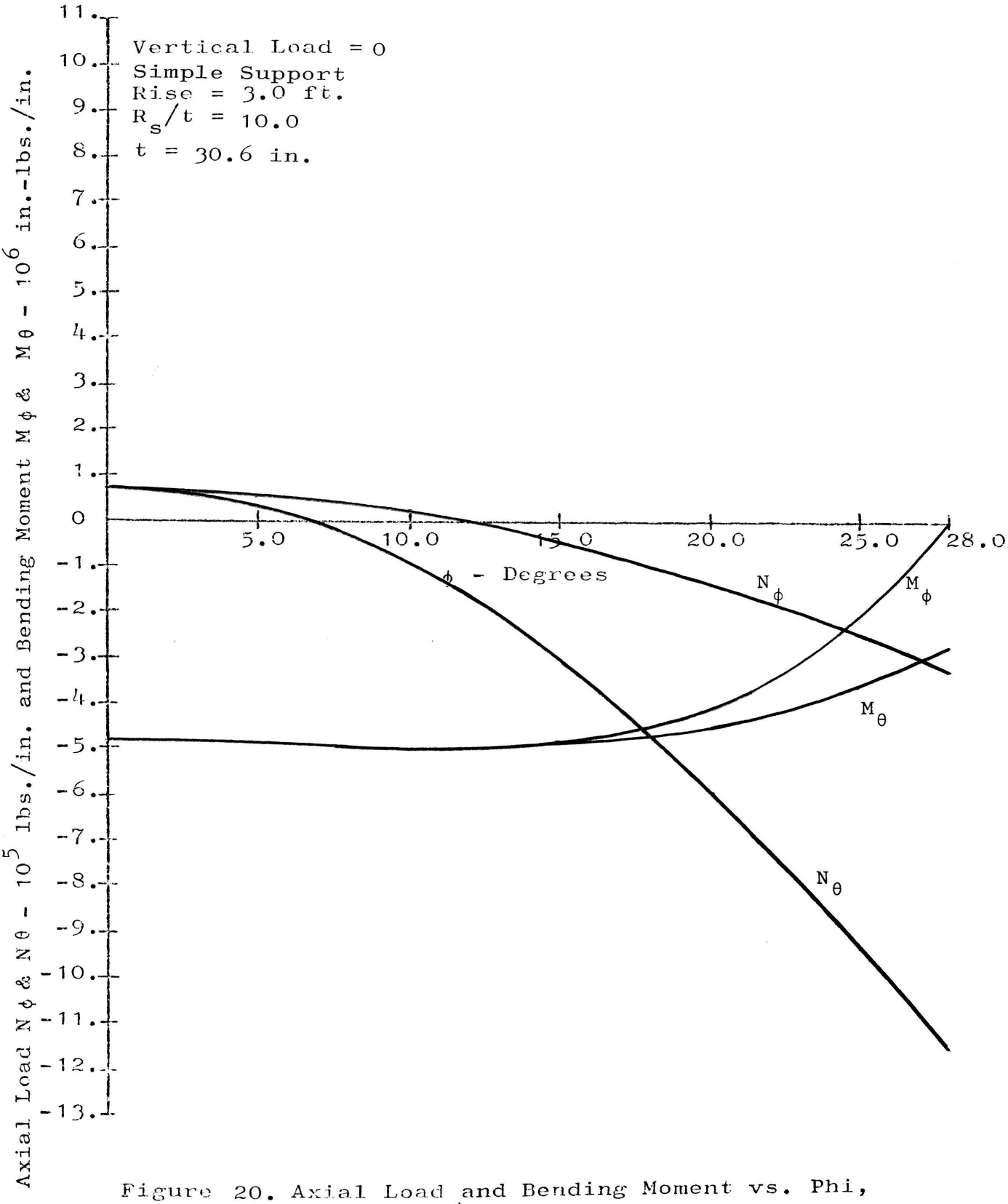

Figure 20. Axial Load and Bending Moment vs. Phi, Case A, R_s/t = 10.0

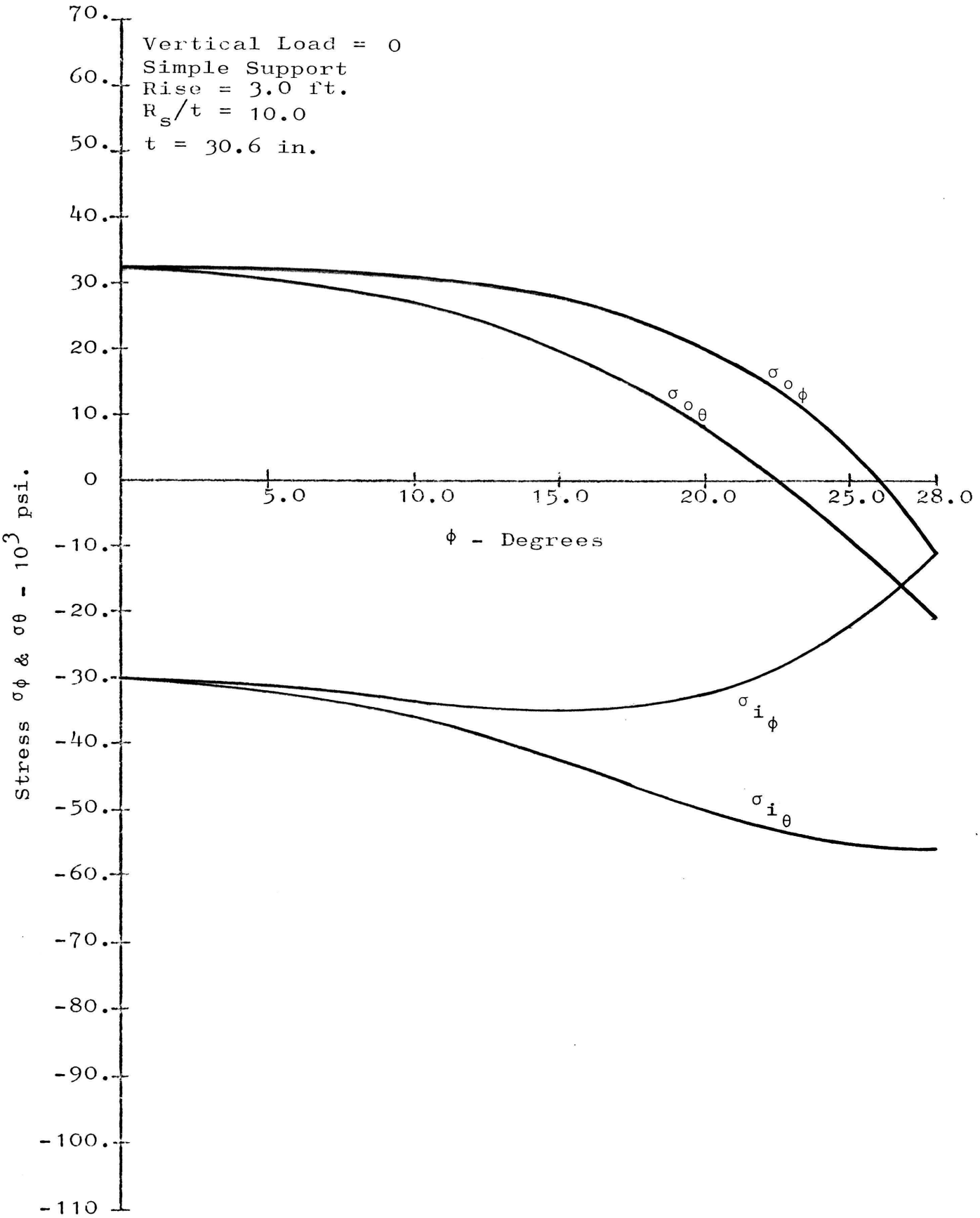

Figure 21. Stress vs. Phi, Case A, R_s/t = 10.0

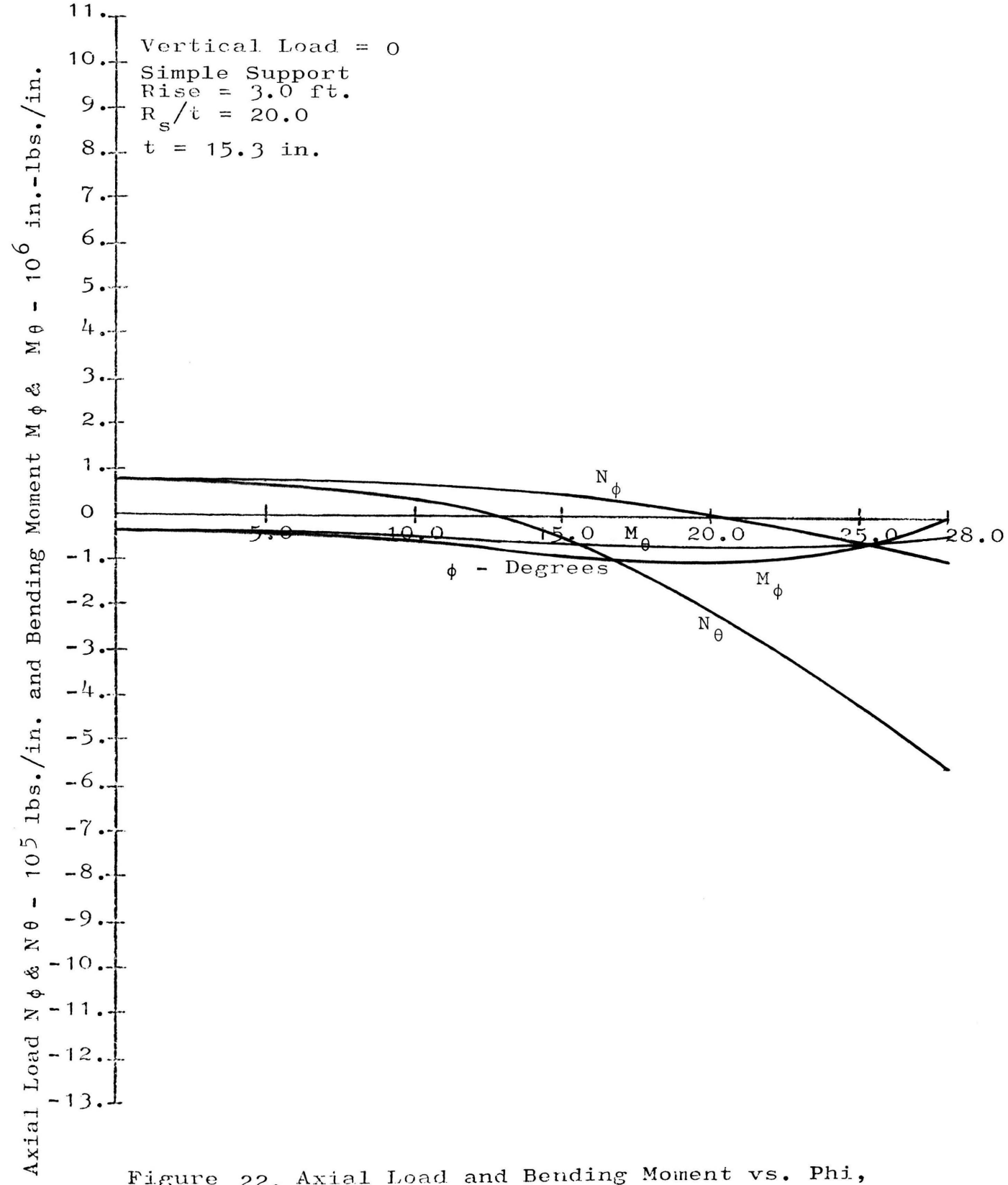

Figure 22. Axial Load and Bending Moment vs. Phi, Case A, R_s/t = 20.0

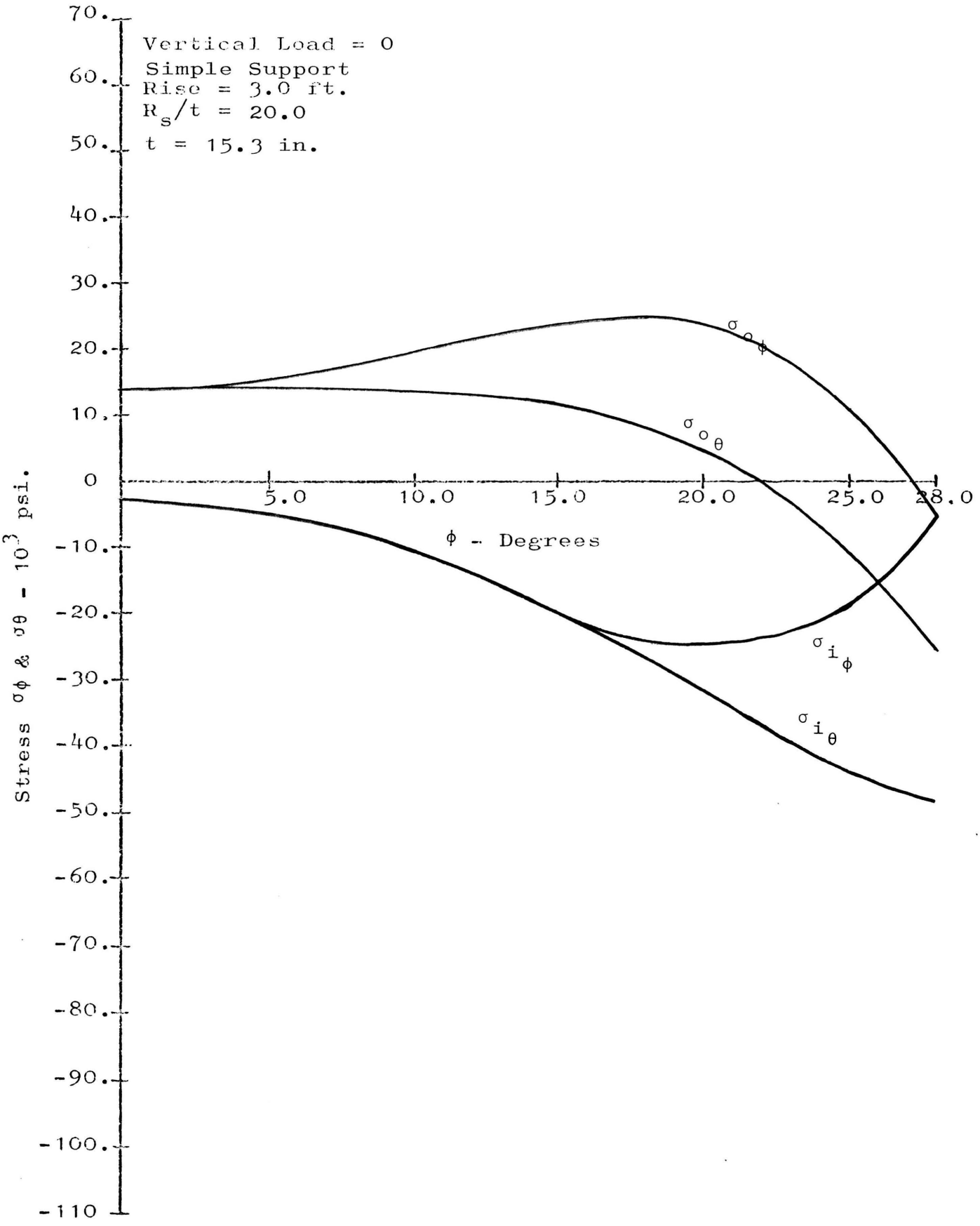

Figure 23. Stress vs. Phi, Case A, R_s/t = 20.0

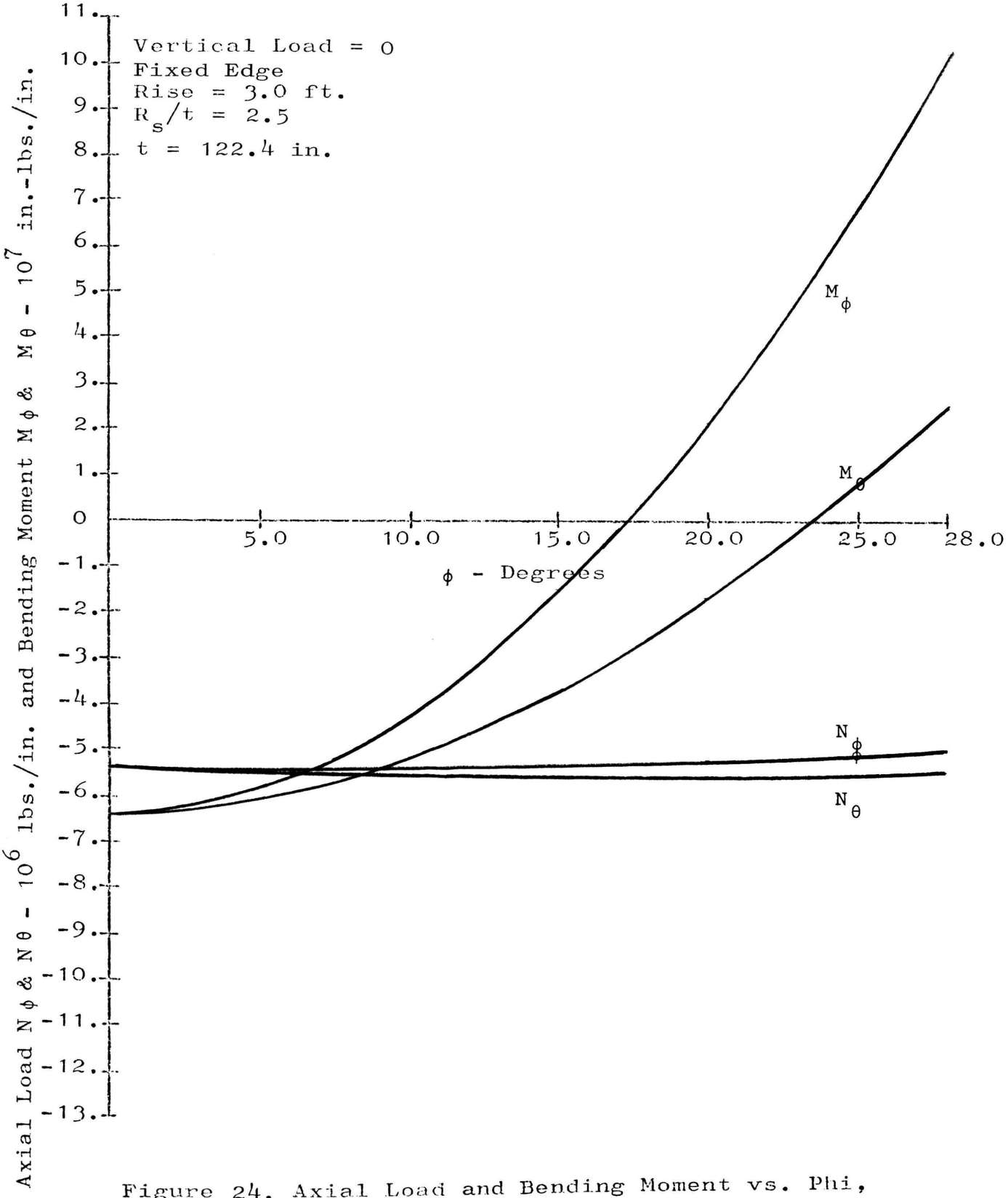

Figure 24. Axial Load and Bending Moment vs. Phi, Case B, R_s/t = 2.5

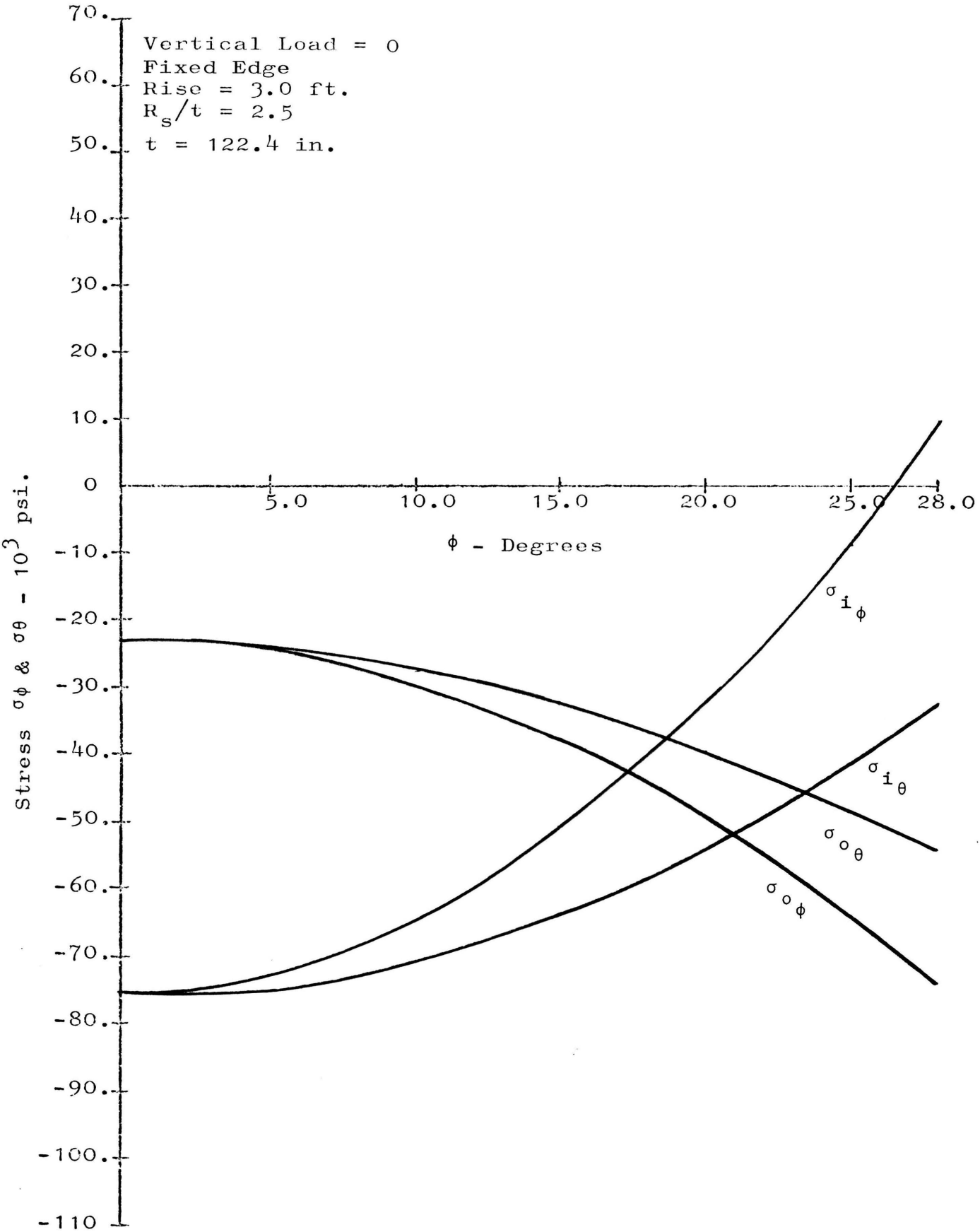

Figure 25. Stress vs. Phi, Case B, R_s/t = 2.5

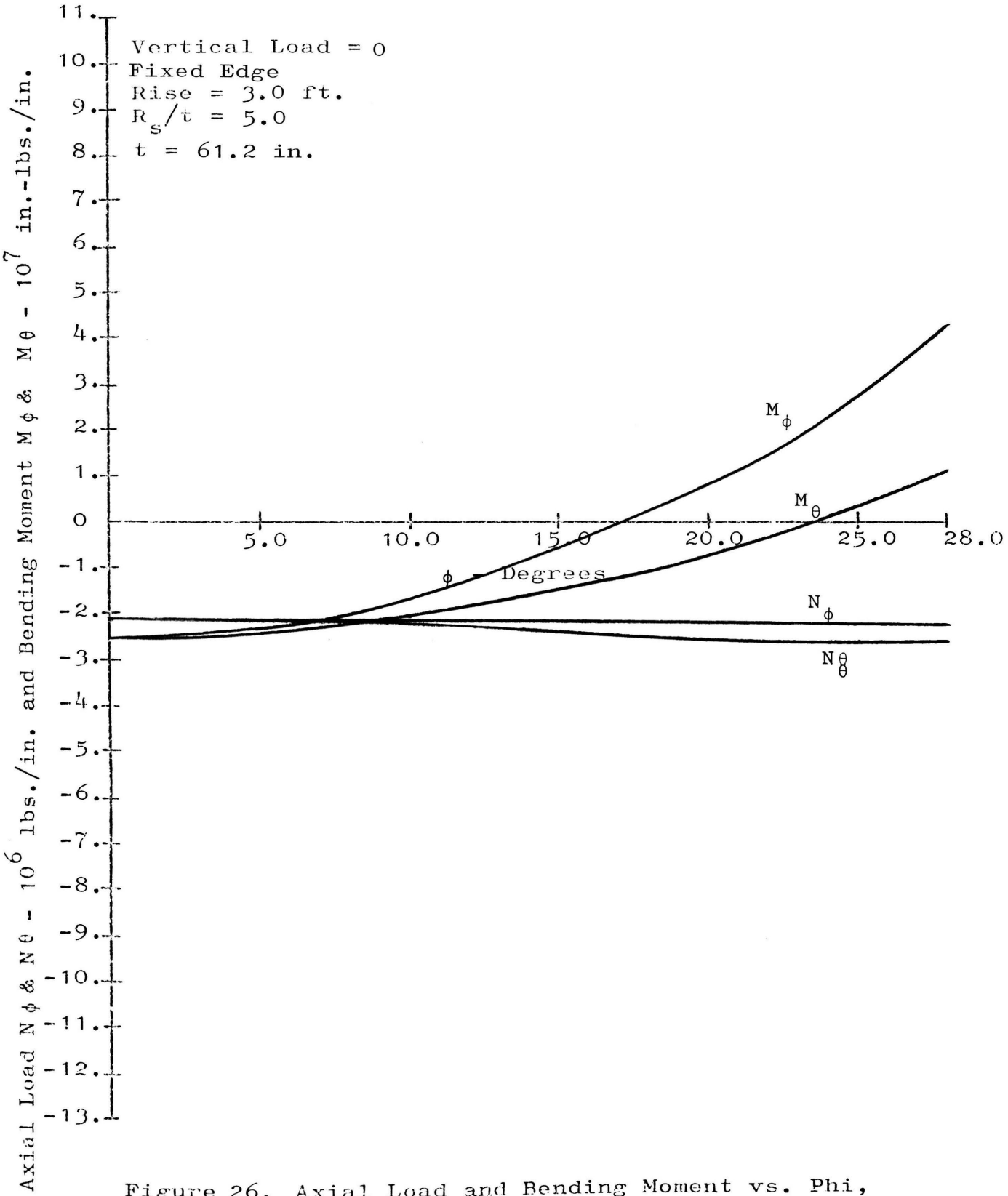

Figure 26. Axial Load and Bending Moment vs. Phi, Case B, R_s/t = 5.0

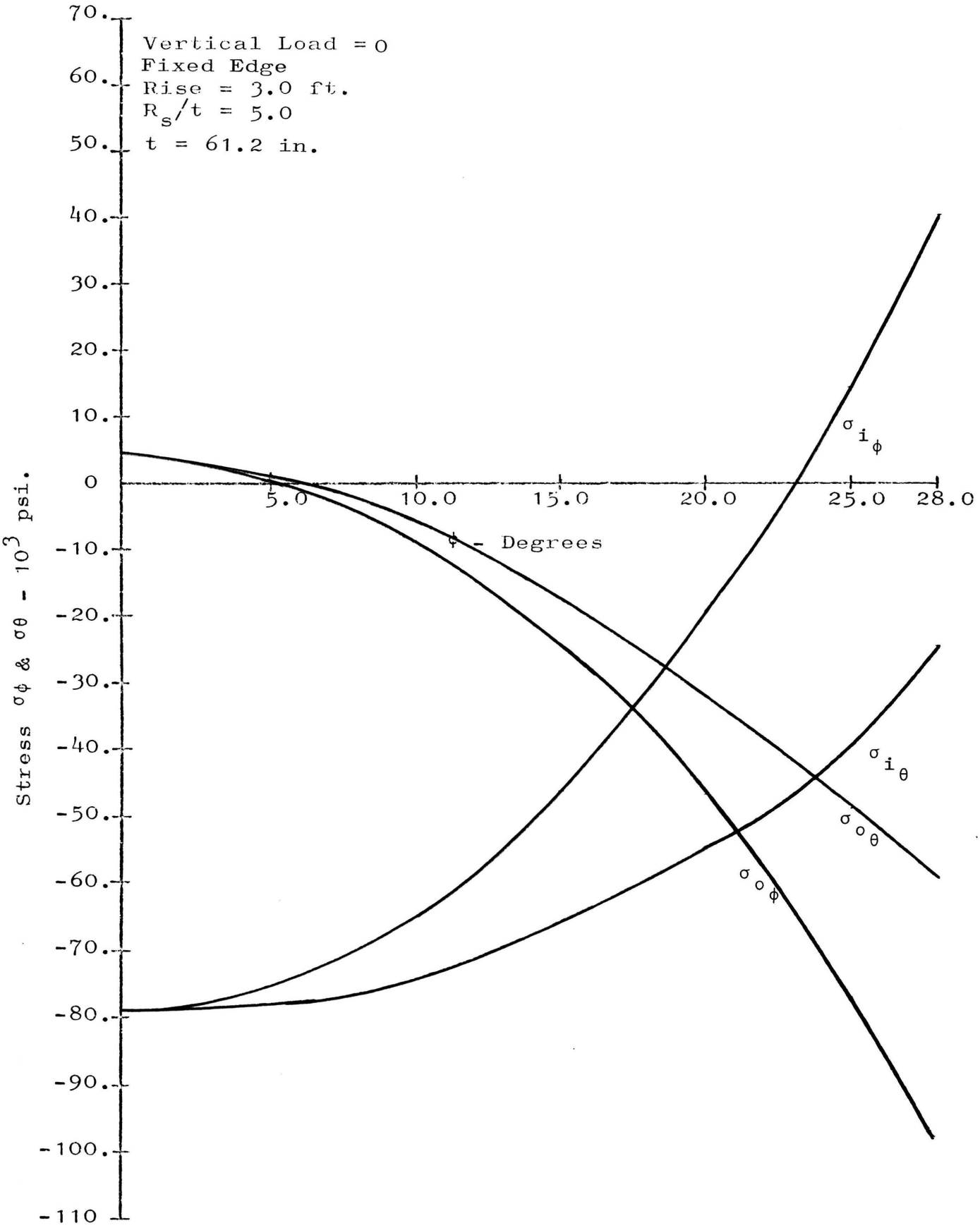

Figure 27. Stress vs. Phi, Case B, R_s/t = 5.0

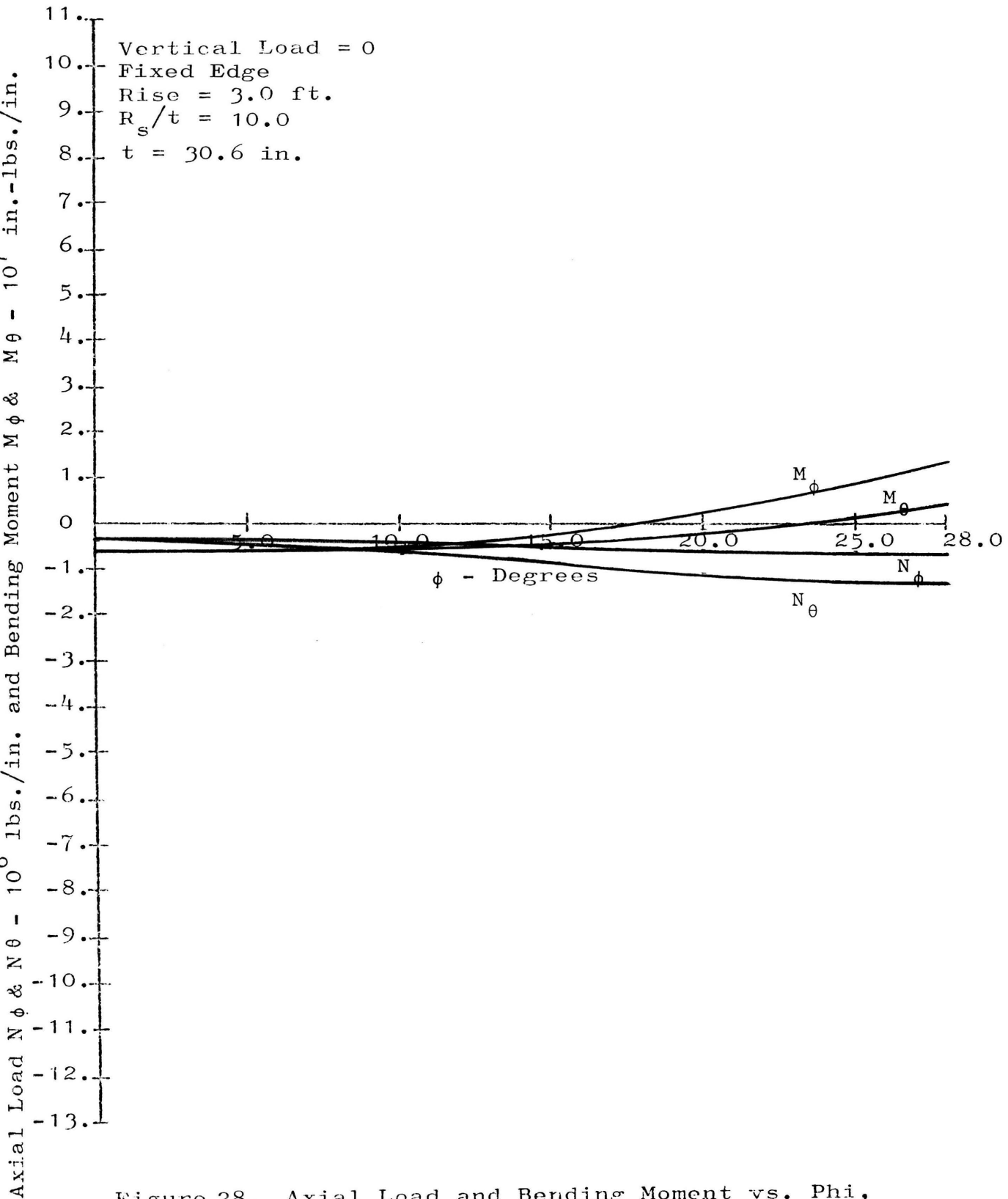

Figure 28. Axial Load and Bending Moment vs. Phi, Case B, R_s/t = 10.0

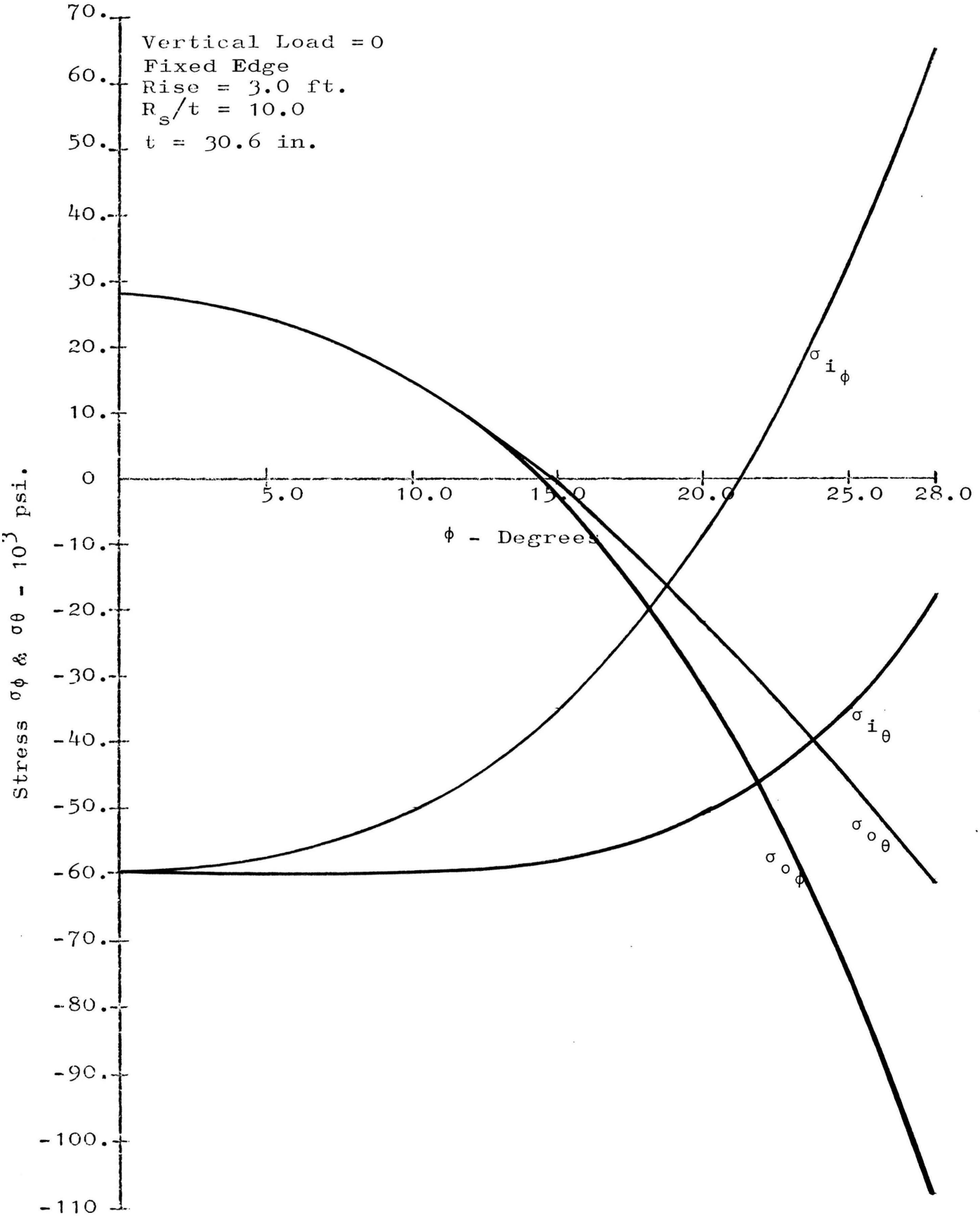

Figure 29. Stress vs. Phi, Case B, R_s/t = 10.0

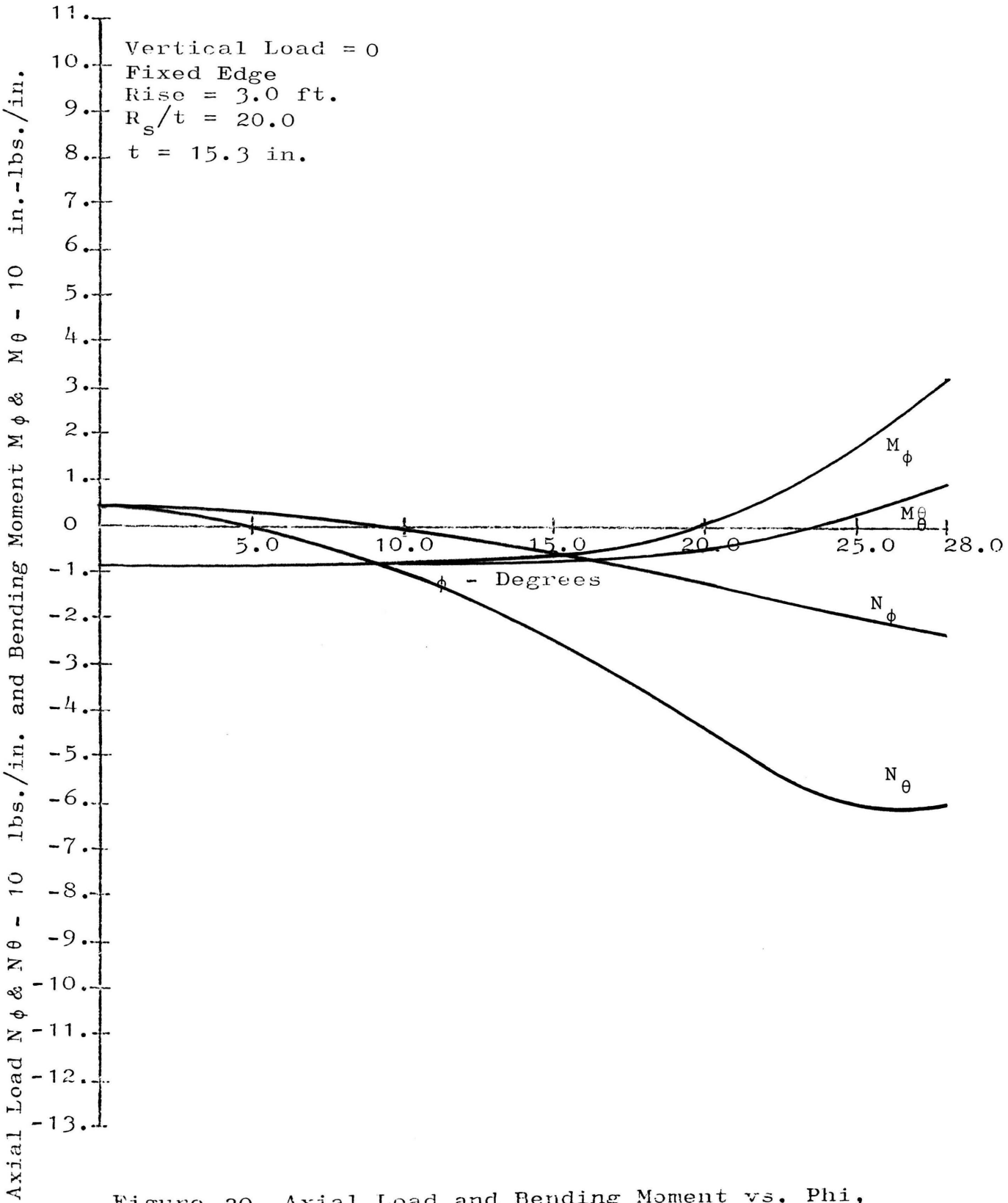

Figure 30. Axial Load and Bending Moment vs. Phi, Case B, R_s/t = 20.0

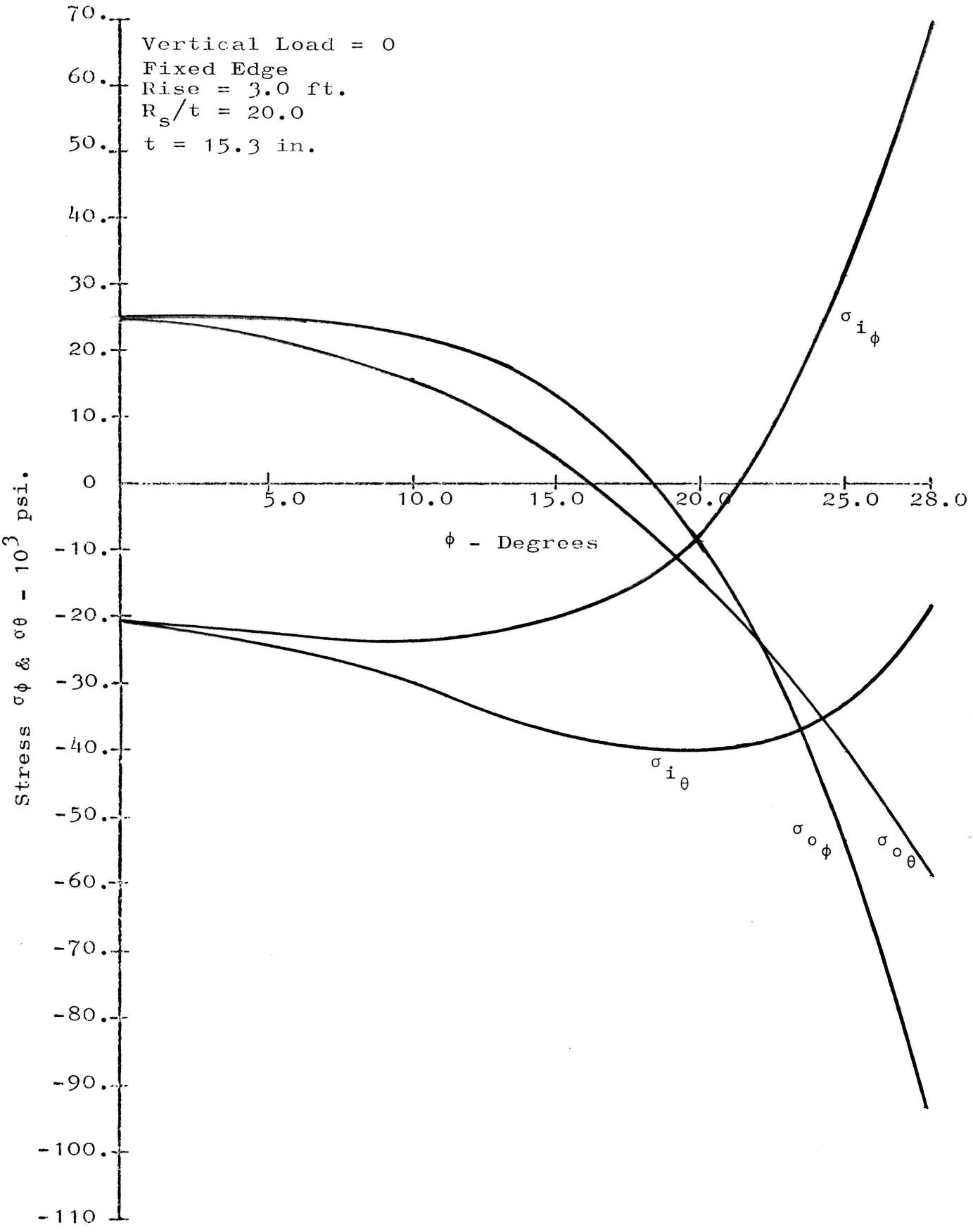

Figure 31. Stress vs. Phi, Case B , R_s/t = 20.0

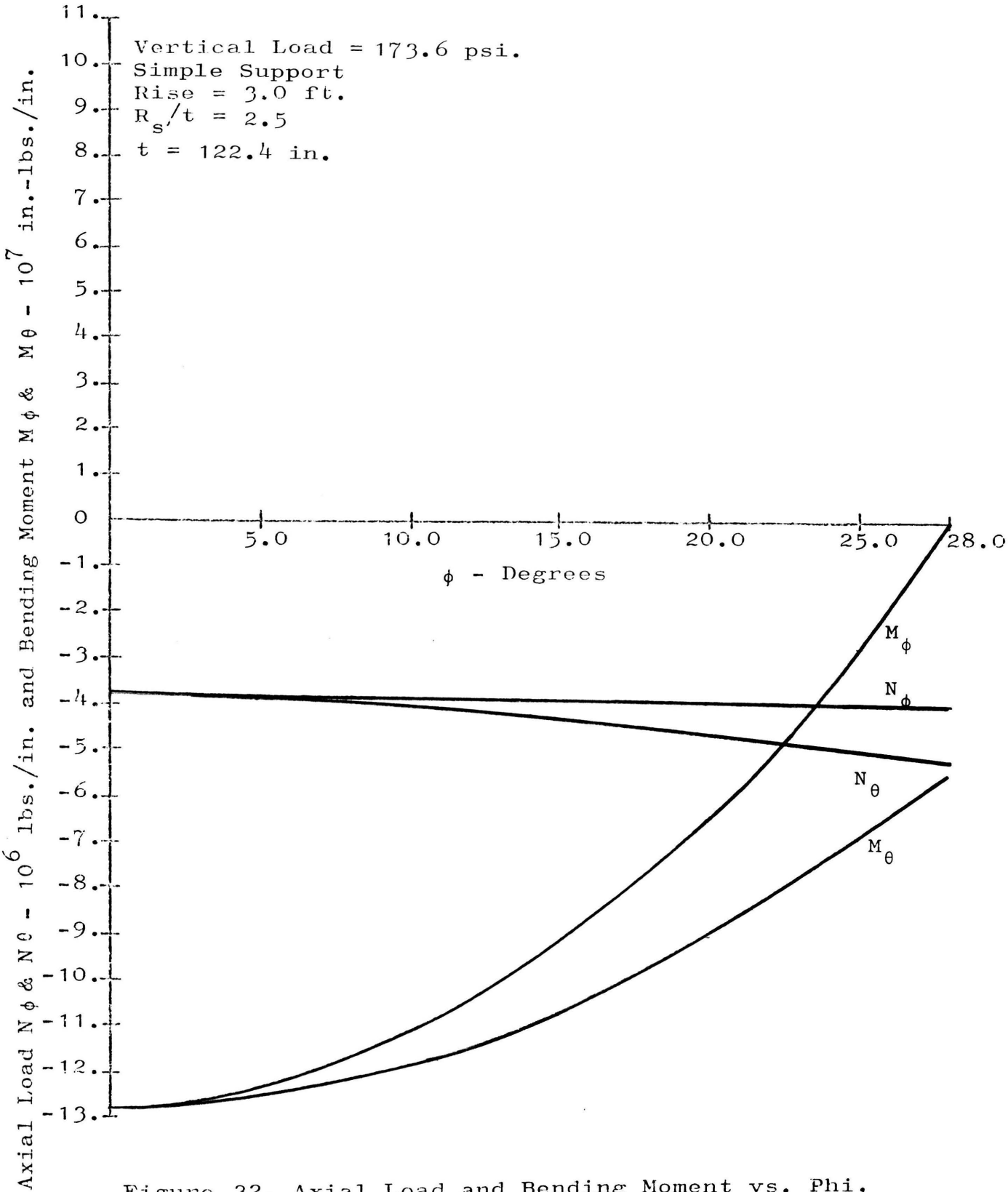

Figure 32. Axial Load and Bending Moment vs. Phi, Case C, R_s/t = 2.5

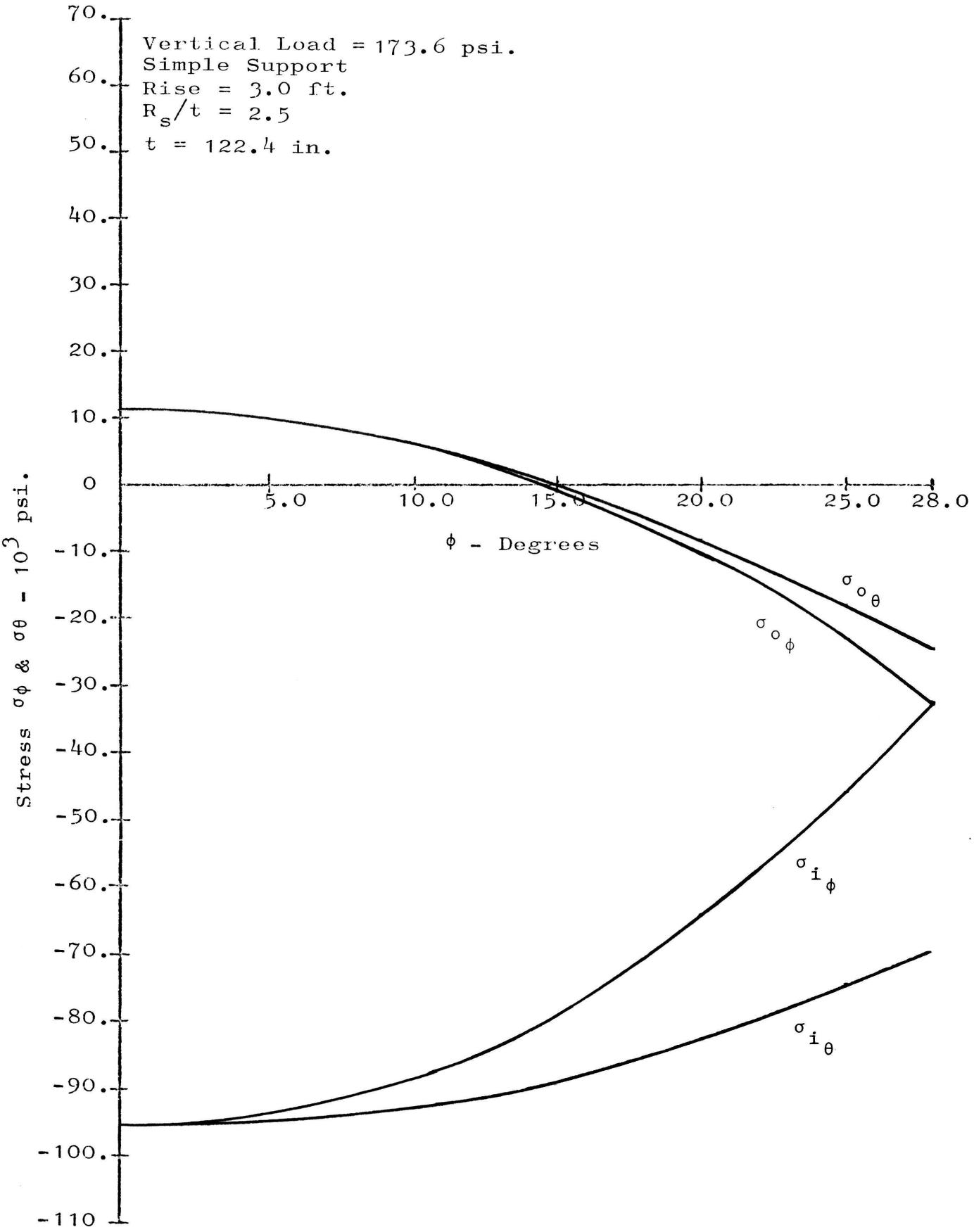

Figure 33. Stress vs. Phi, Case C, R_s/t = 2.5

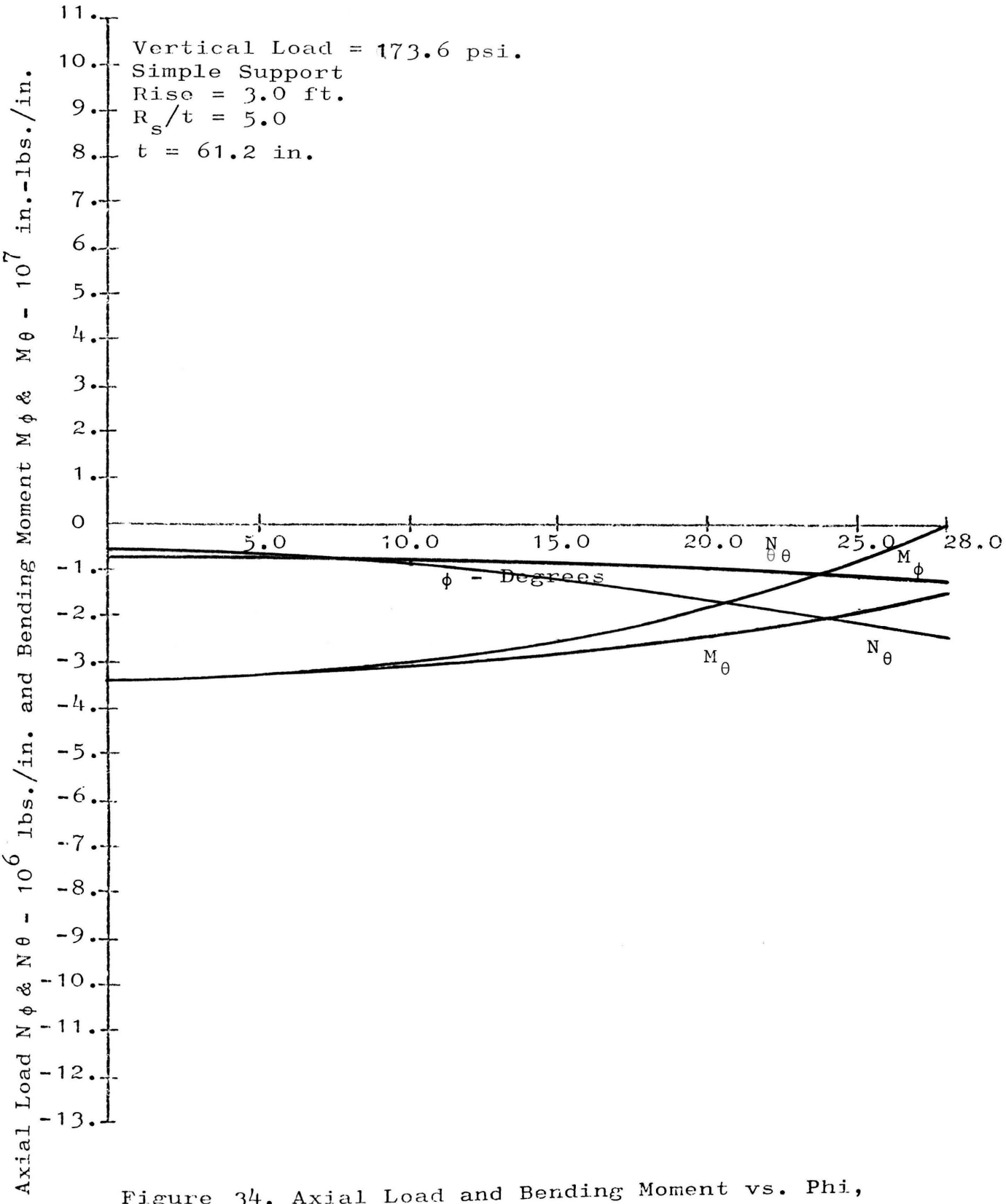

Figure 34. Axial Load and Bending Moment vs. Phi, Case C, R_s/t = 5.0

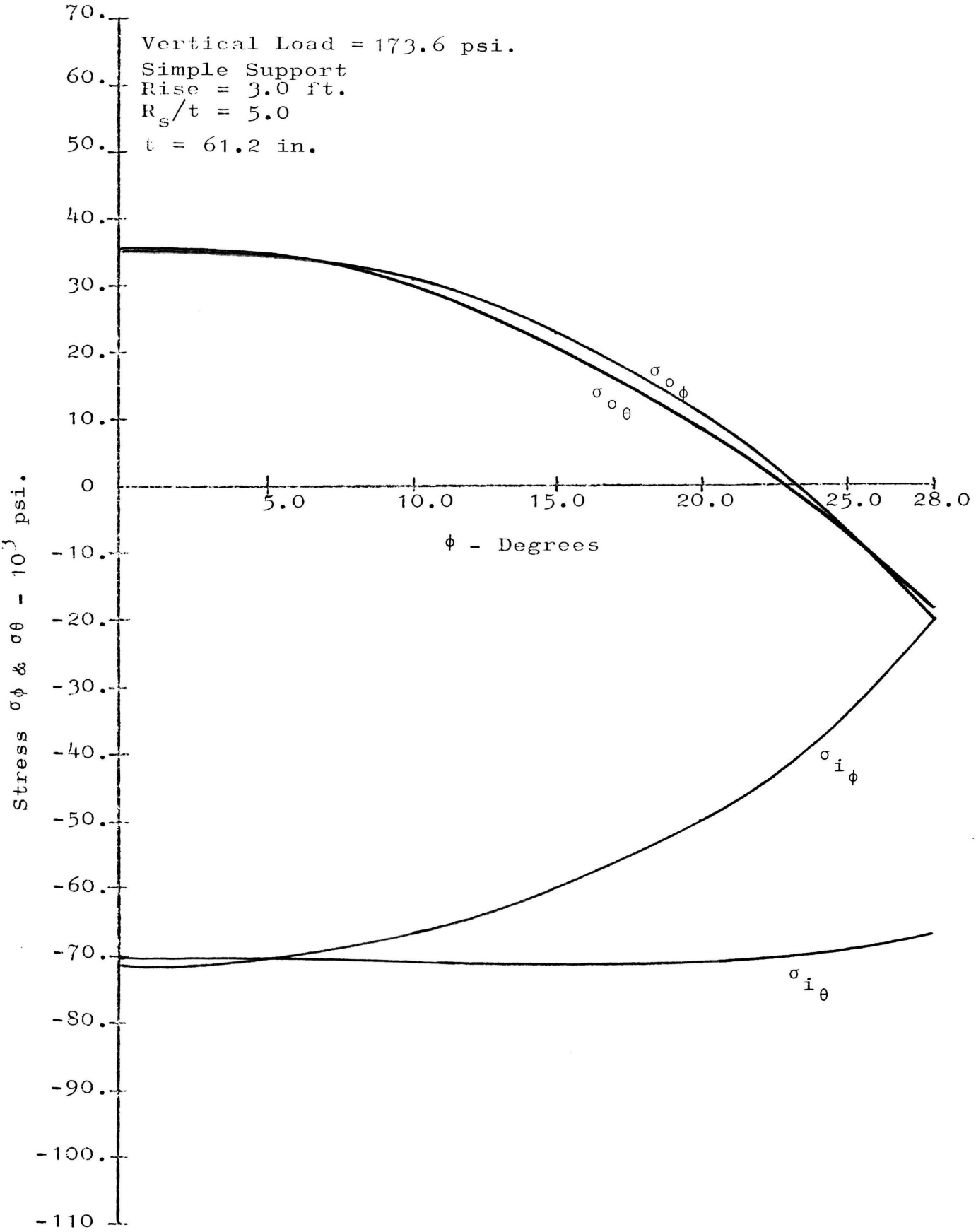

Figure 35. Stress vs. Phi, Case C, R_s/t = 5.0

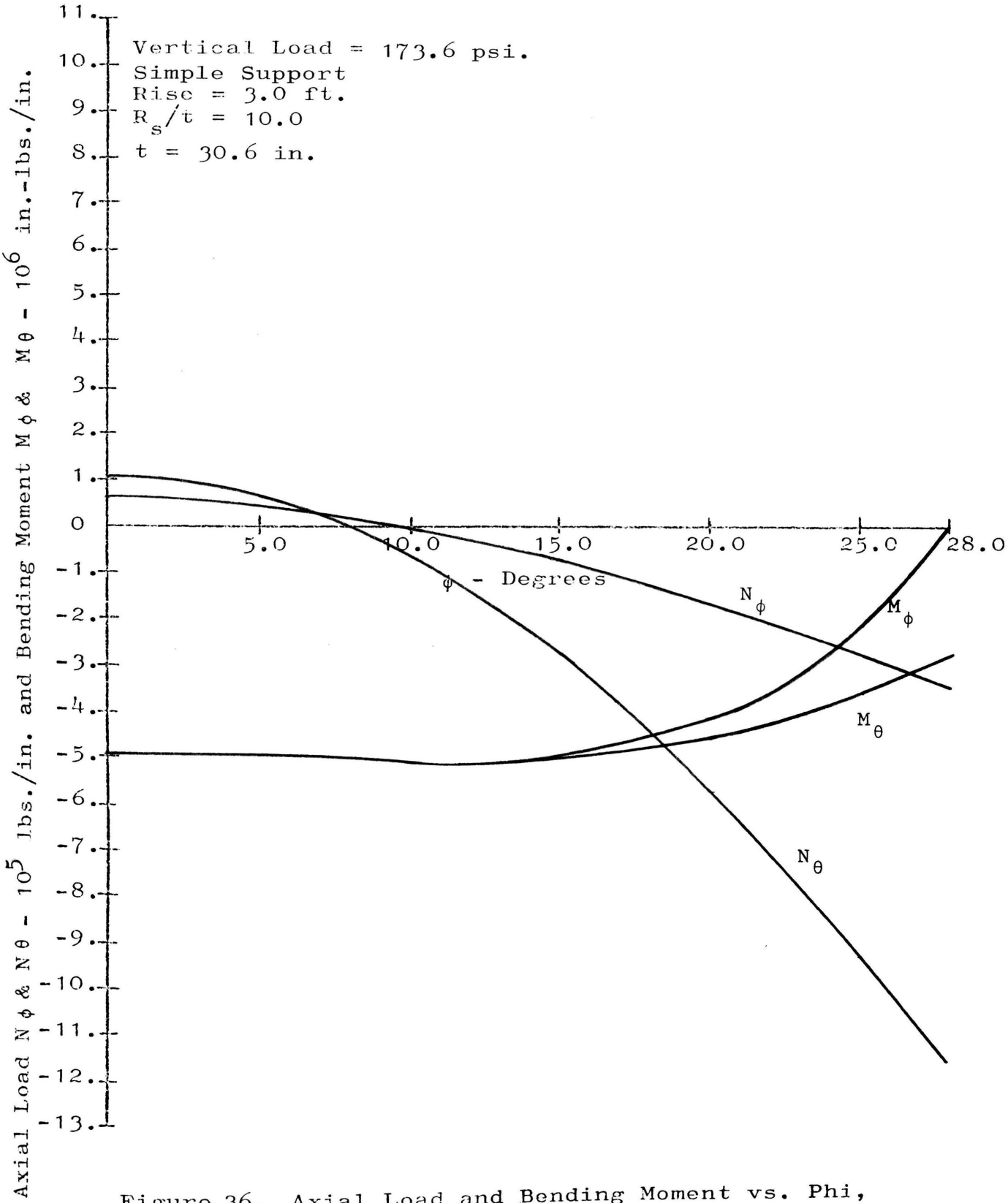

Figure 36. Axial Load and Bending Moment vs. Phi, Case C, R_s/t = 10.0

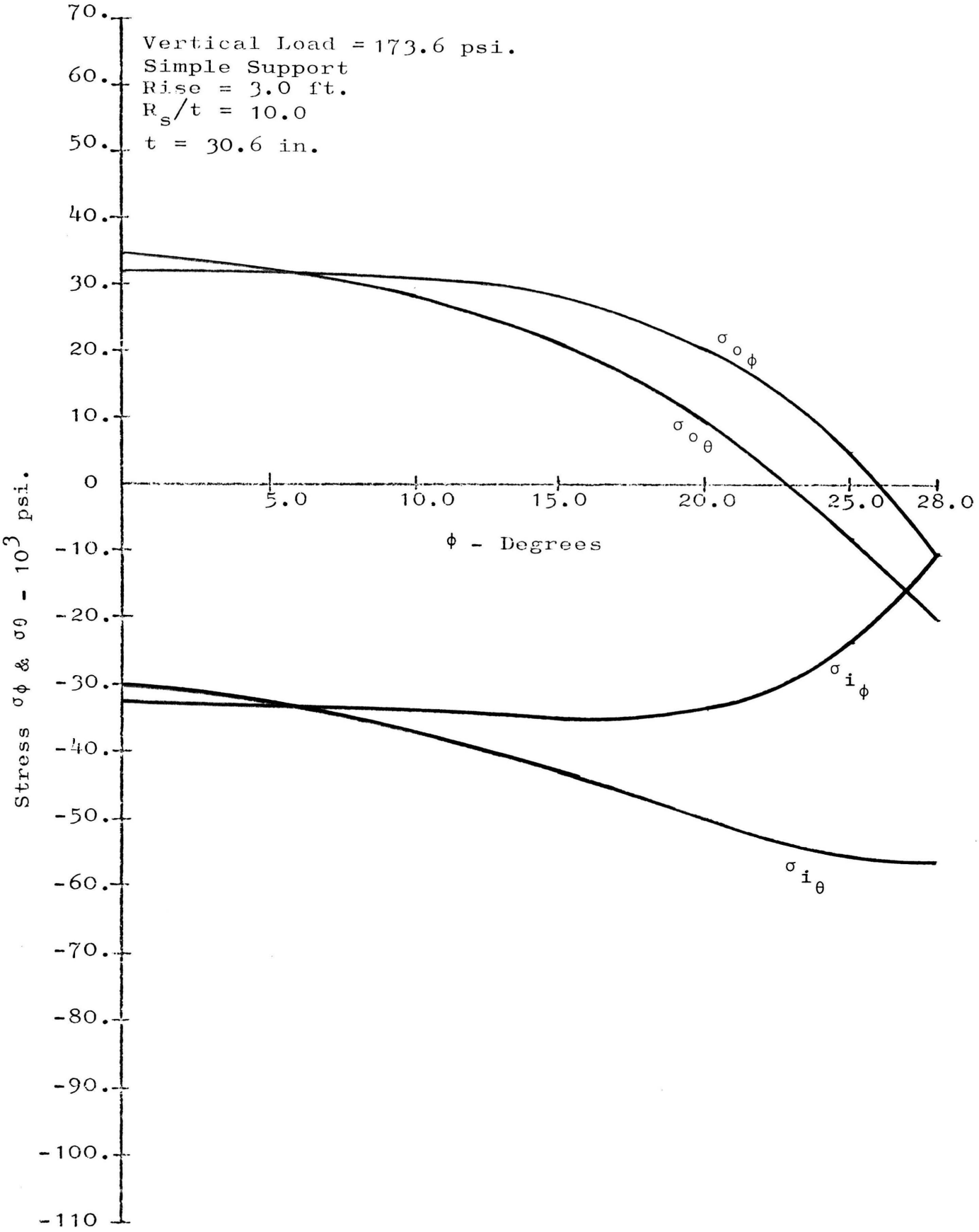

Figure 37. Stress vs. Phi, Case C, R_s/t = 10.0

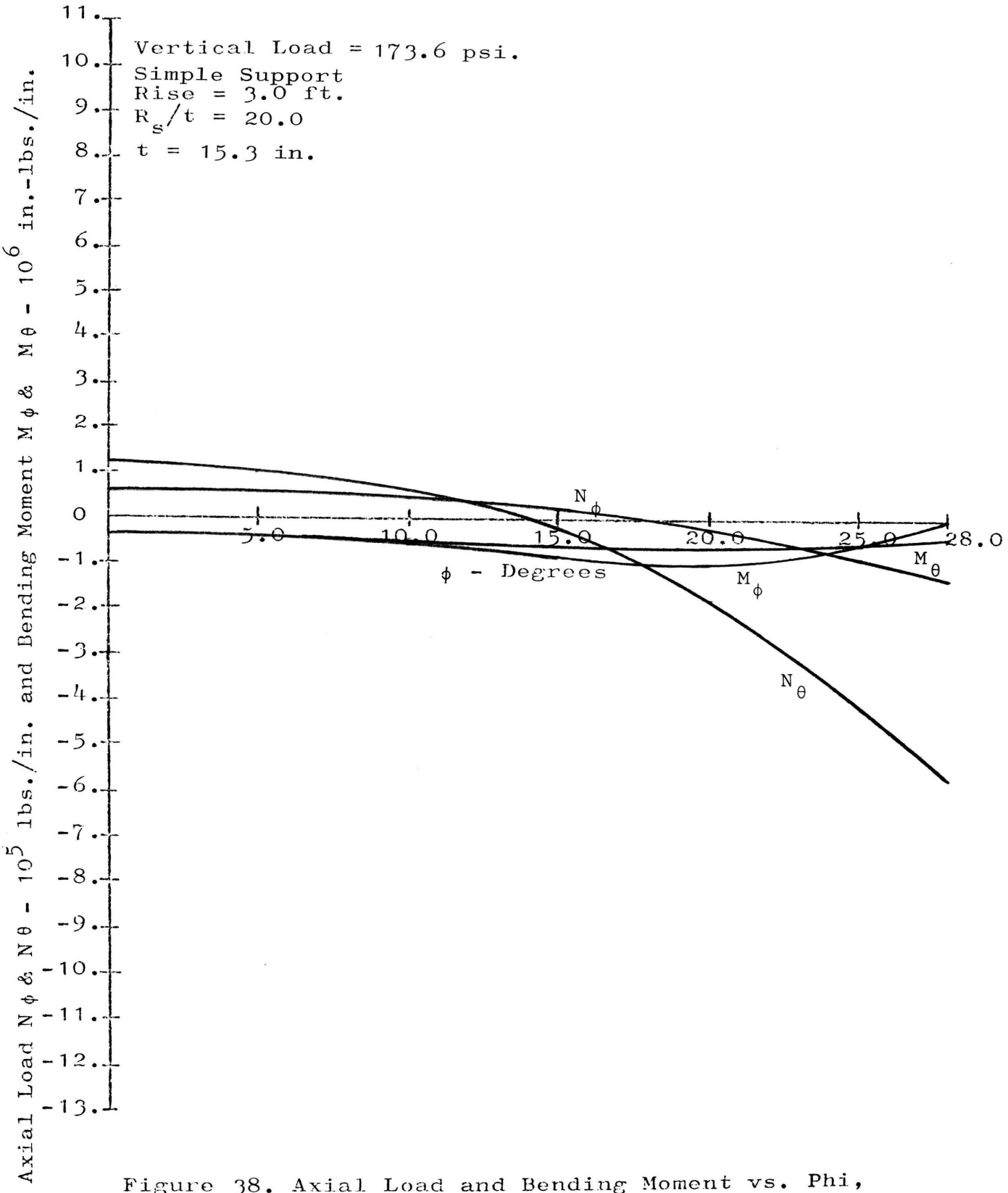

Figure 38. Axial Load and Bending Moment vs. Phi, Case C, R_s/t = 20.0

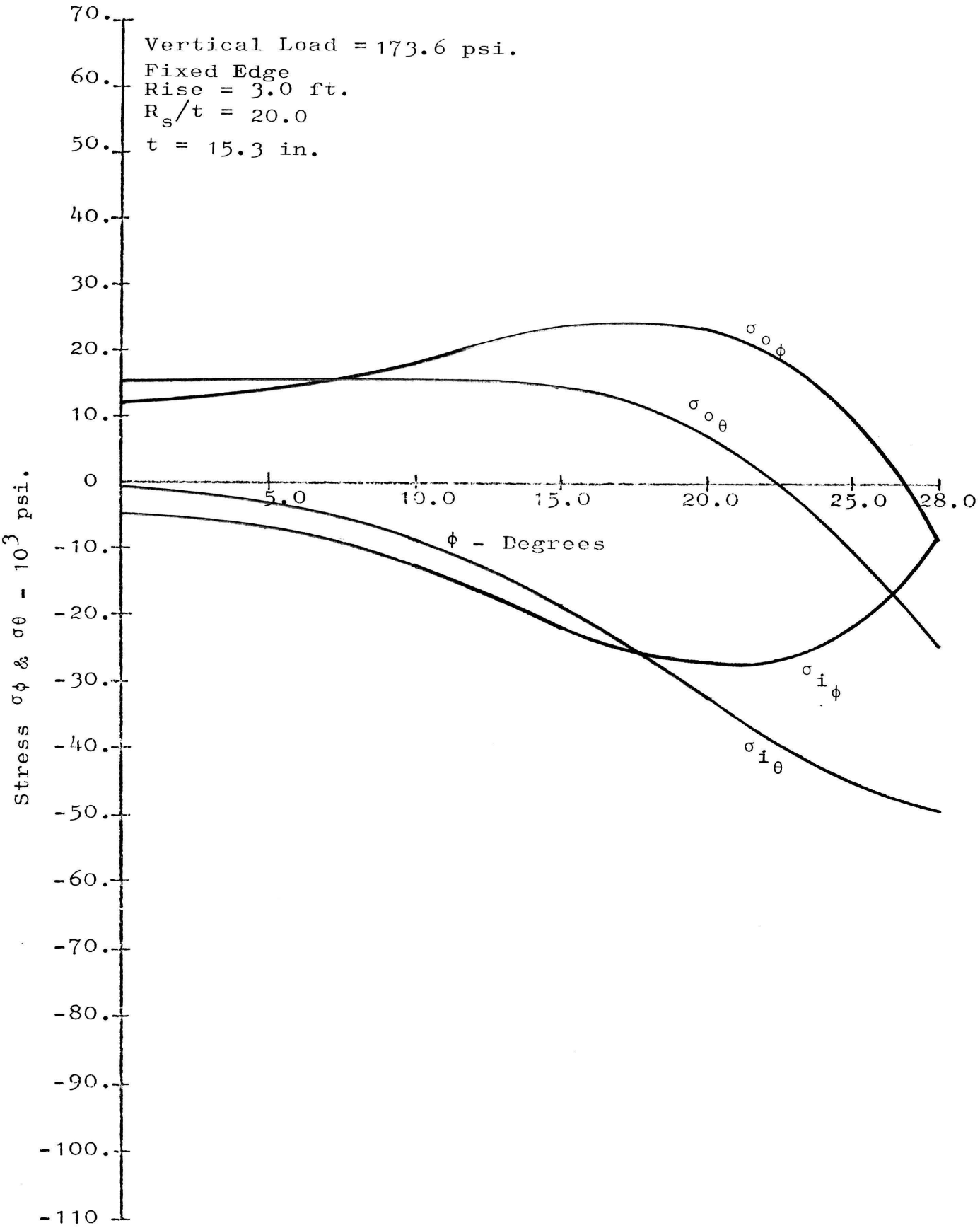

Figure 39. Stress vs. Phi, Case C, R_s/t = 20.0

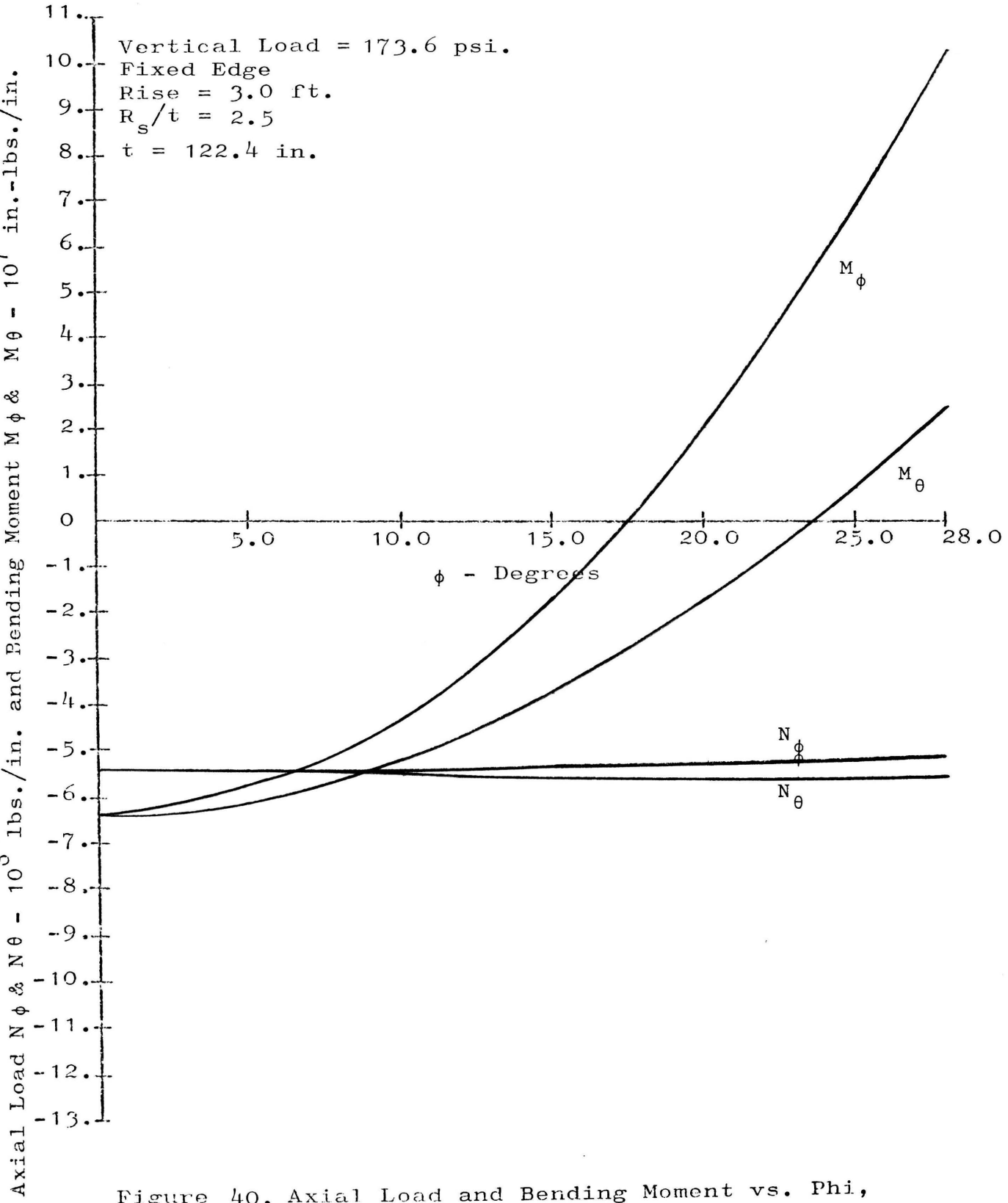

Figure 40. Axial Load and Bending Moment vs. Phi, Case D, R_s/t = 2.5

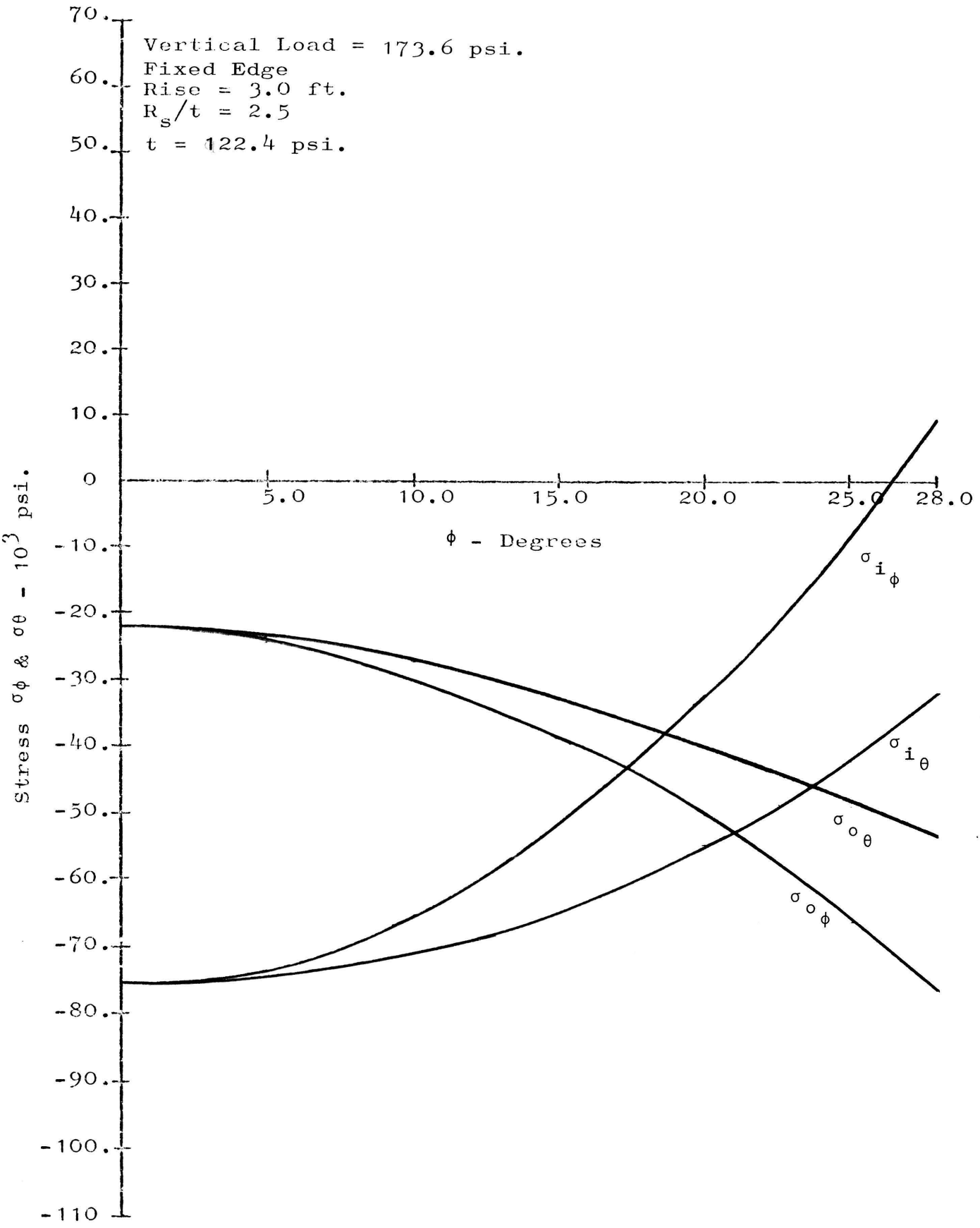

Figure 41. Stress vs. Phi, Case D, R_s/t = 2.5

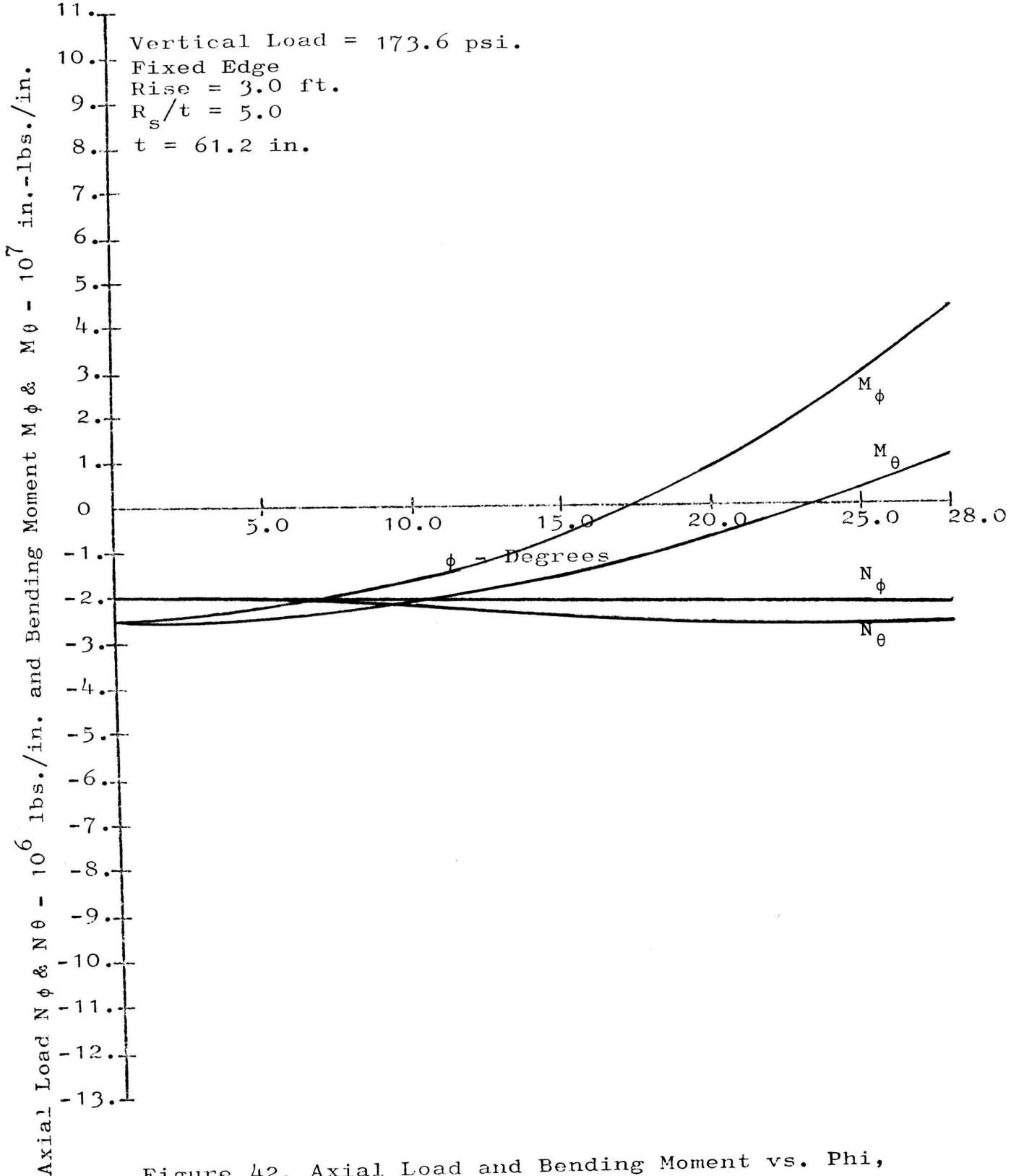

Figure 42. Axial Load and Bending Moment vs. Phi, Case D, R_s/t = 5.0

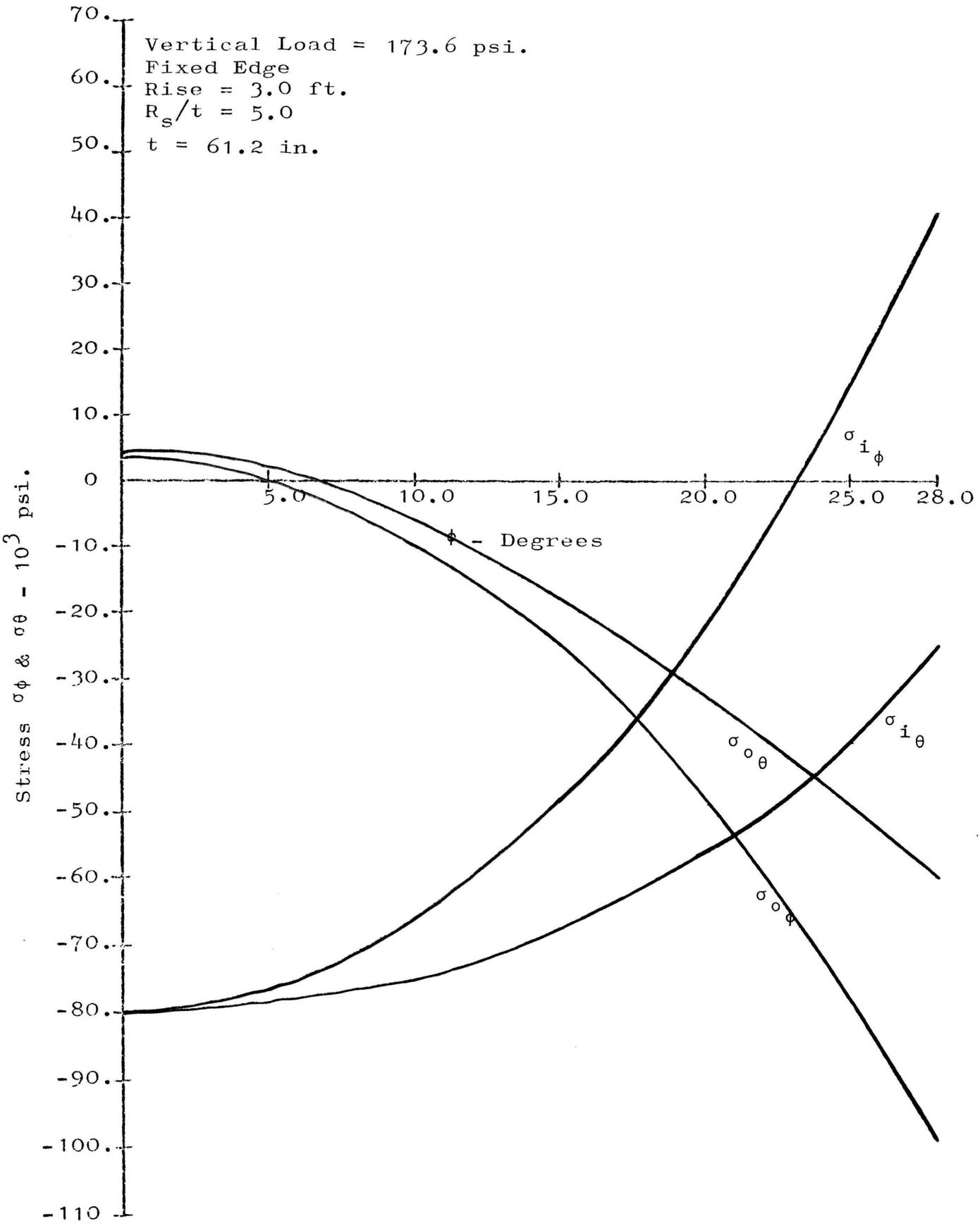

Figure 43. Stress vs. Phi, Case D, R_s/t = 5.0

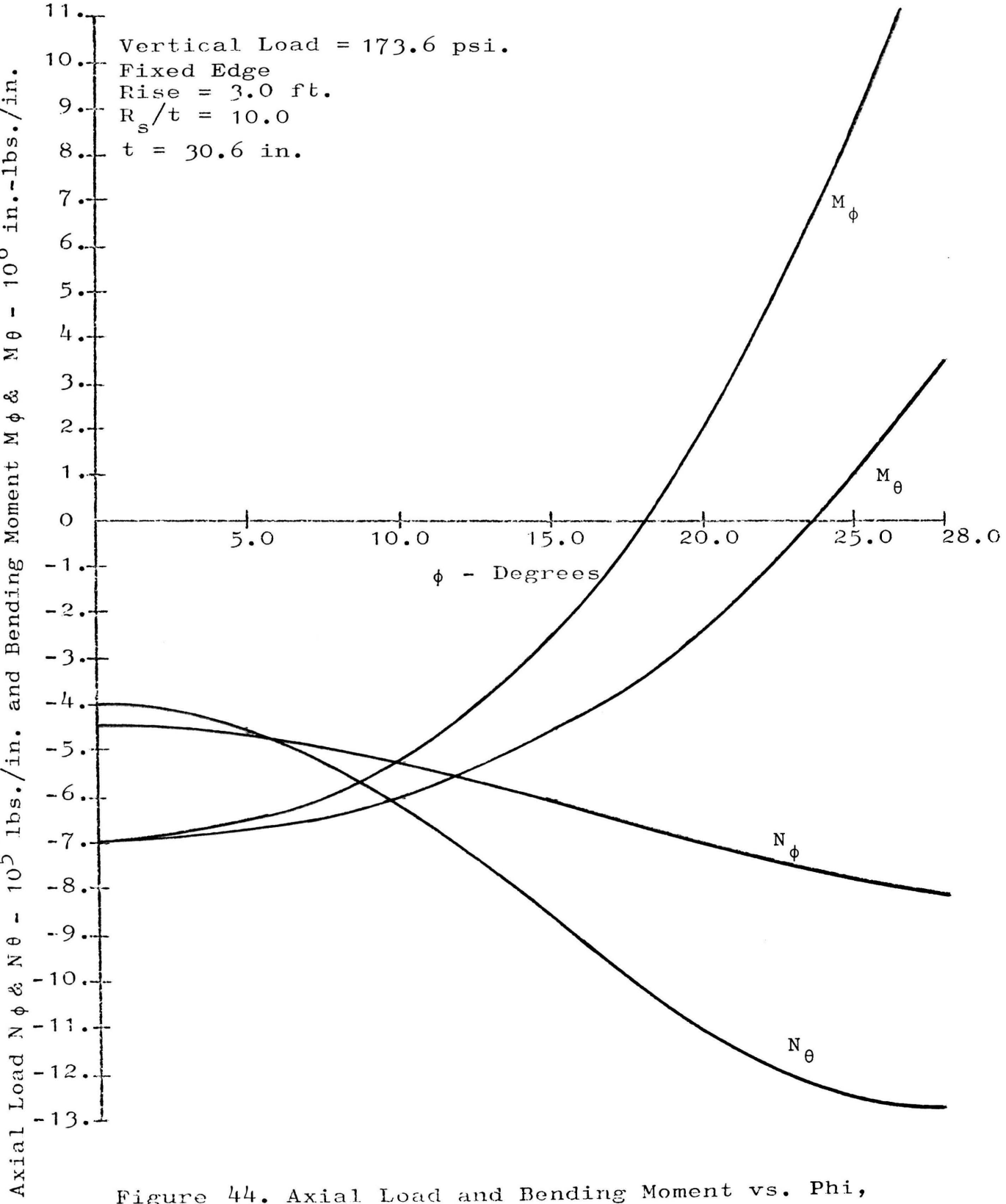

Figure 44. Axial Load and Bending Moment vs. Phi, Case D, R_s/t = 10.0

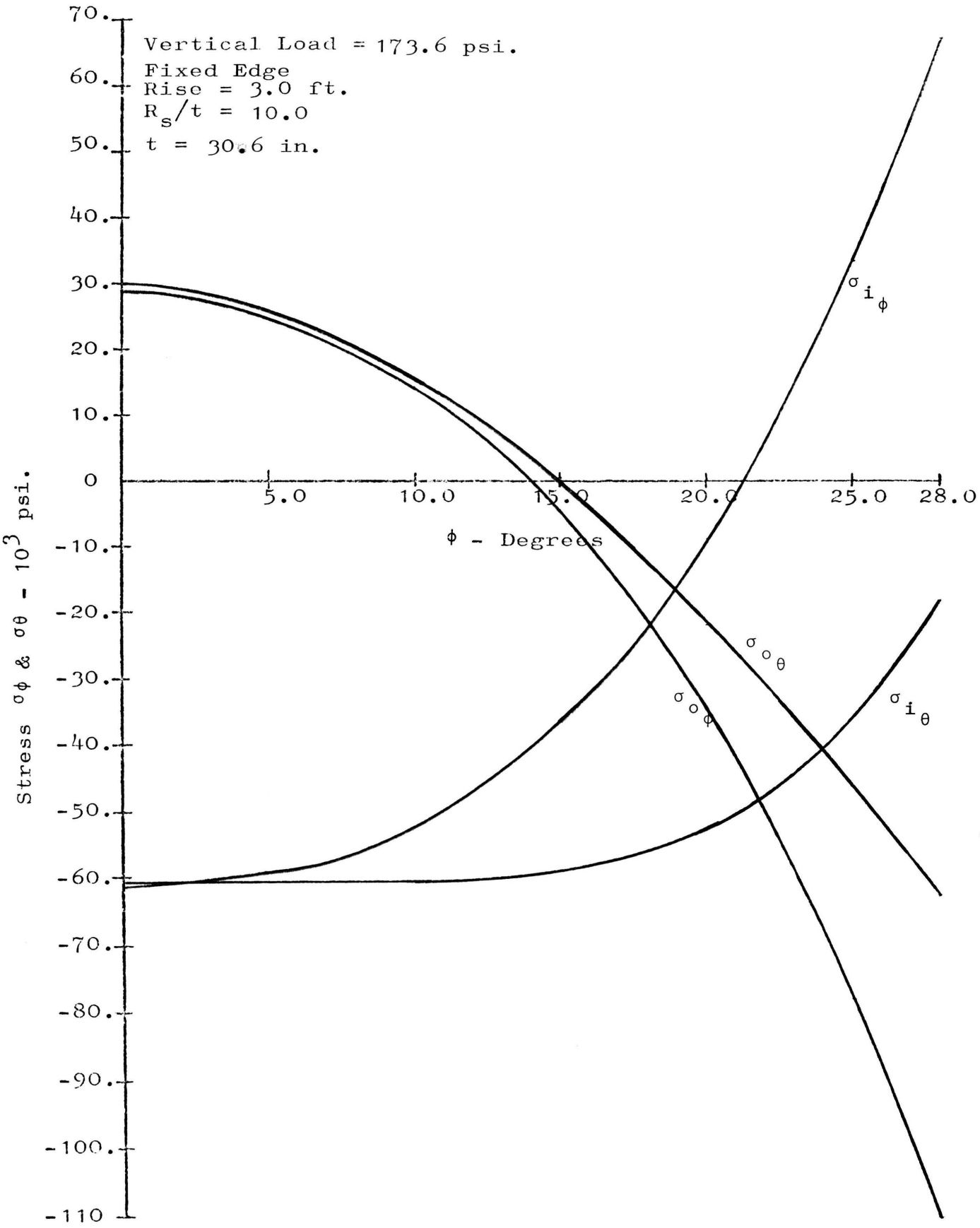

Figure 45. Stress vs. Phi, Case D, R_s/t = 10.0

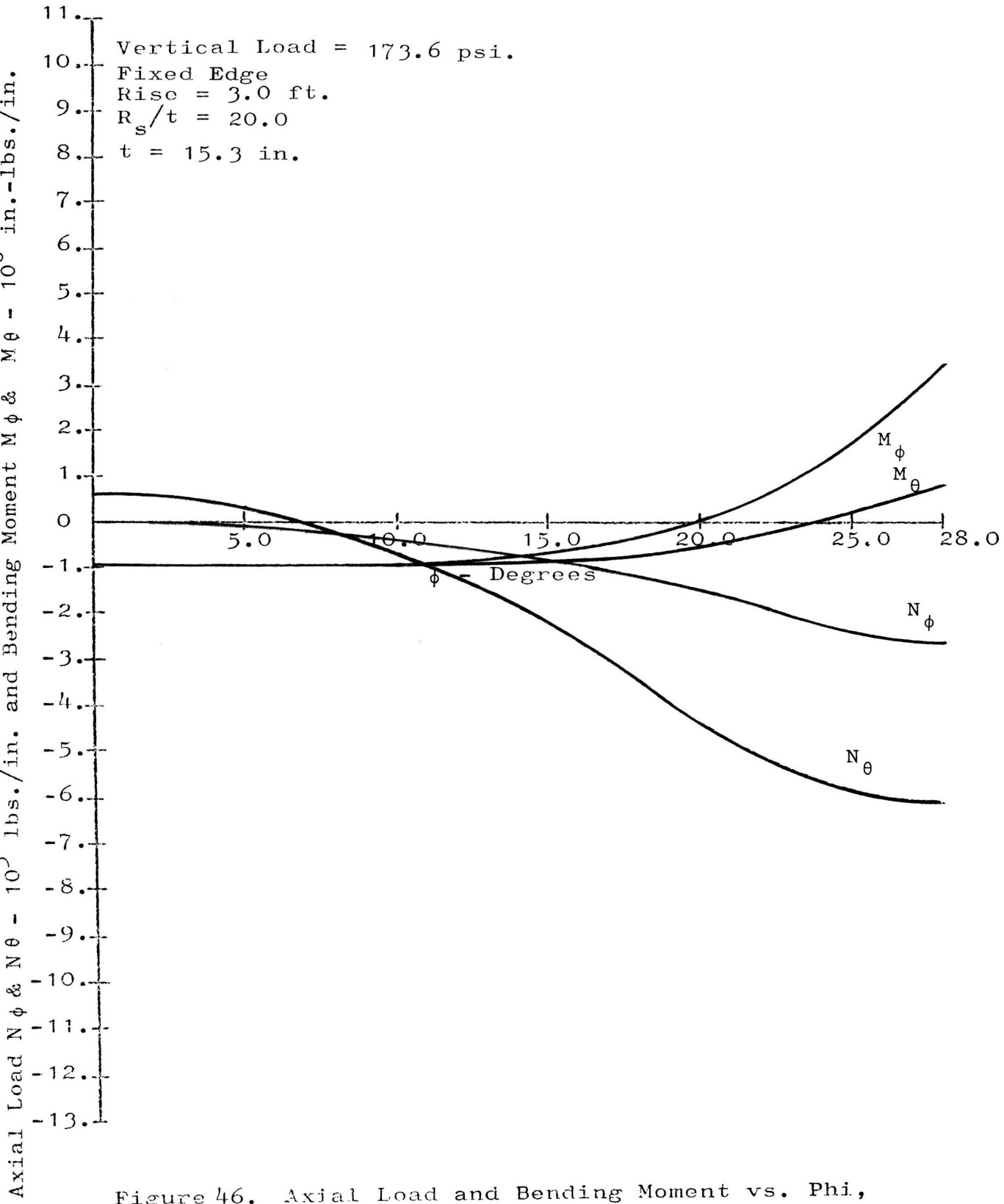

Figure 46. Axial Load and Bending Moment vs. Phi, Case D, R_s/t = 20.0

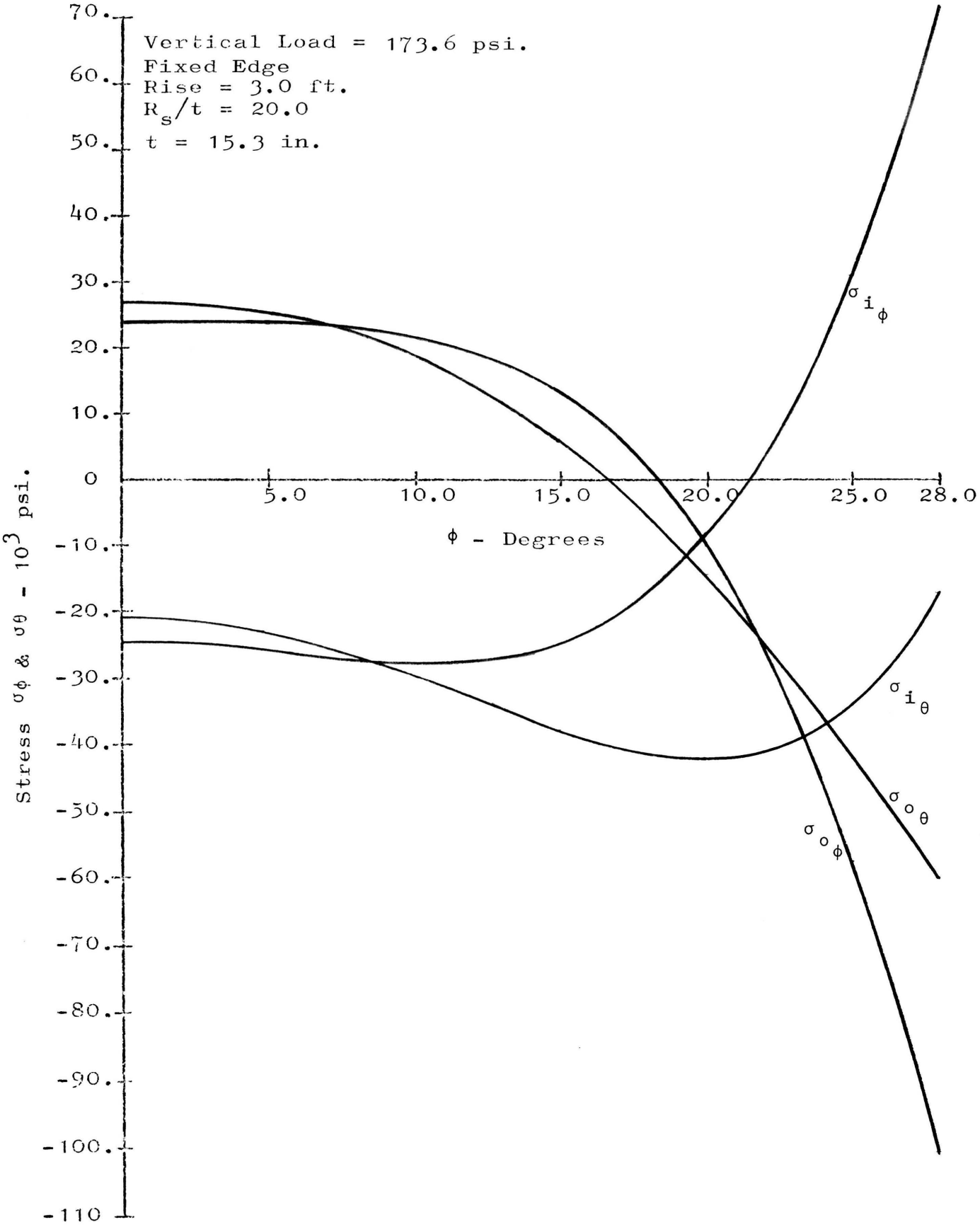

Figure 47. Stress vs. Phi, Case D, R_s/t = 20.0

APPENDIX 1

STRESSES IN SHELL DUE TO ITS OWN WEIGHT

The following is from Fluegge[1] for a spherical shell loaded by its own weight:

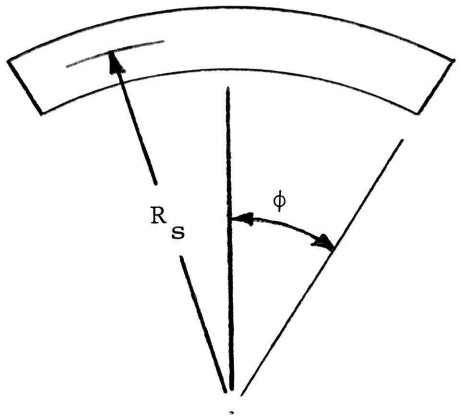

$$N_\phi = - \frac{p_w R_s}{1 + \cos \phi} \qquad (I1)$$

$$N_\theta = p_w R_s \left(\frac{1}{1 + \cos \phi} - \cos \phi\right) \qquad (I2)$$

where

N_ϕ = Meridional axial load in pounds/unit width.

N_θ = Circumferential axial load in pounds/unit width.

p_w = Weight per unit area of middle surface.

R_s = Radius of middle surface.

ϕ = Meridional angle.

Following is a program to calculate the axial loads and the accompanying axial stresses based upon a uniform distribution of the stress across the cross-section. In order to use equations (I1) and (I2) it is necessary to assume that there exists a supporting ring to react the horizontal component of N_ϕ at the free edge. Because this

horizontal component of N_ϕ is relatively small compared to the loads calculated due to the thermal expansion and because the resulting stresses due to the shell weight are small this condition was not superimposed with the stresses due to the thermal expansion.

In the stresses due to the weight of the shell only a membrane solution was used. Fluegge[1] shows that using a membrane solution to this problem rather than the more complex solution considering bending doesn't result in appreciable error. Since the stresses resulting from this approximation are so small it isn't felt that the more exact solution considering bending was warranted.

```
C       MEMBRANE LOADS DUE TO SHELL WEIGHT
        READ (1,10) THICK
        P=0.087*THICK
        READ (1,10) RISE
        RADUS=((144.0+RISE*RISE)/(2.0*RISE))*12.0
        WRITE (3,10) RADUS
        TAN=RISE/12.0
        ALPHA=ATAN(TAN)
        PHINO=2.0*ALPHA*57.2958
        WRITE (3,10) PHINO
  120   PHIRD=PHINO/57.2958
        COSF=COS(PHIRD)
        CSPL1=1.0+COSF
        CNPHI=-P*RADUS/CSPL1
        CNTHA=P*RADUS*(1.0/CSPL1-COSF)
        SNPHI=CNPHI/THICK
        SNTHA=CNTHA/THICK
        WRITE(3,10)PHINO,CNPHI,CNTHA,SNPHI,SNTHA
        PHINO=PHINO-2.0
        IF(PHINO)130,120,120
  130   STOP
   10   FORMAT(5E18.8)
        END
```

ϕ	N_ϕ	N_θ	σ_ϕ	σ_θ
0.36869888E 02	-0.55679932E 03	-0.24499216E 03	-0.11599985E 02	-0.51040030E 01
0.34869888E 02	-0.55054419E 03	-0.27174536E 03	-0.11469670E 02	-0.56613617E 01
0.32869888E 02	-0.54472339E 03	-0.29706250E 03	-0.11348404E 02	-0.61888018E 01
0.30869888E 02	-0.53932104E 03	-0.32093555E 03	-0.11235855E 02	-0.66861572E 01
0.28869888E 02	-0.53432275E 03	-0.34335645E 03	-0.11131723E 02	-0.71532593E 01
0.26869888E 02	-0.52971509E 03	-0.36431763E 03	-0.11035730E 02	-0.75899506E 01
0.24869888E 02	-0.52548511E 03	-0.38381177E 03	-0.10947606E 02	-0.79960785E 01
0.22869888E 02	-0.52162207E 03	-0.40183105E 03	-0.10867126E 02	-0.83714800E 01
0.20869888E 02	-0.51811572E 03	-0.41836841E 03	-0.10794077E 02	-0.87160082E 01
0.18869888E 02	-0.51495776E 03	-0.43341650E 03	-0.10728287E 02	-0.90295105E 01
0.16869888E 02	-0.51213940E 03	-0.44696973E 03	-0.10669571E 02	-0.93118687E 01
0.14869888E 02	-0.50965356E 03	-0.45902173E 03	-0.10617783E 02	-0.95629520E 01
0.12869888E 02	-0.50749414E 03	-0.46956714E 03	-0.10572794E 02	-0.97826481E 01
0.10869888E 02	-0.50565576E 03	-0.47860107E 03	-0.10534494E 02	-0.99708557E 01
0.88698883E 01	-0.50413403E 03	-0.48611938E 03	-0.10502792E 02	-0.10127487E 02
0.68698883E 01	-0.50292505E 03	-0.49211841E 03	-0.10477605E 02	-0.10252466E 02
0.48698883E 01	-0.50202588E 03	-0.49659521E 03	-0.10458872E 02	-0.10345734E 02
0.28698883E 01	-0.50143408E 03	-0.49954785E 03	-0.10446543E 02	-0.10407247E 02
0.86988831E 00	-0.50114844E 03	-0.50097510E 03	-0.10440592E 02	-0.10436981E 02

APPENDIX 2

COMPUTER PROGRAM

```
      DIMENSION RSE(5)
      DIMENSION THCK(5)
      READ (1,14) (RSE(LMM),LMM=1,5)
      READ (1,10) TEMPI
      DO 400 M=1,5
      RISE=RSE(M)
      READ(1,14) (THCK(LMN),LMN=1,4)
      DO 400 L=1,4
      WRITE (3,13) RISE
      THICK=THCK(L)
      WRITE (3,15) THICK
      PRMU=0.25
      AIMPR=1.0-PRMU*PRMU
      RADUS=((144.0+RISE*RISE)/(2.0*RISE))*12.0
      WRITE (3,11) RADUS
      TAN=RISE/12.0
      ALPHA=ATAN(TAN)
      PHINO=2.0*ALPHA*57.2958
      WRITE (3,11) PHINO
      BLAM4=3.0*AIMPR*RADUS*RADUS/(THICK*THICK)-PRMU*PRMU/4.0
      D=2.0*SQRT(BLAM4)
      WRITE (3,11) D
      DWM=0.0
      N=200
      COEFT=0.0000042
      PHIRD = PHINO/57.2958
      DELTA=-COEFT*RADUS*TEMPI*SIN(PHIRD)
      YOMOD=4200000.0
      PRMI1=1.0-PRMU
      PRPL1=1.0+PRMU
      AK=YOMOD*THICK*THICK*THICK/(12.0*AIMPR)
      DDD=YOMOD*THICK/AIMPR
      CMPC=AK/(RADUS*DDD*PRMI1)
      CMPS=AK/(RADUS*DDD*AIMPR)
      A=1.0/8.0
      AZ1=0.0
      AZ2=0.0
      ADZ1=0.0
      ADZ2=0.0
105   B=D/8.0
      AB=1.0
      C=11.0
      PHIRD=PHINO/57.2958
      SINF=SIN(PHIRD)
      SING=SINF*SINF
      SINK=SING
      COSF=COS(PHIRD)
      COSSN=COSF*SINF
```

```
      Z1=1.0+SING/8.0
      Z2=D*SING/8.0
      DZ1=2.0*COSSN/8.0
      DZ2=D*2.0*COSSN/8.0
      DO 50 I=2,N
  115 DENOM=4.0*I*(I+1)
      RLPRT=(A*C-B*D)/DENOM
      AIMPT=(B*C+A*D)/DENOM
      SING=SING*SINK
  120 Z1=Z1+RLPRT*SING
      Z2=Z1+AIMPT*SING
      COSSN=COSSN*SINK
      ANUM=2.0*I*COSSN
      DZ1=DZ1+ANUM*RLPRT
      DZ2=DZ2+ANUM*AIMPT
      IF( ABS(Z1-AZ1)-0.00001)121,121,124
  121 IF(ABS(Z2-AZ2)-0.00001)122,122,124
  122 IF(ABS(DZ1-ADZ1)-0.00001)123,123,124
  123 IF(ABS(DZ2-ADZ2)-0.00001)52,124,124
  124 AZ1=Z1
      AZ2=Z2
      ADZ1=DZ1
      ADZ2=DZ2
      CB=C
      C=C+C-AB+8.0
      AB=CB
      A=RLPRT
  125 B=AIMPT
   50 CONTINUE
   52 WRITE (3,11) AB,Z1,Z2,DZ1,DZ2
      ZNUM1=D*Z2-PRMU*Z1
      ZNUM2=D*Z1+PRMU*Z2
      DZNM1=D*DZ2-PRMU*DZ1
      DZNM2=D*DZ1+PRMU*DZ2
      IF(DWM-1.0)51,300,300
   51 A11=COSF*Z1*PRMI1+SINF*DZ1
      A12=COSF*Z2*PRMI1+SINF*DZ2
      B11= -DELTA*YOMOD*THICK/(RADUS*SINF)+PRPL1*86.805*
           RADUS {USED WITH VERTICAL LOAD}
      B11= -DELTA*YOMOD*THICK/(RADUS*SINF) {USED WITH
           VERTICAL LOAD=0}
      A21=ZNUMI }
      A22=-ANUM2} {USED WITH FIXED EDGE}
      A21=(ZNUM1*COSF+DZNM1*SINF/PRPL1) } {USED WITH SIMPLY}
      A22=-(ZNUM2*COSF+DZNM2*SINF/PRPL1)} {SUPPORTED EDGE  }
      B22=0.0
      IF(A21-A11)200,200,210
  200 A221=-(A21/A11)*A12+A22
      B221=-(A21/A11)*B11
      C2=B221/A221
      C1=(B11-A12*C2)/A11
      GO TO 220
```

```
  210  A121=-(A11/A21)*A22+A12
       B111=B11
       C2=B111/A121
       C1=-(A22*C2)/A21
  220  WRITE (3,11)C1,C2
C      FROM B.C. GET PLOAD
       PLOAD=C1*Z1+C2*Z2 {USED WITH VERTICAL LOAD = 0}
       PLOAD=((C1*Z1+C2*Z2)*SINF+12500.0*COSF)/SINF
                  {USED WITH VERTICAL LOAD}
       WRITE (3,11) PLOAD
  300  BNUM=C1*Z1+C2*Z2
       ANPHI=-COSF*BNUM=86.805*RADUS}          {LAST TERM LEFT
       ANTHA=-COSF*BNUM-SINF*(C1*DZ1+C2*DZ2)+  {OFF WHEN VERTICAL
             86.805*RADUS}                     {LOAD = 0
       QPHI=BNUM*SINF
       FTERM=CMPC*COSF*(ZNUM1*C1-ZNUM2*C2)
       STERM=CMPS*SINF*(DZNM1*C1-DZNM2*C2)
       AMPHI=FTERM+STERM
       AMTHA=FTERM+PRMU*STERM
       WRITE (3,12) PHINO, ANPHI,ANTHA,QPHI,AMPHI,AMTHA
C      PROGRAM MODIFICATION TO GET STRESS AT INNER AND
       OUTER RADUS
       RADS2=RADUS*RADUS
       THCK2=THICK*THICK
       RADOT=RADUS+THICK/2.0
       RADIN=RADUS-THICK/2.0
       SOTNM=RADOT*THICK+6.0*RADS2-RADUS*THICK
       SOTDM=12.0*RADS2+THCK2
       SOTCN=12.0*RADUS/(RADOT*THCK2)
       SOTFR=SOTCN*SOTNM/SOTDM
       SOTHA=ANTHA/THICK-AMTHA*SOTFR
       SOPHI=ANPHI/THICK-AMPHI*SOTFR
       SINNM=RADIN*THICK-6.0*RADS2-RADUS*THICK
       SINCN=12.0*RADUS/(RADIN*THCK2)
       SINFR=SINCN*SINNM/SOTDM
       SITHA=ANTHA/THICK-AMTHA*SINFR
       SIPHI=ANPHI/THICK-AMPHI*SINFR
       WRITE (3,11) SOTHA,SOPHI,SITHA,SIPHI
       PHINO=PHINO-2.0
       DWM=DWM+2.0
       IF(PHINO)600,600,350
  350  GO TO 1
C      PROGRAM MODIFICATION TO GET STRESS DISTRIBUTION
  600  CNTRD=THICK*THICK/(12.0*RADUS)
       ZZA=-(THICK/2.0+CNTRD)
       ZOUT=THICK+ZZA
       SGNM1=12.0*RADUS*RADUS*THICK*THICK
       SGNM2=THICK**4.0
       SPNM3=12.0*RADUS*THICK*THICK
       SPNM4=144.0*RADUS**3.0
       SGCON=12.0*RADUS/*THICK**3.0)
       SGPDM=SPNM4*RADUS+2.0*SGNM1+SGNM2
       SGPNM=SPNM3+SPNM4
```

```
533   SGTNM=SGNM1+SGNM2+SGPNM*ZZA
      SGTDM=SGPDM+SGPNM*ZZA
      SGFRA=SGCON*SGTNM/SGTDM
      SGTHB=-10000.0*SGFRA
      WRITE (3,11) ZZA,SGTHB
      ZZA=ZZA+0.05*THICK
      IF(ZZA-ZOUT)533,533,400
400   CONTINUE
500   STOP
 15   FORMAT (9H THICK = ,E18.8)
 14   FORMAT (5F10.5)
 13   FORMAT (1H1, 7HRISE = ,E18.8)
 12   FORMAT (6E18.8)
 11   FORMAT (5E18.8)
 10   FORMAT (F18.4)
      END
```

APPENDIX 3

The following shows the derivation for the location of the centroid and the "area factor due to curvature" for an element of a spherical shell.

1) Centroid

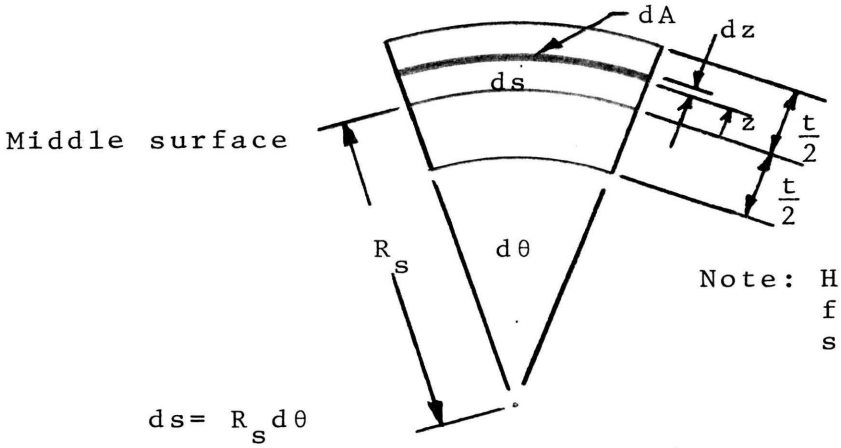

Note: Here z is measured from the middle surface.

$$\text{z centroid relative to middle surface} = \frac{\int z\,dA}{\int dA} = \frac{\int_{-\frac{t}{2}}^{+\frac{t}{2}} z\left[\left(\frac{R_s+z}{R_s}\right)ds\right]dz}{\int_{-\frac{t}{2}}^{+\frac{t}{2}} \left(\frac{R_s+z}{R_s}\right)ds\,dz}$$

$$= \frac{\int_{-\frac{t}{2}}^{+\frac{t}{2}} z\left[\left(\frac{R_s+z}{R_s}\right)(R_s\,d\theta)\right]dz}{\int_{-\frac{t}{2}}^{+\frac{t}{2}} \left(\frac{R_s+z}{R_s}\right)R_s\,d\theta\,dz}$$

$$= \frac{\frac{t^3 \, d\theta}{12}}{R_s \; t \; d\theta}$$

$$\text{z centroid relative to middle surface} = \frac{t^2}{12 \; R_s}$$

$$\text{Therefore } R_c = R_s + \frac{t^2}{12 \; R_s}$$

2) "Area factor due to curvature"

$$Z = - \frac{1}{A} \int_{\text{area}} \frac{z}{R_c + z} \, dA$$

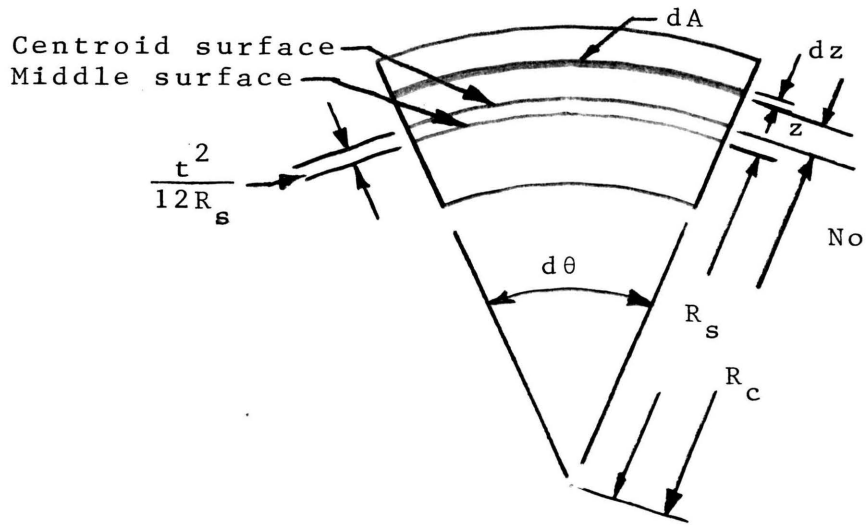

Note: Here z Measured from the centroid surface.

$$dA = d\theta (R_c + z) \, dz$$

$$Z = - \frac{1}{A} \int_{\text{area}} \frac{z \, d\theta (R_c + z) \, dz}{(R_c + z)}$$

$$= -\frac{d\theta}{A}\int_{-\left(\frac{t}{2}+\frac{t^2}{12R_s}\right)}^{\frac{t}{2}-\frac{t^2}{12R_s}} z\,dz = -\frac{d\theta}{A}\frac{z^2}{2}\Bigg|_{-\left(\frac{t}{2}+\frac{t^2}{12R_s}\right)}^{\frac{t}{2}-\frac{t^2}{12R_s}}$$

$$Z = \frac{d\theta t^3}{12R_s A}$$

But $A = R_s t\, d\theta$

so $$Z = \frac{t^2}{12R_s^2}$$

BIBLIOGRAPHY

1. Stresses in Shells; W. Flugge - Springer-Verlag Co., Germany, 1960, pages 7, 312-329.

2. Theory of Elasticity; S. Timoshenko and J. N. Goodier - McGraw-Hill Book Company, Inc., 1951, pages 416-421.

3. Theory of Plates and Shells; S. Timoshenko and S. Woinowsky-Krieger - McGraw-Hill Book Company, Inc., 1959, pages 533-543.

4. Elasticity in Engineering Mechanics; A. P. Boresi - Prentice-Hall, Inc., 1965, pages 224-228.

5. Differential Equations; L. R. Ford - McGraw-Hill Book Company, Inc., 1955, pages 155-157.

6. Advanced Mechanics of Materials; F. B. Seely and J. O. Smith - John Wiley and Sons, Inc., 1952, pages 137-144.

VITA

David Wayne Moore was born July 3, 1938 in St. Louis, Missouri. He was educated in the Ferguson, Missouri elementary schools and graduated from the Hazelwood High School, St. Louis, Missouri in June, 1956. He received a B.S.M.E. Degree from Washington University in St. Louis in June, 1960.

Immediately thereafter he was employed by McDonnell Aircraft Corporation (now McDonnell Douglas Company) in the Strength Department of the Engineering Technology Division. He attained the position of Senior Engineer - Strength before leaving McDonnell in September, 1966.

In September, 1964 the author enrolled at the Graduate Resident Center in St. Louis. Since September, 1966 he has been employed as a graduate assistant in the Engineering Mechanics Department of the University of Missouri at Rolla.